**REPUBLIC OF TURKEY**
**ADANA ALPARSLAN TÜRKEŞ SCIENCE AND TECHNOLOGY UNIVERSITY**

**GRADUATE SCHOOL OF NATURAL AND APPLIED SCIENCES**
**DEPARTMENT OF ELECTRICAL AND ELECTRONIC ENGINEERING**

# EXPERIMENTAL AND THEORETICAL EVALUATION OF HYDROGEN PRODUCTION VIA PV-ASSISTED ALKALINE ELECTROLYSIS

**HÜSEYİN NAZLIGÜL**
**MASTER OF SCIENCE**

**ADANA 2021**

**REPUBLIC OF TURKEY**

**ADANA ALPARSLAN TÜRKEŞ SCIENCE AND TECHNOLOGY UNIVERSITY**

**GRADUATE SCHOOL OF NATURAL AND APPLIED SCIENCES**

**DEPARTMENT OF ELECTRICAL AND ELECTRONIC ENGINEERING**

# EXPERIMENTAL AND THEORETICAL EVALUATION OF HYDROGEN PRODUCTION VIA PV-ASSISTED ALKALINE ELECTROLYSIS

**HÜSEYİN NAZLIGÜL**

**MASTER OF SCIENCE**

**SUPERVISOR**

**ASSOC. PROF. DR. BAŞAK DOĞRU MERT**

**ADANA 2021**

I hereby declare that all information in this thesis has been obtained and presented in accordance with academic rules and ethical conduct. I also declare that, as required by these rules and conduct, I have fully cited and referenced all information that is not original to this work.

[Signature]

Hüseyin NAZLIGÜL

# ABSTRACT

**EXPERIMENTAL AND THEORETICAL EVALUATION OF HYDROGEN PRODUCTION VIA PV-ASSISTED ALKALINE ELECTROLYSIS**

Hüseyin NAZLIGÜL
Department of Electrical Electronic Engineering
Supervisor: Assoc. Prof. Dr. Başak DOĞRU MERT
June 2021, 95 pages

Energy resources have become the most important issue of all countries in the world because of the rapid increase in the population worldwide, the continuous development of technology, the role of the countries in their relations and economic prosperity. On the other hand, due to the decrease in the production rates of these limited resources every year, the depletion of reserves, the increase of awareness about global warming and greenhouse gas emissions, and more restrictive regulations to protect nature, humanity has led to the search for different energy resources. Considering the negative effects of fossil fuels, it has become a necessity to turn to alternative energy sources, especially hydrogen as an energy carrier, and to make maximum use of these sources. However, this demand for clean fuel energy during its production is a critical issue and a completely green production chain should be needed in order not to harm nature. Especially for electrolysis cells, electricity must be supplied from renewable sources. Hydrogen technologies give extremely positive signals for the medium and long term in the energy arena of the future. In particular, it has become a necessity to resort to hydrogen as an energy carrier and to get the maximum benefit from these sources. Because hydrogen emission is only water. It provides zero carbon emissions and is good as a high energy density, it has such advantages as one of the most promising energy carriers for the future.

In order to contribute to this direction, hydrogen production was carried out by alkaline electrolysis method, which can be adapted to the application of an on grid supply system with renewable sources. In this study, a renewable electrolysis system is designed, which provides the necessary voltage for electrolysis from an 80W PV panel with a DC-DC converter and stores the excess electricity in batteries. Firstly, this system was simulated in MATLAB/Simulink and then the experimental part was carried out and the results were compared. All experiments were carried out at 25℃ and 1000 W/m$^2$ irradiation in Adana, Turkey. As a result of the simulation, the PV panel power was found to be 81 W, while it was found to be 77.15 W in the experimental study. Since the results obtained have close values with each other, the results of the system to be simulated can be observed approximately without installing such a system anywhere in the world.

In electrolysis system, Pt with a surface of 2 cm$^2$ was used as the anode, and four different electrodes with a surface of 0.36 cm$^2$ were used as the cathode. A graphite electrode with a surface of 0.36 cm$^2$ was produced and its surface was covered with different metals and decorated. Appropriate cathode performance was determined with the aid of polarization curves. The decomposition potential and hydrogen gas volume were obtained with the two-electrode configuration. The hydrogen gas volume was determined with a graduated cylinder filled with 1 M KOH electrolyte. The hydrogen performance of G, G/Ni, G/NiCo and G/NiCoAg was compared. G, G/Ni, G/NiCo, and G/NiCoAg produced 30 mL, 31 mL, 42 mL and 78 mL of hydrogen gas, respectively, end of 30 minutes of electrolysis time by applying a voltage of 3V. Thanks to these thin coatings and decorations, the electrocatalytic properties of the electrodes were increased and it was proved that there was a serious increase in hydrogen production.

**Keywords:** alkaline electrolysis, hydrogen production, photovoltaic, renewable energy

# ÖZET

**HİDROJEN ÜRETİMİNİN PV DESTEKLİ ALKALİN ELEKTROLİZİ İLE DENEYSEL VE TEORİK DEĞERLENDİRİLMESİ**

Hüseyin NAZLIGÜL
Elektrik Elektronik Mühendisliği Anabilim Dalı
Danışman: Doç. Dr. Başak DOĞRU MERT
Haziran 2021, 95 sayfa

Dünya nüfusunun hızla artması, teknolojinin sürekli gelişmesi, ülkelerin ekonomik refahı ve ilişkilerindeki rolü nedeniyle enerji kaynakları tüm dünya ülkelerinin en önemli sorunu haline gelmiştir. Öte yandan, bu sınırlı kaynakların üretim oranlarının her yıl azalması, rezervlerin tükenmesi, küresel ısınma ve sera gazı emisyonları konusundaki farkındalığın artması ve doğayı korumaya yönelik daha kısıtlayıcı düzenlemeler getirilmesiyle insanlık, farklı enerji kaynakları arayışına yöneldi. Fosil yakıtların olumsuz etkileri göz önüne alındığında, enerji taşıyıcısı olarak hidrojen başta olmak üzere, alternatif enerji kaynaklarına yönelmek ve bu kaynaklardan maksimum düzeyde yararlanmak bir zorunluluk haline gelmiştir. Ancak üretimi sırasında temiz yakıt enerjisine olan bu talep kritik bir konudur ve doğaya zarar vermemek için tamamen yeşil bir üretim zincirine ihtiyaç duyulmaktadır. Özellikle elektroliz hücreleri için elektrik yenilenebilir kaynaklardan sağlanmalıdır. Hidrojen teknolojileri, geleceğin enerji arenasında orta ve uzun vade için son derece olumlu sinyaller veriyor. Özellikle enerji taşıyıcısı olarak hidrojene başvurmak ve bu kaynaklardan maksimum faydayı elde etmek bir zorunluluk haline gelmiştir. Çünkü hidrojen emisyonu sadece sudur. Sıfır karbon emisyonu sağlar ve yüksek enerji yoğunluğu olarak iyidir, gelecek için en umut verici enerji taşıyıcılarından biri gibi avantajlara sahiptir.

Bu yönde katkı sağlamak amacıyla yenilenebilir kaynaklarla şebeke içi besleme sistemi uygulamasına uyarlanabilecek alkali elektroliz yöntemi ile hidrojen üretimi gerçekleştirilmiştir. Bu çalışmada, DC-DC dönüştürücülü 80 W'lık bir PV panelden elektroliz için gerekli voltajı sağlayan ve fazla elektriği akülerde depolayan yenilenebilir bir elektroliz sistemi tasarlanmıştır.

Bu sistem önce MATLAB/Simulink'te simüle edilmiş daha sonra deneysel kısım gerçekleştirilerek sonuçlar karşılaştırılmıştır. Tüm deneyler Adana, Türkiye'de 25℃ ve 1000 W/m$^2$ ışınımda yapılmıştır. Simülasyon sonucunda PV panel gücü 81 W, deneysel çalışmada ise 77.15 W olarak bulunmuştur. Elde edilen sonuçlar birbirine yakın değerlere sahip olduğundan simülasyonu yapılacak sistemin sonuçları dünyanın herhangi bir yerinde böyle bir sistem kurulmadan önce, yaklaşık olarak gözlemlenebilmektedir.

Elektroliz sisteminde anot olarak 2 cm$^2$ yüzeyli Pt, katot olarak 0.36 cm$^2$ yüzeyli dört farklı elektrot kullanılmıştır. 0.36 cm$^2$ yüzeyli grafit elektrot üretilmiş ve yüzeyi farklı metallerle kaplanmış ve dekore edilmiştir. Polarizasyon eğrileri yardımıyla uygun katot performansı belirlendi. Ayrışma potansiyeli ve hidrojen gazı hacmi, iki elektrotlu konfigürasyon ile elde edildi. Hidrojen gazı hacmi, 1 M KOH elektroliti ile doldurulmuş dereceli bir silindir ile belirlendi. G, G/Ni, G/NiCo ve G/NiCoAg'nin hidrojen performansı karşılaştırıldı. G, G/Ni, G/NiCo ve G/NiCoAg, 3V'luk bir voltaj uygulayarak 30 dakikalık elektroliz süresinin sonunda sırasıyla 30 mL, 31 mL, 42 mL ve 78 mL hidrojen gazı üretmiştir. Bu ince kaplamalar ve modifikasyonlar sayesinde elektrotların elektrokatalitik özellikleri artırılmış ve hidrojen üretiminde ciddi bir artış olduğu kanıtlanmıştır.

**Anahtar Kelimeler:** alkali elektroliz, fotovoltaik, hidrojen üretimi, yenilenebilir enerji

*Dedication*

*I would like to dedicate my thesis to our martyrs.*

# TABLE OF CONTENTS

# LIST OF FIGURES

# LIST OF TABLES

# NOMENCLATURE

| | |
|---|---|
| Bcm | : Billion Cubic Meters |
| kWh | : Kilowatt Hour |
| MWh | : Megawatt Hour |
| TWh | : Terawatt Hour |
| W | : Watt |
| kW | : Kilowatt |
| MW | : Megawatt |
| GW | : Gigawatt |
| V | : Volt |
| A | : Amper |
| g | : Gram |
| kg | : Kilogram |
| m | : Meter |
| $m^2$ | : Meter Square |
| cm | : Centimeter |
| $cm^2$ | : Centimeter Square |
| L | : Liter |
| mL | : Milliliter |
| % | : Percent |
| s | : Second |
| ºC | : Celcius |
| ºF | : Fahranheit |
| ºK | : Kelvin |
| I | : Current |
| $E_d$ | : Decomposition Voltage |
| $I_d$ | : Current Density |
| $E_{over}$ | : Over Voltage |
| m | : Mass |
| Ag | : Silver |
| AgCl | : Silver Chloride |

| | |
|---|---|
| KCl | : Potassium Chloride |
| G | : Graphite |
| G/Ni | : Nickel Plated Graphite |
| G/NiCo | : Cobalt Decorated Nickel Plated Graphite |
| G/NiCoAg | : Silver, Cobalt Decorated Nickel Plated Graphite |
| Zn | : Zinc |
| Pt | : Platinum |
| $O_2$ | : Oxygen |
| $H_2$ | : Hydrogen |
| N | : Nitrogen |
| $CO_2$ | : Carbon Dioxide |
| $CH_4$ | : Methane |
| Na | : Sodium |
| NaOH | : Sodium Hydroxide |
| KOH | : Potassium Hydroxide |
| $Cl_2$ | : Chlorine |
| Cu | : Copper |
| Bi | : Bismuth |
| B | : Boron |
| S | : Sulfur |
| M | : Molarity |
| $H_2SO_4$ | : Sulfuric Acid |
| $e^-$ | : Electron |
| PV | : Photovoltaic |
| CIS | : Commonwealth of Independent States |
| DC | : Direct Current |
| AC | : Alternating Current |
| Q | : Total Charge |
| $V_t$ | : Theoretical Hydrogen Volumes |
| $V_e$ | : Experimental Hydrogen Volumes |

# 1. INTRODUCTION

Energy is accepted as a strategic concept that plays a very important role in the continuation of vitality and the socio-economic development of countries. Energy is a major element of economic growth and a key factor for a country's development. Over the years, the demand for energy, especially electrical energy, has been increasing due to modernization, industrialization and population growth as well as the increasing standard of living of people. Especially for people dragged into a technological life, a life without energy has become unthinkable and has pushed people to seek new energy sources. Energy, which is defined as the ability to do work, can be transformed from one type to another with appropriate methods and can be classified in different ways. The resources that can obtain energy for economic purposes using various methods and techniques are called energy resources. Since energy can be in many different forms, its classification is done in different ways. Therefore, classifications in energy are made according to some criteria. Energy sources are generally classified according to their use and recyclability.

According to their recyclability, they are classified as primary and secondary energy sources. If it uses an energy source as it is in nature, this group is called the primary energy source. Crude oil, coal, natural gas, lignite can be given as examples of primary energy sources. The energy obtained by transforming the primary energy resources found in nature through certain processes is grouped as a secondary energy source. Electricity, gasoline, diesel oil, diesel, coke and liquefied petroleum gas are among these types of energy sources.

According to the classification made according to their use, energy resources are renewable and non-renewable. Renewable energy resources to energy resources that can remain the same in a natural cycle process, which do not decrease and never run out despite being used; Energy sources that cannot renew themselves once used are known as non-renewable energy sources. Renewable resources are wind energy, solar energy, hydroelectric energy, hydrogen energy, geothermal energy, wave energy and biomass energy. Non-renewable energy sources are divided into four classes as coal, oil, natural gas and nuclear energy. First of all, it would be useful to refer to statistical information about the most used energy sources, the reserve amounts of these resources and their share in electrical energy production in the world and in Turkey.

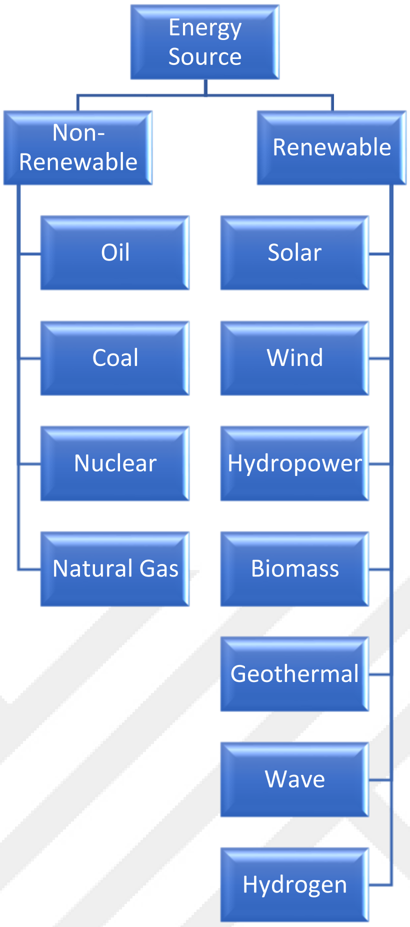


**Figure 1.1.** Renewable and non-renewable energy sources.

**Energy sources**

The continuity of energy resources is an important factor in the progress of the economic level of countries. Today, countries have turned to new investments and new technologies to provide energy from unlimited and sustainable sources instead of limited resources. In this part of the study, types of energy are discussed in two parts as non-renewable and renewable.

### 1.1.1. Non-Renewable sources

Non-renewable energy sources are divided into four classes as coal, oil, natural gas and nuclear energy. Coal, oil and natural gas are also called fossil energy sources. Fossil fuels are formed by living remains under the influence of high temperature and pressure for many years. The existing energy in them is extracted by the extraction of fossil remains, their processing and transformation under various processes. After energy production with fossil resources, these resources cannot be recycled. Therefore, these resources are decreasing day by day. In this section, reserves and production amounts in the world will be examined, as well as our country's reserves.

#### 1.1.1.1. Oil

The usage area of crude oil is limited, but the value of the products obtained after the oil is processed and the usage area increases. The place where oil is processed is called a refinery. Oil is usually ready to use after refinement or refining. The products obtained after the crude oil is processed, in order of importance; Gasoline, Fuel Oil, Diesel, Lipid Petroleum Gas (LPG), Jet Fuel and Asphalt. The petroleum-based raw material is also used in aircraft, automobile, construction, explosive industry, textile industry and paint industry, food processing techniques and agriculture. In addition to these, it is used in the production of plastics, artificial rubber, artificial fiber, fertilizers, detergents, insecticides and various solvents.

The world approved oil reserves are 1295 billion barrels in 2000, while it is 1734 billion barrels at the end of 2019. This corresponds to a significant increase of 25 %. However, this increase is very low in the last decade and the rate of increase is decreasing with each passing year. This situation is an indication that the oil reserve life is reduced and it will be insufficient in the future.

The Figure 1.2. shows the regional shares of world reserves. When we look regionally, almost half of the world's oil reserves are in the Middle East. The middle east is followed by the continent of America with 33%. The remaining 19% of this distribution is respectively CIS (Commonwealth of Independent States), Africa, Asia Pacific and European regions.

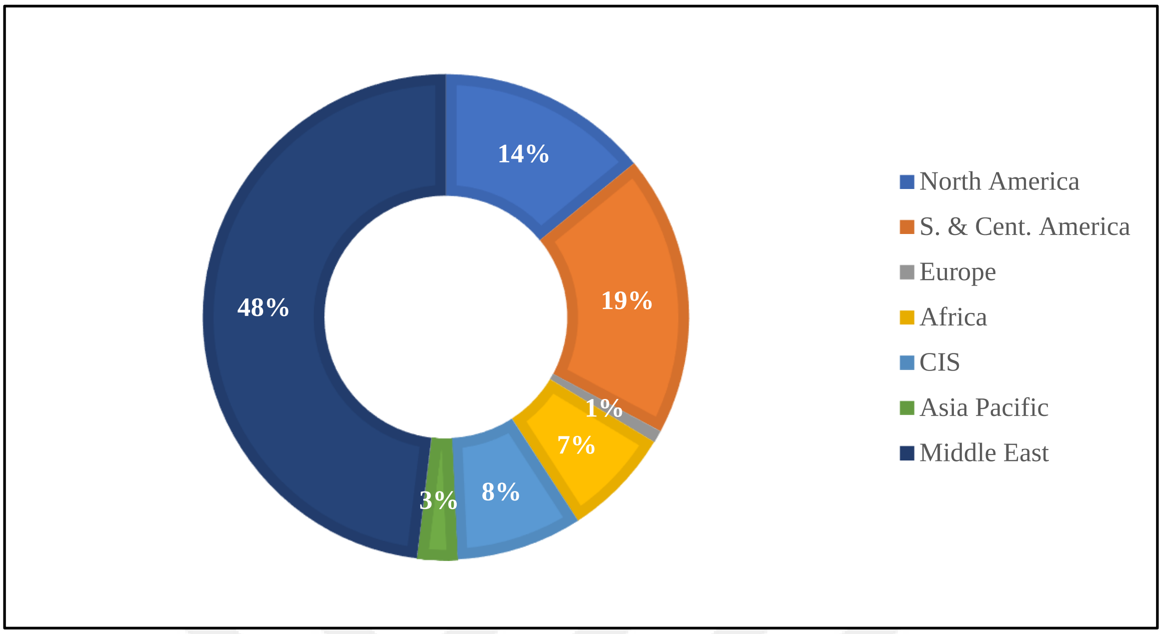


**Figure 1.2.** Oil reserves by continents at the end of 2019.

Some countries have a huge share of oil reserves in the world. As seen in Table 1.1, the first two places are Venezuela and Saudi Arabia. In this way, it makes a great contribution to the income of their country. When the remaining 8 countries are included, 86.4% of the oil reserves are seen in the 10 countries in Table 1.1.

**Table 1.1.** Oil reserves by some country at the end of 2019.

| Countries | Million Tones | 2019(%) |
|---|---|---|
| Venezuela | 303.8 | 17.5 |
| Saudi Arabia | 297.6 | 17.2 |
| Canada | 169.7 | 9.8 |
| Iran | 155.6 | 9.0 |
| Iraq | 145.0 | 8.4 |
| Russian Federation | 107.2 | 6.2 |
| Kuwait | 101.5 | 5.9 |
| United Arab Emirates | 97.8 | 5.6 |
| US | 68.9 | 4.0 |
| Libya | 48.4 | 2.8 |

Countries, where oil is abundant, have established refineries to process and make crude available. Thanks to these refineries, they aim to meet their oil needs and generate income by exporting oil to the world. Among the countries producing oil, the United States realizes as much as 18% with 17045 thousand barrels per day. The other abundant countries in oil production are Saudi Arabia, Russia, Canada, and Iraq with 12.4%, 12.1%, 5.9% and 5% percentages, respectively. As seen in Table 1.2, the first 5 countries meet half of the oil production.

**Table 1.2.** Oil production daily by some country at the end of 2019.

| Countries | Thousand barrels | 2019(%) |
|---|---|---|
| US | 17045 | 17.9 |
| Saudi Arabia | 11832 | 12.4 |
| Russian Federation | 11540 | 12.1 |
| Canada | 5651 | 5.9 |
| Iraq | 4779 | 5.0 |
| United Arab Emirates | 3998 | 4.2 |
| China | 3836 | 4.0 |
| Iran | 3535 | 3.7 |
| Kuwait | 2996 | 3.1 |
| Brazil | 2877 | 3.0 |

It is a fact that oil is the most important primary energy source in the world and will not lose its importance in the long term. The share of oil, which is the main ingredient of the transportation sector, in primary energy use is quite large. In countries where the population and the number of vehicles are high, especially in developed countries, oil consumption is high. For this reason, when we look at Table 1.3, we see the US, China and India, respectively, in the top three with consumption rates. But being in the first three in this table is not very positive for a green world. The remaining countries are developed or crowded countries from different continents.

**Table 1.3.** Coal consumption daily by some country at the end of 2019.

| Countries | Thousand barrels | 2019(%) |
|---|---|---|
| US | 19400 | 19.7 |
| China | 14056 | 14.3 |
| India | 5271 | 5.4 |
| Japan | 3812 | 3.9 |
| Saudi Arabia | 3788 | 3.9 |
| Russian Federation | 3317 | 3.4 |
| South Korea | 2760 | 2.8 |
| Canada | 2403 | 2.4 |
| Brazil | 2398 | 2.4 |
| Germany | 2281 | 2.3 |

Despite the fact that 50% of the world's total oil reserves are found in the neighboring geography of our country, our country is not as rich in oil as its neighbors Iran, Iraq and Syria. This is due to the difference in the geological structure in our country. 70% of the oil produced is met by the Turkish Petroleum Corporation (TPC) from the fields in the Southeastern Anatolia Region (EMRA, 2013). Today, many companies, especially TPC, are engaged in these activities. Petroleum, which ranks first in the world's primary energy consumption, has 42 million tons of reserves in Turkey. Existing oil deposits are mostly in Adıyaman, Batman and Diyarbakır in the Southeastern Anatolia Region. There are also oil fields in Siirt, Şanlıurfa and Mardin. The oil produced meets a very small portion (1/7) of Turkey's needs. The rest is financed externally. Refineries have been established in Turkey for the refining of crude oil. Some of the crude oil produced in the Southeastern Anatolia Region is sent to the Batman Refinery, and some to Dörtyol via the Batman-Iskenderun pipeline. From here, it is transported to Izmir and Izmit refineries by tankers. Crude oil is transferred to Kırıkkale Refinery via the oil pipeline between İskenderun Bay and Kırıkkale. In addition, some of the Iraqi oil is transported to Yumurtalık Port by the Turkey-Iraq pipeline. Turkey provides a significant income from this transportation. Azerbaijani oil is transported to the Iskenderun Bay via the Baku-Tbilisi-Ceyhan Oil Pipeline.
In recent years, Turkey has been conducting natural gas and oil exploration activities on land and in the eastern Mediterranean. As a result of these searches, new reserves have been found and it is predicted that new reserves will be found.

#### 1.1.1.2. Coal

The material formed by the transformation of organic materials under water and under the soil in the case of suitable environment acid values in humid and hot regions is called coal (Savrul, 2010). The lifetime of the coals varies between 15 million and 400 million years in terms of geology. As the age of the coal, their qualities increase. The coal group is classified into different varieties. There are three types of coal: anthracite, hard coal and lignite. It has been revealed as a result of the studies that anthracite coal contains 95% carbon. This type of coal is a very valuable type and its structure is quite durable and hard. For this reason, more calories are released as a result of the burning process compared to other types of coal. 70% of hard coal and less than 50% of lignite give heat. (Kuzoluk,2014)
It is known that the total coal reserve of the world is approximately 1.1 trillion tons. According to the researches of the World Energy Council; The proven and exploitable coal reserves in the

world total 891 billion tons. Of the said reserve; 403 billion tons of anthracite and bituminous coal, 287 billion tons of sub-bituminous coal and 201 billion tons of lignite are in the category. Coal production in the world has increased 2-fold in the last 30 years. The biggest factor in this increase is the increased energy need due to technological development in China and the Asian continent. Countries producing coal in the world are examined in Table 1.4, which shows that 10 countries in the world account for 91.5% of total coal production. China ranks first in coal producing countries with the highest share of 46.6%. This country is followed by India 9.7%, USA 8.1%, Indonesia 7.8%.

**Table 1.4.** Coal production by some country at the end of 2019.

| Countries | Million tones | 2019 (%) |
|---|---|---|
| China | 3 693 | 46.6 |
| India | 769 | 9.7 |
| United States | 640 | 8.1 |
| Indonesia | 616 | 7.8 |
| Australia | 503 | 6.4 |
| Russian Federation | 418 | 5.3 |
| South Africa | 254 | 3.2 |
| Germany | 131 | 1.7 |
| Poland | 112 | 1.4 |
| Kazakhstan | 105 | 1.3 |
| Rest of the world | 680 | 8.5 |
| Total World | 7921 | 100.0 |

Coal, which is the first source that comes to mind when it comes to fossil resources, is found in many parts of the world and has taken its place as an indispensable energy source in our daily lives. The most important advantage of coal as a reliable fuel, low production cost and also not showing the need for advanced technology at this production stage are among the main reasons for preference. It is mostly used in industry, electricity production and home heating. Coal is one of the most important raw materials required to generate heat energy in all areas of industrialization. For example, in the iron and steel industry, we can see the high efficiency of coal in industrial production systems. (Demir, 2013).

**Table 1.5.** Coal consumption by some country from 2000 to 2019.

| Countries | 2000 | 2005 | 2010 | 2015 | 2019 | 2019 (%) |
|---|---|---|---|---|---|---|
| China | 29.56 | 55.46 | 73.22 | 80.13 | 81.67 | 51.70 |
| India | 6.88 | 8.84 | 12.16 | 16.55 | 18.62 | 11.80 |
| United States | 22.63 | 22.85 | 20.88 | 15.58 | 11.34 | 7.20 |
| Japan | 4.00 | 4.81 | 4.87 | 5.03 | 4.91 | 3.10 |
| South Africa | 3.12 | 3.35 | 3.89 | 3.52 | 3.81 | 2.40 |
| Russian Federation | 4.43 | 3.96 | 3.79 | 3.86 | 3.63 | 2.30 |
| South Korea | 1.80 | 2.29 | 3.23 | 3.58 | 3.44 | 2.20 |
| Indonesia | 0.55 | 1.02 | 1.65 | 2.14 | 3.41 | 2.20 |
| Germany | 3.57 | 3.40 | 3.23 | 3.29 | 2.30 | 1.50 |
| Poland | 2.35 | 2.31 | 2.31 | 2.04 | 1.91 | 1.20 |
| Turkey | 0.94 | 0.93 | 1.32 | 1.45 | 1.70 | 1.10 |
| Kazakhstan | 0.75 | 1.13 | 1.40 | 1.43 | 1.67 | 1.10 |
| Total World | 98.70 | 130.21 | 151.19 | 157.84 | 157.86 | 100.00 |

As seen in Table 1.5, the largest part of coal consumption is in China with 81.67 exajoules in 2019. China's coal consumption is just over half of the world's total coal consumption. China's coal consumption is followed by India, the US, Japan and South Africa, respectively. Thus, more than 75% of the world's coal consumption has been accumulated in the first five countries.

Thermal power plants, where coal resources are used as raw materials in electricity generation, are the most used power plants today. Although these power plants appear as power plants that can be easily obtained as raw materials, they also have disadvantages for humanity and our world. When we look at the damage to the environment, it is in the first place. Thermal power plants emit many harmful solid and gaseous substances as waste to the environment. The most important of these substances are substances such as sulfur dioxide, carbon monoxide, nitrous oxide, which negatively affect human, social and natural health (Akdoğan, 2018). In recent years, interest in coal has been declining worldwide for these reasons. Consumption decreases every year in developed countries such as the United States, Germany, Japan and Russia. More environmentally friendly resources are preferred over coal. Unfortunately, increases in coal consumption in developing countries have been very serious. For example, from 2000 to 2019, Indonesia also increased from 0.55 exajoules to 3.41 exajoules.

Our country has 1.1% of the world's total coal reserves in Turkey. The total coal resource of our country, including lignite, asphaltite and hard coal, is approximately 20.84 billion tons

(MTA, 2019; TKİ, 2019). The most important hard coal resource is in Zonguldak and its vicinity. According to the current reports of Mineral Research and Exploration of Turkey, hard coal resource constitutes 7.3% with 1.52 billion tons of which 736 million tons are visible, and Lignite and asphaltite constitute 92.7% with 19.32 billion tons in total. (TTK, 2020) Since the survey and feasibility studies of only one third of our country's coal resources have been completed, very few of them are considered as reserves.

The coal consumed in Turkey in 2018, 1.10 million tons of domestic coal, 39.14 million tons of imported coal, 82.48 million tons of lignite and asphaltite, including a total of 122.82 million tons. Therefore, in 2018, compared to the previous year, imported and domestic coal consumption increased by 1.7% and lignite-asphaltite consumption increased by 13.09%.
The increase in total coal consumption is 8.9%. In 2018, thermal power plants had the largest share of coal consumption in Turkey. The share of power plants in the consumption of coal is steadily increasing. This share, which was 20% ten years ago, is close to 60.7% as of 2018. The remaining consumption was 15.7% coke plants and 23.6% other industries.

Lignite coals produced in our country are consumed in thermal power plants and industrial sectors for the purpose of electricity generation, as well as in housing and workplaces for heating purposes. In 2018, 73.5% of the total lignite supply, which was 80.9 million tons, was consumed in electricity generation and heat generation. The share of usage in industrial sectors is 4.8% and the share of usage in residential and workplaces is 4.2%. However, the thermal values of lignite used in electricity production are much lower than those of coals used in industry or heating. Calculation based on total thermal value; 72.9% of the lignite energy supplied in 2018 was consumed in electricity generation, 13.8% in industrial sectors and 10.7% in residential and workplaces. In the same year, almost all of the 1,405 thousand tons of asphaltite supply was consumed for electricity generation purposes.

#### 1.1.1.3. Natural Gas

Natural gas, just like coal, is fossil fuel formed as a result of the exchange of organic materials that have remained under high pressure and heat for millions of years. Natural gas, which is a fossil-based energy source, is squeezed between underground porous rocks or exists in a large volume above the oil basins. In terms of content, natural gas consists of 95% methane and trace amounts of ethane, propane, atom, butane and carbon dioxide gases. However, natural gas is the only hydrocarbon energy source that can lead to further reductions in global carbon density by reducing carbon dioxide emissions easily and at a manageable cost.

Natural gas, which has an important place among the primary energy sources all over the world, will maintain its strategic position similar to oil in the long term. When we look at the world, there are 198.8 trillion cubic meters of proven natural gas reserves. It is predicted that this reserve will last for less than 60 years in the market. In the distribution between countries, the top ten countries with the highest proven natural gas reserves in the world in 2019 are given in Table 1.6. When we examine the regions of the world, natural gas reserves are mostly in the Middle East region with 75.6 trillion cubic meters (38%). Among the Middle Eastern countries, there are Iran, Qatar, Saudi Arabian United Arab Emirates and Iraq. The Middle East is followed by CIS countries, including Russia and Turkmenistan, which have 64.2 trillion cubic meters (32.3%) of reserves. respectively, Europe, Asia Pacific, South and Central America are the regions with the least natural gas reserves with 8 trillion cubic meters.

**Table 1.6.** Naturel gas reserves by some country at the end of 2019.

| Countries | Trillion cubic meters | 2019(%) |
|---|---|---|
| Russian Federation | 38.0 | 19.1 |
| Iran | 32.0 | 16.1 |
| Qatar | 24.7 | 12.4 |
| Turkmenistan | 19.5 | 9.8 |
| US | 12.9 | 6.5 |
| China | 8.4 | 4.2 |
| Venezuela | 6.3 | 3.2 |
| Saudi Arabia | 6.0 | 3.0 |
| United Arab Emirates | 5.9 | 3.0 |
| Nigeria | 5.4 | 2.7 |
| Algeria | 4.3 | 2.2 |
| Iraq | 3.5 | 1.8 |

It is important for countries to put the natural gas reserve into production, to meet the energy demand and to generate income by exporting the surplus. World natural gas production has increased by approximately 2.5% each year in the last decade and reached 3929 billion cubic meters (bcm) by the end of 2019. As seen in Table 1.7, although it is in fifth place in terms of reserves, the US is in the first place with 23% in production. Russia ranks second with 17% but meets the natural gas needs of the majority of European and Asian countries.

**Table 1.7.** Naturel gas production by some country at the end of 2019.

| Countries | Billion cubic meters | 2019(%) |
|---|---|---|
| US | 920.8 | 23.1 |
| Russian Federation | 679.0 | 17.0 |
| Iran | 244.2 | 6.1 |
| Qatar | 178.1 | 4.5 |
| China | 177.6 | 4.5 |
| Canada | 173.1 | 4.3 |
| Australia | 153.5 | 3.8 |
| Norway | 114.4 | 2.9 |
| Saudi Arabia | 113.6 | 2.8 |
| Algeria | 86.2 | 2.2 |

In the New Policies Scenario of the report published by the International Energy Agency in 2013; gas demand is expected to increase 1.6% annually on average until 2035 to reach 5 tcm, and 85% of this increase will result from the demand of non-OECD countries. The top countries in natural gas consumption are given in Table 1.8 and as can be seen, these countries are generally developed countries. It is estimated that the gas demand in Asia Pacific, whose share in energy consumption is limited, will increase four times due to the expected high demand especially in China. The European Union (EU), which has low natural gas production and high consumption, is dependent on foreign sources in approximately 58% of its energy needs. 40% of the natural gas and oil exported to EU countries comes from the Russian Federation. The EU will remain the largest gas importer in the future. It has been calculated that European natural gas consumption, which was 496 bcm in 2001, will reach 634 bcm in 2021 (UNECE, 2016).

**Table 1.8.** Naturel gas consumption by some country at the end of 2019.

| Countries | Billion cubic meters | 2019(%) |
|---|---|---|
| US | 846.6 | 21.5 |
| Russian Federation | 444.3 | 11.3 |
| China | 307.3 | 7.8 |
| Iran | 223.6 | 5.7 |
| Canada | 120.3 | 3.1 |
| Saudi Arabia | 113.6 | 2.9 |
| Japan | 108.1 | 2.8 |

| | | |
|---|---|---|
| Mexico | 90.7 | 2.3 |
| Germany | 88.7 | 2.3 |
| United Kingdom | 78.8 | 2.0 |

Since natural gas consumption in Turkey in 2000, rising levels of household spending growth and economic activity have led to a gradual increase. Increasing energy imports together with the lack of energy production also increased the external deficit in our country. The main reasons for the increase in natural gas consumption stem from the increase in electricity consumption depending on industrial production and individual consumption. Due to very little of the natural gas production in Turkey, close to the entire portion of the natural gas consumed it is met through imports. Turkey's annual natural gas needs are about 45 bcm in 2019. Turkey shares its annual natural gas consumption in electricity generation, industry, residence and other sectors as 25%, 27%, 32% and 16% respectively. Turkey's natural gas needs are met by pipelines from the Russian Federation, Turkmenistan, Azerbaijan and Iran, and by tankers with LNG liquefied from Nigeria and Algeria. Our country continues its natural gas exploration efforts in the Black Sea and the Eastern Mediterranean. 320 billion cubic meters of natural gas reserves were found in the Black Sea in 2020. Available reserves will meet very short-term needs. Because of this, more exploration and drilling efforts should be carried out and a serious amount of budget should be allocated to these exploration efforts.

#### 1.1.1.4. Nuclear

Nuclear Energy is defined as the energy obtained by fusion and fission reactions as a result of the collision of atomic nuclei that reach high energy at high temperatures. The fission reaction that occurs as a result of the fragmentation of the atomic nucleus during the production of nuclear energy poses significant dangers. The energy-controlled and continuous energy production systems released as a result of this division are called nuclear power plants. For this reason, the establishment of nuclear power plants is carried out with high costs and investments. The heat energy generated as a result of atom fragmentation in nuclear power plants is first converted into mechanical energy and then electrical energy and offered for use in commercial areas.

The fuel used in these power plants is mostly enriched uranium. The first studies on this subject were carried out in the USA in 1945. With the increase in search for alternative energy after the oil crisis in the 1970s, nuclear power plants began to be established in the world. 448 nuclear energy reactors are continuing to operate in the world. Here the USA takes the lead with 100 reactors. This country is followed by France with 58 reactors, Japan with 43 reactors, China with 35 reactors and Russia with 36 reactors. Many countries in the world have increased their efforts day by day to establish their nuclear power plant. The amount of electricity generated from nuclear reactors in some countries in Table 1.9. In the world, the countries' rate of meeting the electricity demand from nuclear energy was the first in France with 73%, while Ukraine was the second with 52% and Belgium with 51%.

**Table 1.9.** The amount of electricity generated from nuclear reactors in some countries.

| Countries | Production (TWh) |
|---|---|
| US | 852.00 |
| France | 399.43 |
| China | 348.70 |
| Russian Federation | 208.98 |
| South Korea | 145.98 |
| Canada | 100.48 |
| Ukraine | 83.00 |
| Germany | 75.07 |
| Sweden | 67.01 |
| Japan | 65.63 |
| Spain | 58.43 |
| United Kingdom | 56.18 |
| India | 45.16 |

Founded in 1956, the world has been included in the international atomic energy agency IEA board the anniversary of Turkey. Turkey working for the first nuclear power plant by the year 1965 is taken first, too scope of the license for the first nuclear power plants in 1974. This license is currently valid for the Akkuyu field. The first nuclear agreements with Russia were made in 2010 for the Akkuyu nuclear power plant. According to the agreement, the plant to be installed will have 4 units of VVER-1200 type and the total installed power will be 4,800 MW. The first unit of this power plant will be put into operation in 2021 and the whole will be operational in 2024 (Bartik, 2018). Turkey's 2nd nuclear power plant, which will be of interest to the nuclear power plant in Sinop treaties were made with Japan in 2013. The plant to be built according to the agreement will have 4 units of ATMEA-1 type and a total of 4,480 MW of installed power, and the first two units of the power plant will be commissioned in 2023-2024 and the whole will be completed in 2028 (Bartik, 2018).

Work is underway in the third nuclear power plant, and agreements have been made between EÜAŞ, Westinghouse Electric and SNPTC (State Nuclear Power Technology Corporation) in 2014. Currently, the development report is being studied with these companies. There are some conditions that are important criteria for us in the transition phase of our country to nuclear energy (Bartik, 2018).

### 1.1.2. Renewable Sources

Increasing energy needs and increasing electricity consumption have led countries to seek alternative energy sources. The gradual decrease in the lifespan of exhaustible resources has increased the interest and investment levels in these resources. If we list the renewable energy sources: wind, solar, hydrogen, hydroelectric, geothermal, sea wave and biomass energy.

#### 1.1.2.1. Wind energy

The change in the distance of the earth from the sun at any moment and the different heat balance on the earth affect the temperature, humidity and pressure in the air. In line with these variables, a reaction occurs in the air, the rotation of the earth can be interpreted as the air movement resulting from the temperature and pressure difference. (Bartik, 2018). We call this situation the wind. Wind Energy has emerged by taking advantage of the power of these air flow reactions. The process of utilizing wind energy, which dates back about 4000 years, has been used in processes such as moving ships with sails and grinding wheat. Today, this process is mostly used for electricity generation. Although this energy is used in many different ways, the wind turbine is used to convert this wind energy into motion energy and then to generate electrical energy. On the other hand, wind energy has a discrete and random nature, since the direction and speed of wind flow are variables depending on climatic conditions. In order to prevent the negative effects of this situation, blades and controllers are designed in different structures.

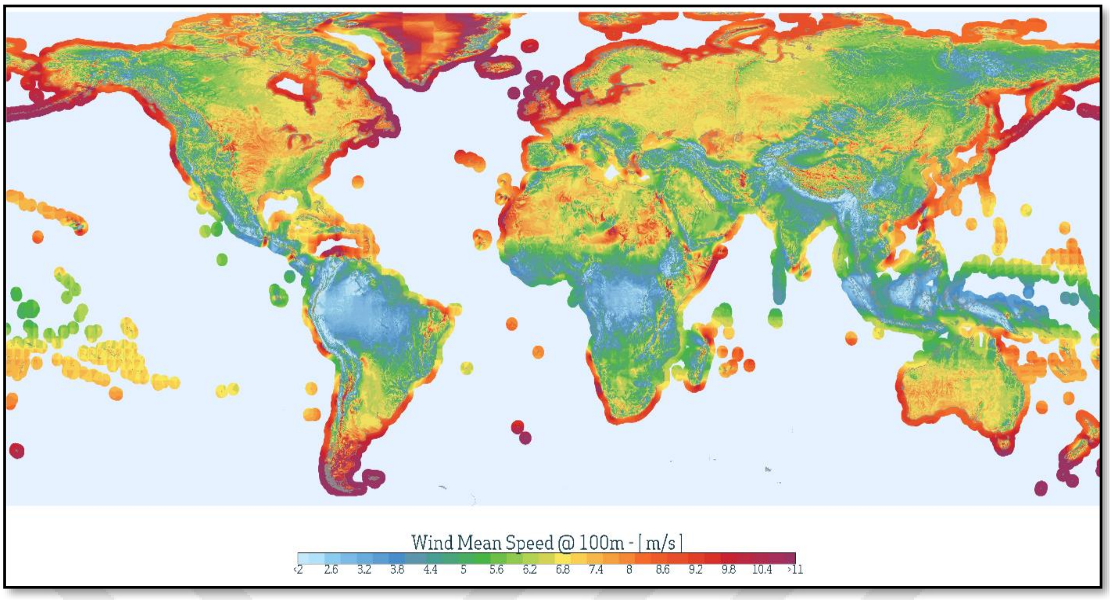


**Figure 1.3.** Atlas of world wind potential at 100 meters. (vortexfdc.com)

Undoubtedly, as long as the world exists, the wind will always exist actively on the world. There are two different approaches to the installation of wind power generation systems for the use of wind energy in electrical power generation. These are onshore installation and offshore installation. Although there are many onshore wind turbines today, offshore wind farms will increase rapidly in the coming years after it is seen that offshore wind farms are more efficient than onshore ones.

The wind potential is seen as the energy we will use the most in the future. When Figure 1.3 is examined, the wind energy potential of our world is quite high. The distribution of wind potential on the basis of regions in the world is shown in Table 1.10. North America (14000 TW/year) stands out as the region with the highest wind potential in the world.

**Table 1.10.** Annual wind potential power by continent.

| Region | Annual Wind Potential (TW/Year) |
|---|---|
| North America | 14,000 |
| Eastern Europe/Russia | 10,600 |
| Africa | 10,600 |
| South America | 5,400 |
| West Europe | 4,800 |
| Asia | 4.600 |

As of 2008, 440,000 people participated in wind energy employment. It is predicted that this number will be 1,500,000 people by 2024. According to IEA data, it is estimated that 18% of the world's electrical energy will be produced from wind in 2050. This shows that the current capacity will need to be increased approximately 8 times. Countries around the world continue to increase their wind energy production efforts. The amount of installed wind farm power capacity is given in some countries in Table 1.11. In this regard, China ranks first as the established power.

**Table 1.11.** Top ten countries by installed wind farm power in world.

| Countries | Production (TWh) | 2019(%) |
|---|---|---|
| China | 405.7 | 28.4 |
| US | 303.1 | 21.2 |
| Germany | 126.0 | 8.8 |
| United Kingdom | 64.1 | 4.5 |
| India | 63.3 | 4.4 |
| Spain | 56.2 | 3.9 |
| Brazil | 55.8 | 3.9 |
| France | 34.5 | 2.4 |
| Canada | 34.2 | 2.4 |
| Turkey | 21.7 | 1.5 |

With new investments and new projects, wind energy has consolidated its place in the edible energy sector. The Global Wind Energy Council (GWEC) estimates that about 344 GW of new onshore and offshore wind power capacity could be installed worldwide by 2020-2024, taking into account the impact of COVID-19. The total power of the installed offshore and onshore wind farms in the world in 2020 is given in Figure 1.4.

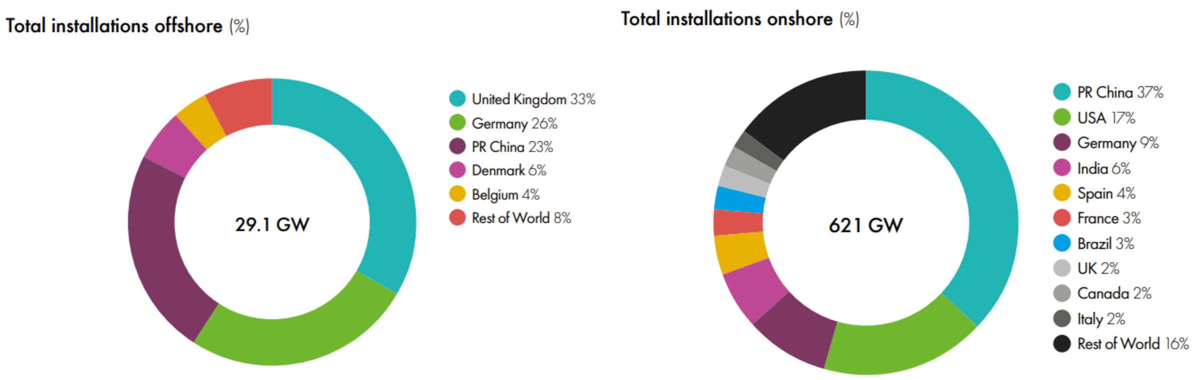


**Figure 1.4.** Total power of installed offshore and onshore wind farms in the world.

In our country, studies for wind and wind energy have started to be carried out since 1990. Strong winds blow from the sea to the land during the day because the seas warm up after the land masses during the day, and from the land to the sea because the land parts cool late at night. In our peninsular country, both land and sea have a very high wind potential. Our country, which has a coastline of 3,500 km, is in a very good state in terms of wind potential with these characteristics. The best wind resource potentials of our country are located near the coastlines, high slopes and mountain tops or near open areas. In Turkey, especially along the coast and in the mountains to the east, stronger wind speeds are observed in winter.

In 2006, an atlas of wind potential was created at the regional base of Turkey. REPA (Atlas Of Wind Energy Potential) is a wind atlas produced by running back three separate numerical weather analysis models with meteorological parameters realized for many years to cover all land and sea areas of the geography of Turkey and realized with advanced techniques. As seen in Figure 1.5 in this atlas, Turkey's medium-sized numerical weather forecast model and wind source information are given.

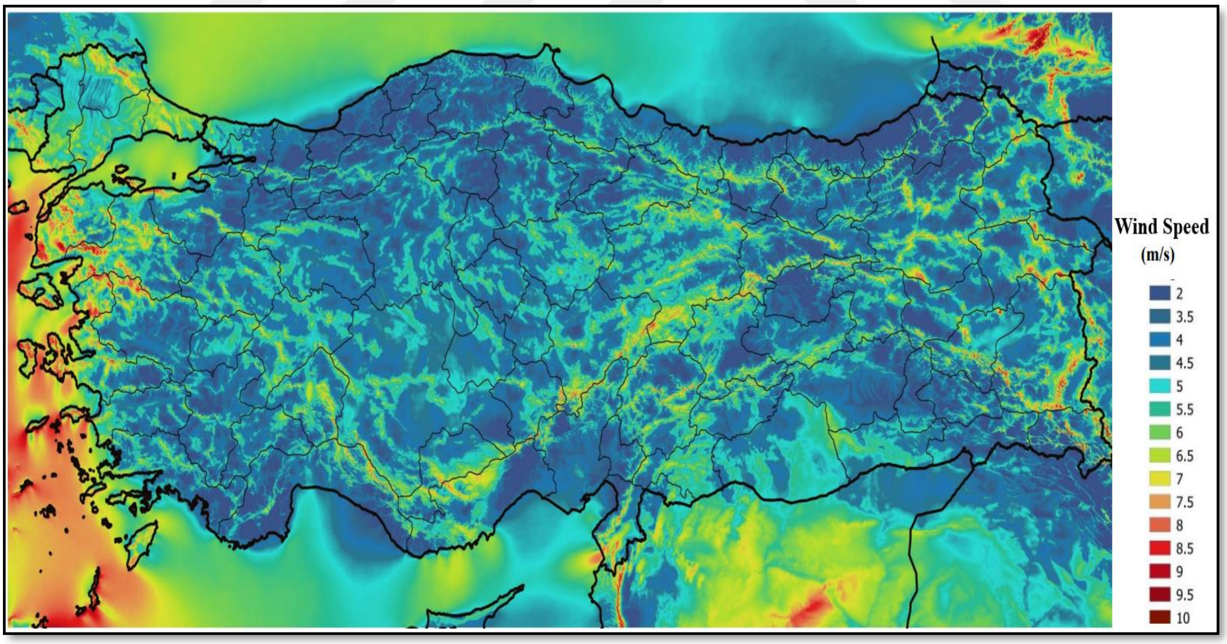


**Figure 1.5.** Atlas of Turkey wind speed potential at 100 meters.

The installed power of wind power shows the trend that has increased in the past day. In our country, the wind potential is technically known to be 48,000 MW. The area required to meet this potential is equivalent to 1.3% of the territory of our country. 5 MW power plants can be installed in places with a height of 50 meters and a wind speed above 7.5 m/s. Looking at the regional base in Table 1.12, our region with the highest wind potential is the Marmara region. The average wind power was 51.91 W/m$^2$, while the average annual wind speed was 3.29 m/s.

**Table 1.12.** Average wind power density and average annual wind speed by region in Turkey.

| Region Name | Average Wind Power Density (W/m$^2$) | **Average Annual Wind Speed (m/s)** |
|---|---|---|
| Marmara | 51.91 | 3.29 |
| Southeastern Anatolia | 29.33 | 2.69 |
| Mediterranean | 21.36 | 2.45 |
| Aegean | 23.47 | 2.65 |
| Black Sea | 21.31 | 2.38 |
| Central Anatolia | 20.14 | 2.46 |
| Eastern Anatolia | 13.19 | 2.12 |
| Average | 25.82 | 2.58 |

Over the years, wind power capacity in our country continues to develop by increasing. At the beginning of the 2000s, the power level of 19 MW increased to 9294 MW by 2019. Wind farms with the highest installed power in Turkey are given in Table 1.13 and the total number of wind farms is 268.

**Table 1.13.** The highest installed power capacity wind farms in Turkey.

| Power Plant Name | State | Power (MW) |
|---|---|---|
| Soma Wind Farm | Manisa | 288 |
| Karaburun Wind Farm | İzmir | 223 |
| Dinar Wind Farm | Afyonkarahisar | 200 |
| Geycek Wind Farm | Kırşehir | 168 |
| Balıkesir Wind Farm | Balıkesir | 143 |
| Osmaniye Gökçedağ Wind Farm | Osmaniye | 135 |
| Saros Wind Farm | Çanakkale | 133 |
| Kangal Wind Farm | Sivas | 128 |
| Şamlı Wind Farm | Balıkesir | 127 |
| Bergama Wind Farm | İzmir | 120 |
| Bilgin Enerji Soma Wind Farm | Manisa | 120 |

Wind energy is a clean, environmentally friendly, domestic and national resource that minimizes dependence on other countries that do not have short-term or long-term price imbalance that does not have raw material costs. Although the area where wind farms are established seems to require large land, the main covered by wind turbines is about 1-2%. The remaining 98-99% can be easily evaluated as an agricultural area. In addition, wind power plants do not harm the agricultural structure and provide job opportunities to the people living in the region where they are established. 14.200 people are employed in the wind sector in our country. Wind energy after hydroelectric power, Turkey has also managed to become the most important renewable energy source. However, in a country with a potential of 48,000 MW technically, the value of 9294 MW remains very low.

#### 1.1.2.2. Hydropower energy

The source of hydroelectric power is water. Hydroelectric power is a type of energy derived from the movement of water in the flow below a high point. This energy is produced by hydroelectric power plants and turned into a usable resource. It has been the most widely used type of energy in the world with the developments in its field during the past time. Especially its contribution to electricity generation is very important. The idea of obtaining high efficiency and storing water in hydroelectric power plants that control water power has allowed the emergence of large dams. Although power plants with turbines without dams placed on small canals and rivers have gained speed in recent years, countries with hydroelectric power plants with large dams can supply their energy needs for many years.

When we compare hydroelectric energy with other types of renewable energy in terms of cost and we can see that it is superior. Geographical location is an important element for hydroelectric power generation. High rugged and water-rich regions are advantageous for this energy. The amount of energy generation is determined by the flow and fall of the water. The energy yield of the water in the big river is more. Likewise, the energy level of the water with a higher height will also be higher. The potential energy in the stagnant water in the dams goes to the turbine through pipes or channels and is converted into kinetic energy by the movement of the water. The water reaching the propellers rotates the propellers connected to the generators and electrical energy is produced. The structure of a simple hydroelectric power plant is given in Figure 1.6.

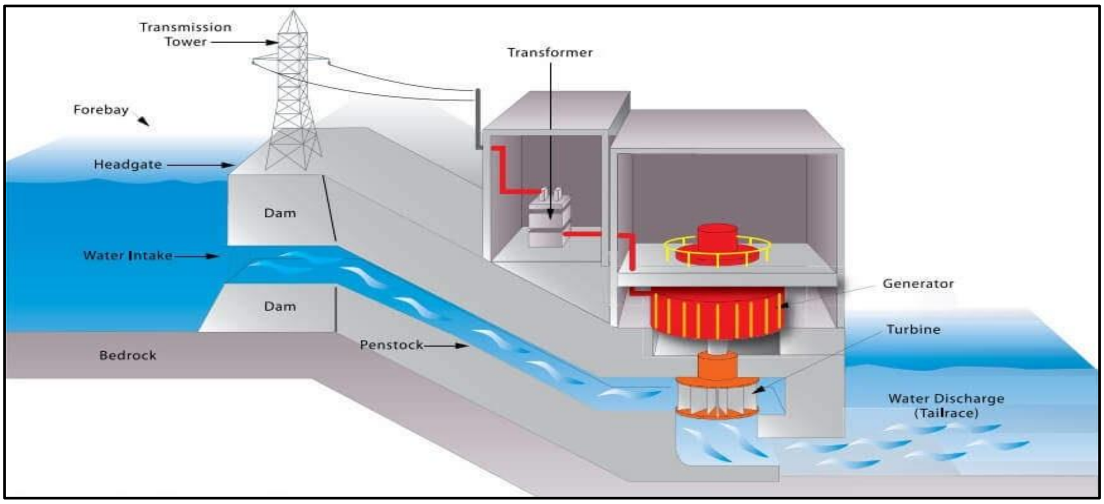


**Figure 1.6.** The structure of a simple hydroelectric power plant.

Approximately 20% (2,600 TWh/year) of the world's electricity consumption, which was 13,000 TWh/year at the beginning of the 2000s, was obtained from hydroelectric power plants. Of the 150 countries that benefit from hydraulic energy, 65 meet more than 50% of their electricity needs. and of these, more than 90% of 24 countries derive from hydroelectric power plants. By 2050, hydroelectric power is expected to reach 200 GW of global capacity and reach 700 TWh of energy. Hydroelectric energy constitutes approximately 17% of the world's electrical energy. Although the development phase of hydroelectric energy seems to have slowed down in recent years, an increase of 119 GW is expected by 2022 (Deniz, 2018). A large part of this share is formed by China, Brazil and Canada. About half of the world's hydroelectric production is concentrated in these three countries.

**Table 1.14.** The amount of electricity generated from hydroelectric power plants in some countries.

| Countries | Production (TWh) | **2019(%)** |
|---|---|---|
| China | 1269.7 | 30.1 |
| Brazil | 399.3 | 9.5 |
| Canada | 382.0 | 9.0 |
| US | 271.2 | 6.4 |
| Russian Federation | 194.4 | 4.6 |
| India | 161.8 | 3.8 |
| Norway | 125.3 | 3.0 |
| Turkey | 89.2 | 2.1 |
| Japan | 73.9 | 1.8 |
| Eastern Africa | 68.9 | 1.6 |

The fact that hydroelectric power plants are advantageous in many ways has increased the reasons for preferring these power plants. In terms of installation cost, we encounter a more economical cost table than all other power plants, except for natural gas thermal power plants. The most important reasons for this are that about 75-80% of the vehicle and equipment procurement process during the installation phase of these power plants can be met by domestic manufacturers. These power plants are more advantageous during the operation phase as well as during the installation phase. In addition, considering that a hydroelectric power plant has a minimum life of 75 years, it stands out with its long service life compared to other power plants (Koçak, 2011).

Our country is in a geographical position to be considered lucky in this regard. It has very important water basins in almost every region. Technically, Turkey ranks 2nd in Europe with 17.6%. Russia took first place in this category. As seen in Table 1.14, it is in 8th place in the world with a hydroelectric potential of 2.1%.

**Table 1.15.** The highest installed power capacity hydroelectric power plant in Turkey.

| Power Plant Name | State | Power (MW) |
|---|---|---|
| Atatürk Dam and HPP | Şanlıurfa | 2.405 |
| Karakaya Dam and HPP | Diyarbakır | 1.800 |
| Keban Dam and HPP | Elazığ | 1.330 |
| Ilısu Dam and HPP | Mardin | 1.209 |
| Altınkaya Dam and HPP | Samsun | 703 |
| Birecik Dam and HPP | Şanlıurfa | 672 |
| Deriner Dam and HPP | Artvin | 670 |
| Yukarı Kaleköy Dam and HPP | Bingöl | 627 |
| Beyhan Dam and HPP | Elazığ | 582 |
| Oymapınar Dam and HPP | Antalya | 540 |

The hydroelectric power plant in our country was built in Tarsus in 1902. Afterward, structures such as the Visera power plant in 1929 and the Ivriz power plant in 1940 were built. But the real acceleration took place after the 1950s. Sarıyar, Hirfanlı, Kesikköprü Seyhan dams and hydroelectric power plants were built. In the 1970s, the Keban dam and power plant were built. The breakthrough projects of the Republic of Turkey in the field of hydroelectric energy were also implemented with the GAP project. Today, there are 685 hydroelectric power plants in total. Total installed power of Hydroelectric Power Plants in Turkey is 31,346 MW. The hydroelectric power plants with the highest installed capacity in Turkey are given in Table 1.15. In 2019, 88 850 GWh electricity was produced with Hydroelectric Power Plants. This corresponds to 28 percent of the country's total electricity production. When the hydroelectric power plants are in the stage of installation, project and licensing, production will increase by 50 percent.

As a result of the researches, the hydroelectric potential of our country is 433 billion kWh. While the technically usable potential is 216 billion kWh, the economic potential is calculated as 140 billion kWh/Year (Doğan, 2019). When we turn this disadvantageous situation into an advantage, renewable energy power plants whose raw material is water will reduce the electrical energy production costs to a very low level and hydroelectric power plants will be the most important energy generating plants in our country.

#### 1.1.2.3. Biomass energy

Biomass energy is a source of energy that includes all kinds of substances produced by living organisms. It can be preferred due to sustainability, easy availability, environmental awareness and energy efficiency (Akdoğan, 2018).

The most commonly used materials as biomass fuel today are corn grain for etonel and soybean for biodiesel. Biological materials and wastes that absorb solar energy form the raw material for biomass, and the energy obtained from these materials is called biomass energy (Akdoğan, 2018).

When we look at renewable energy sources, biomass energy is an energy source that can be stored continuously and uninterruptedly. In addition, biomass energy is a type of energy that is environmentally friendly and has an economic impact on the region with its employment-increasing effect (Akdoğan, 2018).

Electricity generation from biomass energy sources is based on two basic principles. The first is the thermochemical transformation, the second is the biochemical transformation. The thermochemical conversion process consists of combustion, pyrolysis, gasification and liquefaction stages, while the biochemical conversion process can be staged as digestion and fermentation. Waste and biological resources as fuel sources are used in both processes. Biomass energy is the most used energy type in the world after oil, natural gas and coal. Biomass energy, which is used in many areas such as heating, energy and transportation, corresponds to 9.47% of the total energy consumed on earth. However, a significant portion of this amount, 4.33%, is used for heating purposes, especially in developing countries, by burning directly with classical methods. The remaining 5.14% is bioenergy produced using various conversion methods. The energy produced in this context is easily used in many areas of the industry instead of petroleum and its derivatives. The most common liquid biomass fuels are biodiesel and bioethanol. Gaseous biomass fuel is biogas. Solid forms are called biochar and bio-briquette. However, although there are many common types, when it comes to biomass energy, the most used ones are biodiesel and bioethanol. As can be seen from Figure 1.7, when we look at the installed capacity of biomass, China is first followed by Brazil and America.

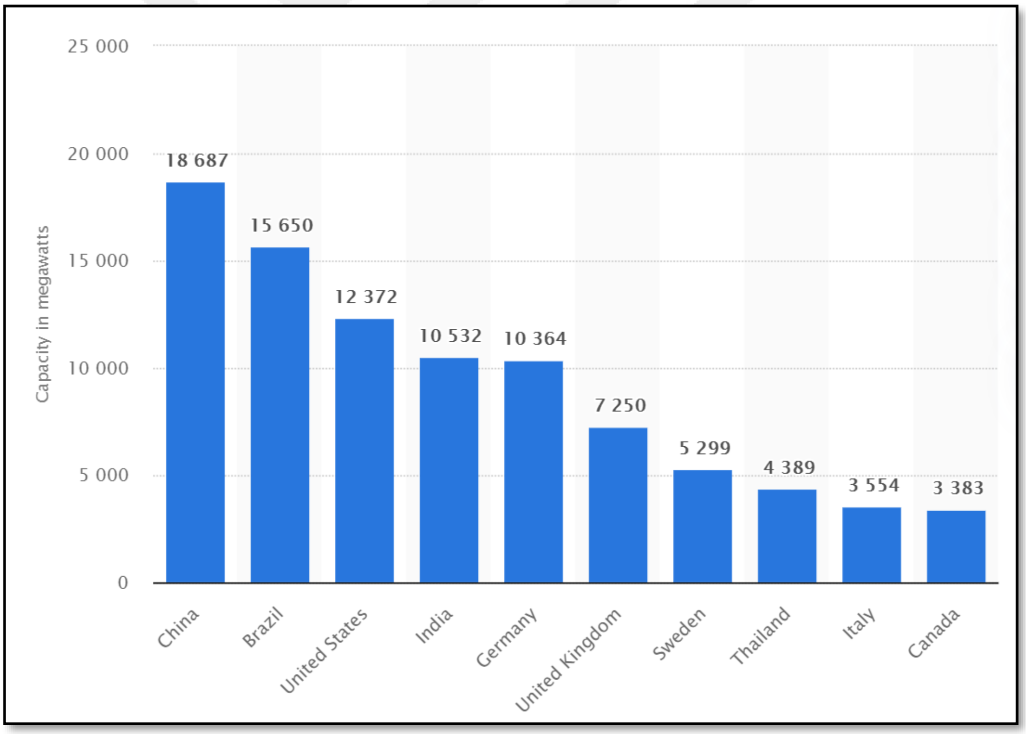


**Figure 1.7.** Top ten countries by installed biomass power plant in the world.

In parallel with the increasing interest in biomass energy in the world, investments in various energy production from biomass have increased in Turkey. It has been in high demand in recent years, especially in rural areas, as it accelerates socio-economic developments. When we look at the fields of biomass energy production and application in Turkey, we observe that there are various recycling methods of various wastes. As a result of these cycles, different fuels are obtained from each other. Generally, heat energy is produced from the products obtained. Heat energy is also converted into electrical energy. The total installed power of Biogas, Biomass, Waste Heat and Pyrolytic Oil Power Plants in Turkey is 1,144 MW. The biomass and landfill gas power plants with the highest installed capacity in Turkey are given in Table 1.16. In 2019, 4.266 GWh of electricity was produced with Biogas, Biomass, Waste Heat and Pyrolytic Oil Power Plants.

**Table 1.16.** The highest installed power capacity biomass and landfill gas power plant in Turkey.

| Power Plant Name | State | Power (MW) |
|---|---|---|
| Odayeri Landfill Gas Power Plants | İstanbul | 34 |
| Toros Tarım Samsun Waste Heat Plant | Samsun | 31 |
| Mutlular Biomass Power Plant | Balıkesir | 30 |
| ITC Antalya Biomass Power Plant | Antalya | 25 |
| Mamak Landfill Gas Power Plants | Ankara | 25 |
| Çadırtepe Biomass Power Plant | Ankara | 23 |
| Sofulu Landfill Gas Power Plants | Adana | 16 |
| Akçansa Çimento Waste Heat Plant | Çanakkale | 15 |
| Kömürcüoda Landfill Gas Power Plants | İstanbul | 14 |
| Eti Alüminyum Waste Heat Plant | Konya | 13 |

#### 1.1.2.4. Geothermal energy

Geothermal resource is a source of ground heat in a sense, and it is hot water, steam and gases containing dense minerals, formed by the heat accumulated in various depths of the earth's crust (Arslan, 2006). Geothermal energy is simply the internal heat of the earth. It has great potential especially in regions located on the tectonic belt. Porous, cracked rock masses underground form geothermal reservoirs by being fed by rain, snow, sea and magmatic waters. In short, the geothermal regions formed by the rising or removing of the water heated underground, actually emerge as a result of more complicated geological events. If rain and melting snow and underground water meet with the impermeable layer, they accumulate here. If these impermeable layers are near magma or an active volcano, they allow the accumulating water to heat up. If these heated groundwaters are in an active tectonic region, they can rise to the surface thanks to faults and fractures.

Geothermal energy is a renewable, sustainable and reliable energy source. Compared to today's renewable energy sources such as sun, wind, and waves, geothermal energy seems to have an attractive position due to its uninterrupted nature (Karagöl and Kavaz 2017). However, although it is defined as continuous and renewable, in order for this situation to be uninterrupted, the geothermal reserves formed by rain, snow, sea and magma waters feeding the porous and cracked rock masses underground depend on the continuity of the underground conditions. They are not affected by short-term changes in atmospheric conditions.

Geothermal fields are classified depending on their temperature. Although there is no precise classification range in the literature, they are classified as low, medium and high temperature sources with different approaches. They are classified as having a temperature lower than 100℃, those between 100℃ and 180℃, and those with a temperature higher than 180℃. Geothermal regions are generally not very common due to their presence in special geological environments. Only 5 percent of the world geographically has geothermal resources. The map shows the places in Figure 1.8 where active geothermal zones are present, which are spread along the borders of this plate.

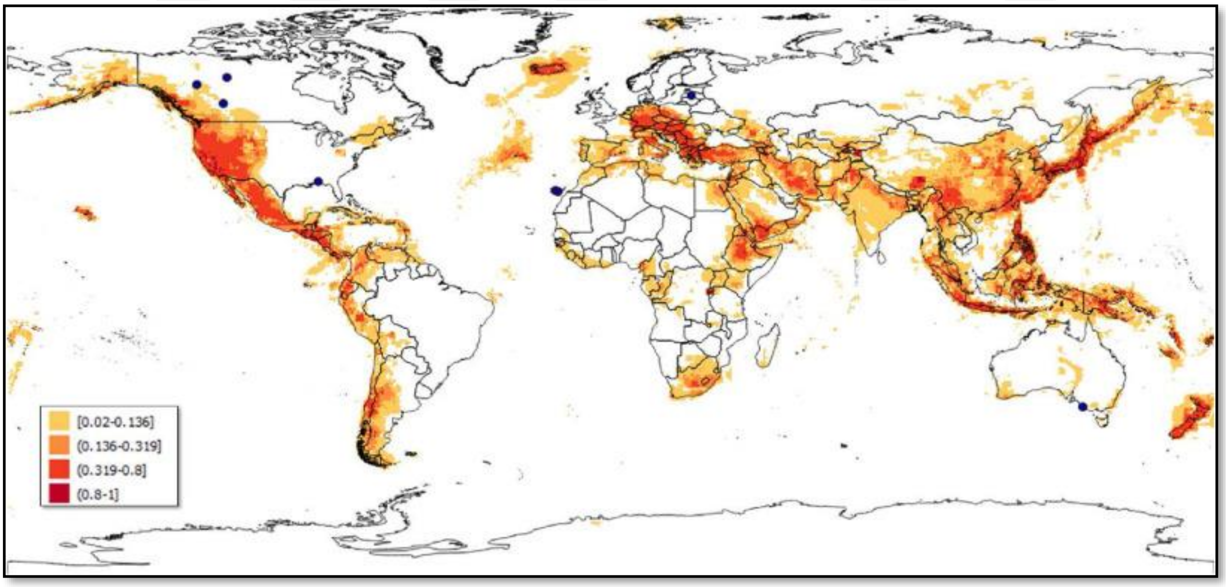


**Figure 1.8.** Map of geothermal energy sources in world. (Coro and Trumpy,2020)

From the past to the present, the main use of geothermal energy sources has been accumulated by natural or artificial methods in places such as hot springs or baths for health purposes.

Currently, geothermal energy is used along with many methods to obtain residential, greenhouse heating and electrical energy. Obtaining electricity at high enthalpy sites is the primary goal and the use of the source is possible with applications in other areas listed above. The best countries in electricity generation with the highest installed capacity of geothermal energy are given in Table 1.17. We see America in the first place by a wide margin. America is followed by Indonesia, Philippines and Turkey.

**Table 1.17.** Top ten countries by installed geothermal electric power capacity in world.

| Countries | Installed Power (MW) |
|---|---|
| US | 3.714 |
| Indonesia | 2.133 |
| Philippines | 1.918 |
| Turkey | 1.624 |
| New Zealand | 1.005 |
| Mexican | 963 |
| Italy | 944 |
| Kenya | 861 |
| Iceland | 755 |
| Japan | 603 |

Turkey is located above the system where there is an area with high geothermal potential called the ring of fire. For this reason, Turkey is one of the lucky countries in the world that can use geothermal energy. Turkey is a country rich in geothermal energy and ranks first in Europe and fourth in the world. Due to its tectonic structure, high-temperature geothermal fields are observed, especially in western Anatolia. In addition to the ongoing hot spring applications in our country, there are electricity generation, residential heating, greenhouse and industrial uses of geothermal resources. As Turkey is located on the Alpine-Himalayan belt, it is a country with significant potential for geothermal energy. The potential of our country in the geothermal field is theoretically estimated to be 31,500 MW. The highest installed power capacity geothermal electric power plants are given in Table 1.18 in Turkey.

**Table 1.18.** The highest installed power capacity geothermal electric power plants in Turkey.

| Power Plant Name | State | Power (MW) |
|---|---|---|
| Kızıldere 3 JEP | Denizli | 165 |
| Efeler JEP | Aydın | 115 |
| Kızıldere 2 JEP | Denizli | 80 |
| Pamukören JEP | Aydın | 68 |
| Mis 3 JEP | Manisa | 48 |
| Galip Hoca Germencik JEP | Aydın | 47 |
| Alaşehir JEP | Manisa | 45 |
| Maren JEP | Aydın | 44 |
| Dora 3 JEP | Aydın | 34 |
| Melih JEP | Aydın | 33 |

The total installed power of the Geothermal Power Plants in Turkey is 1,624 MW. In 2019, 10,060 GWh of electricity was produced with 60 Geothermal Power Plants. In our country, 78% of geothermal fields, especially potential areas, are located in western Anatolia, 9% in Central Anatolia, 7% in the Marmara region, 5% in eastern Anatolia, and 1% in other regions. 90% of our geothermal resources are low and medium temperature and direct applications (heating, thermal tourism, etc.s.) suitable for. The remaining 10% is suitable for indirect applications such as electric power generation.

#### 1.1.2.5. Wave energy

The oceans on earth are a great source of energy. The way to get this energy is by using Waves. The potential energy on the wave is converted into kinetic energy by the circular motion of the water bubbles. With the effect of wind, waves up to 50 meters can be formed in the high seas and a body of water with a lot of weight is displaced. Latitudes between 30-60 degrees on earth are suitable regions to take advantage of this natural event. It is a type of energy that is not very common compared to other types of energy. But it is suitable for countries where energy logistics are difficult, for example, island countries. However, facilities installed on the coast are damaged by the storms and their costs are increasing. Economically, this type of energy has not yet reached a level that can compete with fossil fuels. But in recent years, a rapid decline in the costs of these facilities has been observed. Companies target costs that can fall to less than 10 cents/kW h or even 5 cents/kWh during design. In this way, it allows wave energy plants to compete with other traditional power plants. In areas where the winds act strongly, it is more possible to use wave energy. These regions with high wind and wave potential are listed as follows on earth. The coasts of England are the coasts of South Africa, the coasts of North and South America and Australia.

There is no investment in marine energy production in our country. Although various studies and experiences have been made on this subject, no investment has yet been made in the commercial and industrial fields. In theoretical studies, it has been determined that our country carries very appropriate conditions in order to benefit from this type of energy. It has been determined that the most suitable region for the use of wave energy is the region between Izmir and Antalya. In addition, when we look at the provincial basis, our provinces such as Istanbul, Düzce, Bartın, Sinop, Kırklareli and Sakarya are seen as suitable places. In our country, which is surrounded by seas, it is necessary to increase the work on this environmental, cheap, energy source and reduce the cost. In our country, which has a wave height of approximately 1 meter, the energy obtained from this will greatly reduce our commitment to fossil fuels. Our country's offshore coastline is 8,210 km. However, it is not possible to evaluate all coasts in this way. But if 20% of the current coastline is evaluated, this is equivalent to annual energy of 18.5 TWh.

#### 1.1.2.6. Solar Energy

Solar energy is a kind of radiant energy. It is the energy released during the conversion of hydrogen gas in the sun's core to helium. Solar energy first entered our lives as heating energy, but today the uses of solar energy have become very diverse. There are situations where we benefit from solar energy in many areas of social life. But in the last 10 years, this solar energy has been used in electricity generation. Solar energy has emerged as a highly demanded resource in electrical energy generation in recent years. Electricity is produced with photovoltaic systems (PV) and concentrated solar energy systems (CSP). Radiation energy reaching our world is very important for electricity generation from these systems. The SI unit of irradiance is watt per square meter ($W/m^2$). The average annual solar radiation arriving at the top of the Earth's atmosphere is roughly 1361 $W/m^2$. The sun's rays weaken as they pass through the atmosphere, and when the sun is at the zenith in a cloudless sky, on a horizontal surface at ground level, the global radiation is about 1120 $W/m^2$. The atmospheric positions of the earth and the sun differ in terms of benefiting from solar radiation. In addition, sea level, water vapor level in the atmosphere, cloud cover and pollutant factors cause differentiation in this radiation level. Figure 1.9 shows a global map of global horizontal radiation. While the most ideal region in the world in terms of solar irradiation is the equatorial region, the Mediterranean climate zone comes second, which is in this climate zone in Turkey.

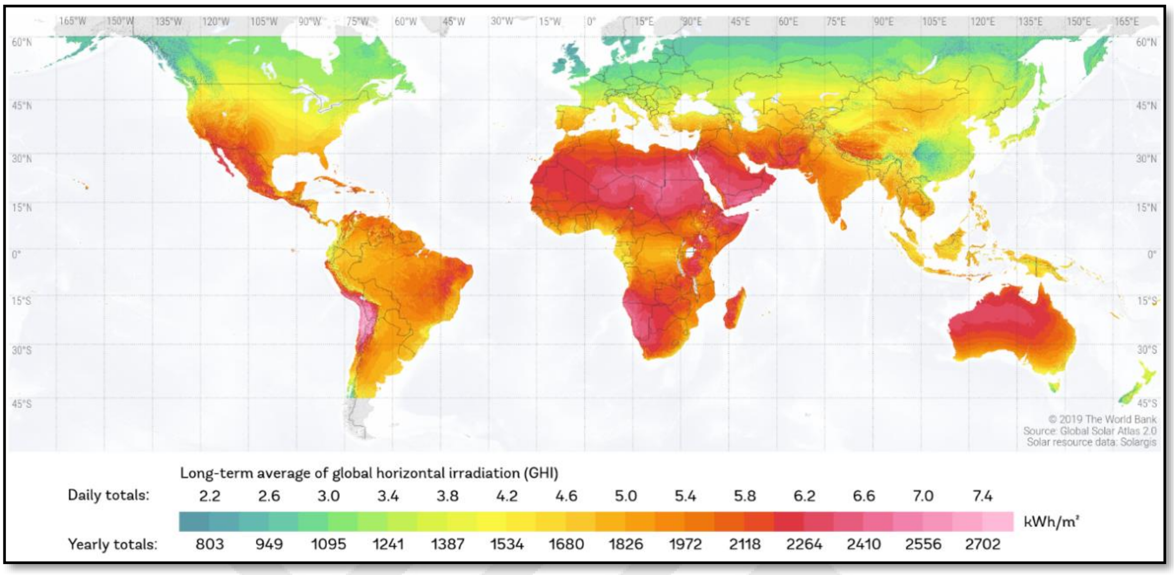


**Figure 1.9.** Global map of global horizontal radiation. (globalsolaratlas.info/download/)

Solar technology is predicted to constitute a significant part of future electricity generation systems. According to the amount of installed capacity, the solar energy sector is the fastest growing energy technology worldwide. The initial investment cost of solar energy systems seemed high. With the technological developments experienced, major developments in the PV sector and the decrease in the prices of PV modules made the unit price of electrical energy generated by these panels very low cost. In the past, the difference between the estimates of solar energy use and the actual number of uses was large, but in recent years this gap has closed. After the system was established, the operating cost is very low and government incentives ensured a rapid increase in the amount of installed power in this sector. Therefore, the cost of using solar energy in the long term may become more advantageous than other energy sources.

Especially in developed countries, solar panels consisting of photovoltaic (PV) cells that can generate electricity directly from solar energy are widely used. Countries with a high share of solar energy in renewable energy use are given in Table 1.19. When we look at these countries, we see that European countries are predominant. Europe provides 20% of all its energy needs from renewable energy. The country with high solar energy use is seen as Norway with 97%. It provides 80% of all energy needs from renewable energy. Although these countries are not as suitable as equatorial countries in terms of climate, it is noteworthy that they rank first. We can say that Europe's clean energy policy and state supports are effective in solar energy use.

**Table 1.19.** The share of solar energy in renewable in electricity production in some countries.

| Countries | 2019(%) |
|---|---|
| Norway | 97.6 |
| Brazil | 82.3 |
| New Zealand | 81.9 |
| Venezuela | 73.7 |
| Colombia | 72.6 |
| Canada | 64.9 |
| Sweden | 58.7 |
| Portugal | 55.0 |
| Chile | 45.1 |
| Turkey | 44.2 |
| Germany | 41.2 |
| Romania | 41.2 |

Table 1.20 shows the share of the total energy obtained from solar energy in the world among states. China takes first place with 30.9%, followed by the United States, Japan and Germany, respectively. The high population of China and especially the air pollution caused by the industry have led to electricity from solar panels. In European countries, Germany takes the lead. 6.6% of the electricity produced from solar energy in the world belongs to Germany.

**Table 1.20.** The amount of electricity generated from solar panels in the world.

| Countries | TWh | 2019(%) |
|---|---|---|
| China | 223.8 | 30.9 |
| US | 108.4 | 15.0 |
| Japan | 75.3 | 10.4 |
| Germany | 47.5 | 6.6 |
| India | 46.3 | 6.4 |
| Italy | 24.3 | 3.4 |
| Australia | 18.0 | 2.5 |
| Spain | 15.0 | 2.1 |
| United Kingdom | 12.7 | 1.8 |
| Mexico | 12.4 | 1.7 |
| South Korea | 12.1 | 1.7 |
| France | 11.7 | 1.6 |
| Turkey | 10.9 | 1.5 |

In this Table 1.20, it is seen that developed countries are included, and Turkey is the developing country. Turkey is shown among the countries with rich resources in terms of current solar energy. Our country's annual sunshine duration has been determined as 2737 hours. This corresponds to approximately 7.5 hours on a daily basis. If we consider the energy from the sun on a daily basis of 1527 kWh / m², it has become 4.2 kWh / m², as it can be seen in the figure, the solar potential decreases as it moves from south to north in our country. Except for the northern parts of Turkey, a very intense solar energy potential is observed. The Black Sea region appears to be our region with little potential to benefit from the sun due to the high number of rainy days due to its location. The regions that turn from yellow to red are the regions where the sun's rays are most efficient and where the energy potential is high. As can be seen, when Figure 1.10 is examined, the Southeastern Anatolia region is seen as the region where the highest solar energy can be used and the Mediterranean region is seen as the second.

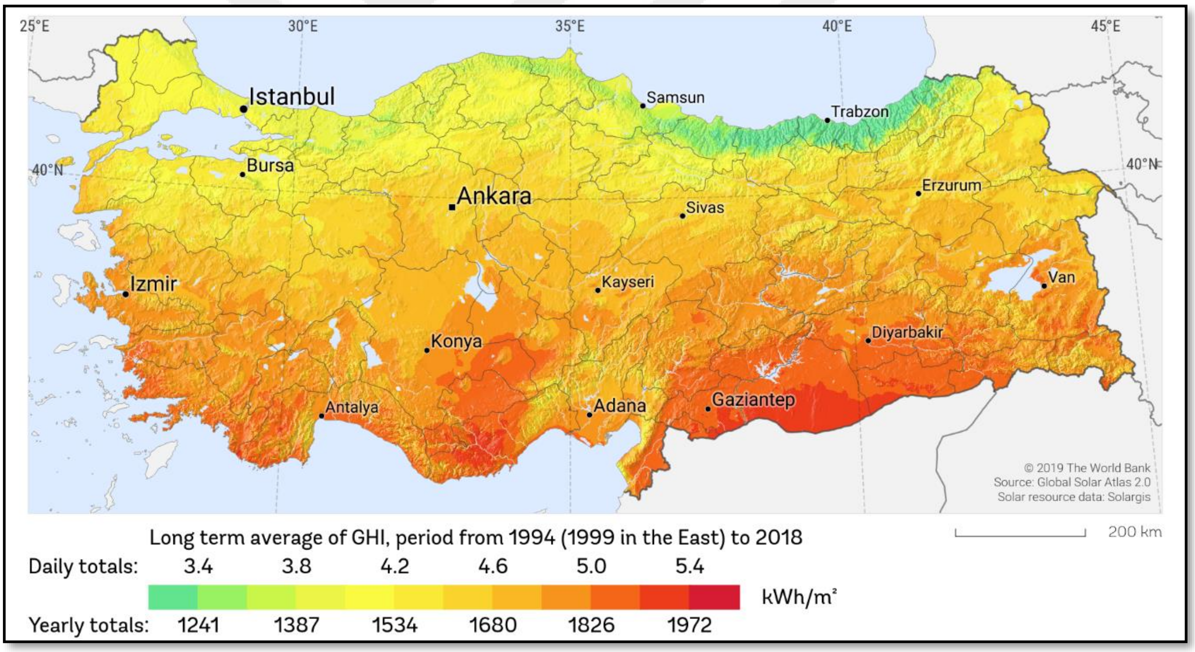


**Figure 1.10.** Turkey's solar energy potential atlas. (globalsolaratlas.info/download/)

The active use of solar energy systems in our country dates back to the recent past. Until 2010, it appears as thermal solar systems on roofs, mainly as an individual water heating system. After 2010, legal regulations paved the way for solar energy electricity generation and from that date studies started for electricity generation. While only power plants with an installed power of more than 1MW were allowed in the first stage, as a result of legal regulations, solar power plants established in our country were separated as unlicensed and licensed. Power plants with power below 1 MW can produce without a license for licensed production, all renewable energy resources in Turkey are subject to licensing conditions. While our installed power was 0 in 2013, 6.9% of Turkey's electricity was provided by solar energy in November 2020 and reached 6.185 MW.

**Table 1.21.** Solar power plants with the most installed power in Turkey.

| Power Plant Name | Province | Installed Power (MW) |
|---|---|---|
| Karapınar YEKA-1 | Konya | 1000 |
| Naturel & Esenboga Enerji | Ankara | 118 |
| Kayseri OSB | Kayseri | 50 |
| Özkoyuncu Madencilik Balıkesir | Balıkesir | 40 |
| Teksin Enerji | Karaman | 33 |
| Cıngıllı | Niğde | 26 |
| Fernas 4 | Burdur | 20 |
| Küçükköy | Antalya | 19 |
| Alibeyhöyüğü | Konya | 18 |
| Konya Karatay Kızören | Konya | 18 |

Solar power plants with the highest installed capacity in Turkey are given in Table 1.21. It is seen that solar power plants are mostly established in the inner Anatolia and the Mediterranean region. The reason for being installed in these regions is that the solar panels are close to the optimum temperature values in electricity generation and they make use of the flat, arid land in these regions instead of agricultural land.

# 2. LITERATURE REVIEW

In MATLAB /Simulink, a PV panel power system connected directly to the electrolysis cell was applied for hydrogen production. Only theoretical and simulated, the experimental part was not done. Alkaline electrolysis, a more common method for obtaining hydrogen from water, was preferred. Electrolysis I-V curve, radiation-current curve and radiation-voltage curve were extracted in MATLAB/Simulink using temperature and radiation from New Zealand meteorological data. Overall electrolyzer efficiency of 68.48% for summer and 63.32% for winter agrees with results provided in the referred published articles. (Martinez and Zamora, 2018)

A mathematical model was implemented to determine solar radiation due to the shortage of measurement stations in Egypt. The values obtained in this model have been compared with previously obtained global solar radiation data and their accuracy has been confirmed. The solar radiation obtained as a result of the experiments was used for hydrogen production from the PV panel and PEM electrolysis system modeled in MATLAB. Thanks to this model, hydrogen production has been increased and the experimental results are shared. (Tamer M. Ismail et al, 2019)

In another study, a system consisting of a PV panel, electrolyzer and hydrogen tank was established. Each stage of this system is modeled in MATLAB/Simulink. It consists of short circuit current 5 A and open circuit voltage 22.1 V PV panel, 500 W electrolyzer and 3 $m^3$ hydrogen tank. According to the temperature and radiation inputs, the hydrogen amount and hydrogen tank pressure graphs per second are shown. The amount of hydrogen obtained per second is given as 3.6 moles. ( Mustafa A. Al-Refai , 2014)

A hydrogen charging station has been simulated for electric vehicles with fuel cells. Fuel stations produce hydrogen using the alkaline electrolysis method with the power obtained from the solar panel and wind turbine hybrid system and store them in a tank. This hybrid system is designed as 12 kW wind turbine 18 kW solar panel in MATLAB/Simulink. In addition, electrolysis and tank parts were simulated, and the effect of temperature on hydrogen flow and Faraday efficiency was observed. In order to obtain the best efficiency, different currents, temperatures and scenarios are tested and presented in a comparative table. In the shortest time, the greatest amount of hydrogen was obtained at a temperature of 40 ℃ and a current density of 100 mA $cm^{-2}$. (Pei-Hsing Huang et al, 2016)

Polymer Electrolyte Membrane electrolysis method with solar energy was used to produce hydrogen. The system created was analyzed under different loads, ambient conditions and seasons. First, the electrolysis part of the system was developed in MATLAB and the power part was tested in the TRNSYS environment. The simulation data obtained are almost exactly compatible with the experimental part. The amount of hydrogen obtained is graphically shown at what times of the day and in which seasons of the year. From March to October, the system is able to perform electrolysis directly connected to the solar panel without the need for any electronic equipment. In summer, the system produces from 5 am to 8 pm during the day, and from 10 am to 5 pm in winter. It has been observed that hydrogen production is difficult without an auxiliary power supply during the winter months. The simulation and experimental parts were carried out successfully and became exemplary study for larger projects. (Seyedmehdi Sharifian at al, 2019)

The electrochemical and thermal parts of a 200 kW alkaline electrolysis were modeled in MATLAB/Simulink. There are two stacks and each stack contains 90 electrolyzer cells. First, the mathematical formulas of the electrochemical part are explained and in the simulation part, cell voltage, thermoneutral voltage, Faraday efficiency, general efficiency of the system and hydrogen production amount are obtained. The hydrogen flow rate is 0.65 $Nm^3$/sec per stack for an electrolyzer stack current of 725A. It is quite obvious that hydrogen production will be increased as electrolyzer current increases. In the thermal part, the heat generation, heat loss and auxiliary cooling requirements in the system were examined and modeled. It has been observed that the amount of heat does not increase much during the operation of the system and works stably. All the data obtained are given in the graphic and the time is set as 24 hours to make the simulation realistic. In addition, this modeling is designed to be integrated with other renewable hybrid systems. (Md. Maruf-ul-Karimand and M. T. Iqbal,2019)

In this study, the effect of shading on production was demonstrated by using four different electrodes. These studies focused mainly on electrolysis in cells with a fluctuating power supply. The reaction of the cell is analyzed by monitoring the voltage, temperature and pressure, current efficiency, time variations in oxygen, and hydrogen concentration. The best performance has shown the Cu/NiMo electrode. 40% of the produced energy was used in hydrogen production and the residue energy was stored. Results showed that the most effective electrode was Cu/NiMo according to Cu, Cu/Ni, and Cu/NiBi, and the highest hydrogen production was achieved for both electrodes on 23.09.2018. The obtained hydrogen gas was 8.18 L per $cm^2$ cathode surface, on September in the region of Adana under 50% partial shading condition in case of Cu/NiMo electrode was used so if we obtained experiments with 1 $dm^2$ total electrode area and predicted approximately 60% total efficiency for whole system steps. ( Başak Doğru Mert at al, 2019)

The novel solar-wind integrated system has been firstly used for hydrogen production in literature with validating theoretical, simulated and experimental studies. This integrated system consists of two main parts; a solar-assisted wind turbine and an alkaline electrolysis cell. In the first part of this system, the semi-flexible PV panels are smoothly integrated on the vertical axis wind turbine blade. This is a unique design in literature, unlike the hybrid systems that include wind turbines and solar PV panels in published literature. The second part includes hydrogen production via an alkaline electrolysis system. The cathodes consist of nickel coated copper (Cu/Ni) and nickel-vanadium binary coated copper (Cu/NiV), that was produced via electrodeposition technique by self-supporting. The performance of electrodes was compared in 1 M KOH solution via I-V behavior, electrochemical impedance spectroscopy, and long term cathodic polarization analysis. Results showed that polarization resistance was decreased almost 4 times by NiV when comparing the Ni. The surface inhomogeneity values were 0.91 and 0.81 for Cu/Ni and Cu/NiV respectively. The hydrogen gas evolved at the cathodes was also measured and higher volumes were detected for NiV binary coating. (Tuğçe Demirdelen at al,2020)

In this study, the proton exchange membrane electrolyzer was developed for separating the water into hydrogen and oxygen gas. The set-up is powering the electrolyzer with a small PV solar panel that produces 2 V and 1 A. The hydrogen was produced and stocked into the tank. The mathematical model of the electrolysis, DC/DC buck converter, PV panel has been implemented in MATLAB/Simulink. The amount of hydrogen that is obtained from the simulation is 7.461 mL/min, and the value from the experiments amounts to 7.0 mL/min. The discrepancy is depending on the weather such as cloud and the sun variability, In addition, the hydrogen production depending on the current and power is shown in the graph and it is observed that it is linear. (Mohamed Albarghot and Luc Rolland,2016)

A mathematical model for an advanced alkaline electrolyzer has been developed based on a combination of fundamental thermodynamics and empirical electrochemical relationships. The model shows that the electrochemical part of the model accurately predicts the cell voltage, hydrogen production, and efficiencies The results show that several improved electrolyzer operating strategies can be identified with the developed system simulation model. The modeling outcomes of this system were performed using MATLAB code. Simulation studies were carried at different temperatures. The highest operating cell voltage occurs at 40°C, while the lowest occurred at 80°C with the cell voltage of 2.395 V and 2.359 V respectively. the hydrogen flow rate observed at different temperatures. There is no significance change in hydrogen flow rates at these temperatures. ( Alhassan Salami Tijani at al,2014)

In this study, the effects of which are compared on hydrogen production using different renewable energy methods, a 10 kW alkaline electrolyser model was used. It is based on combination of empirical electrochemical relationships, thermodynamics, and heat transfer theory. The nominal power values of solar, wind and hybrid systems are 12.1 kW, 11 kW and 16.1 kW respectively. Solar radiation, wind speed and ambient temperature were used as inputs. Using only the solar panel, the hydrogen production rate is 0.0076 mol/s and the hydrogen produced is 4592 moles. Using only wind turbine, hydrogen production rate is 0.0137 mol/s and produced hydrogen is 8297 mol/s. In the hybrid system consisting of a wind turbine and solar panel, the hydrogen production rate is 0.0173 mol/s and the hydrogen produced is 10462 moles. When Faraday efficiencies are compared, it is seen that the hybrid system gives the best result with 0.8568. (A. Khalilnejad and G.H. Riahy ,2014)

In this study, a new MATLAB/Simulink model was developed to analyze large-scale electrolysis models by simplifying them. Alkaline electrolysis and proton exchange membrane electrolysis were used in the study. While performing the simulation, the lookup table was taken as a reference and thus the simulation time was reduced from 142 seconds to 125 seconds. Also, by improving the DC / DC converter used in the system, ripple content decreased from 6.65% to 5.6%. According to the reference model, the normalized square root error in current values passing through the electrolysis cell is 0.975 at 80 degrees Celsius and a value close to 1 indicates a good result. When looking at the current-voltage graph in the literature and in the compared model, successful results are seen. (David Martinez and Ramon Zamora,2019)

Kim Hoong Ng et al. (2020) claim that solar powered photocatalytic water splitting is a practically impossible way of using both thermodynamic and solar energy to intentionally generate $H_2$. They say photocatalytic water splitting, which has been widely studied for $H_2$ production, does not promise to be used commercially with its low solar to hydrogen (STH) efficiency (<10%) and high cost of hydrogen (> 2-4 USD/kg). Although the problems have been overcome, it is impossible to outperform the thermodynamic hurdle of 18% STH as it often needs to be greater than 2.0 eV for significant water splitting. Photon energy losses are inevitable during mid-medium transfer in photocatalytic water splitting, and therefore sacrifice yields the best STH of only 3.32% even in the presence of reagent.

D.Martinez and R.Zamora (2017) discussed the application of a MATLAB/ Simulink/Simscape power system of an alkaline electrolyzer directly coupled to a photovoltaic module. They added a variable input to measure the response of the models to temperature and a variable resistor for the PV module. They observed that the voltage variation for certain temperatures did not affect the PV module acting as a current source proportional to module heating. The amount of electrical energy entering the system changes seasonally. There was more electricity input in the summer than in the winter. The efficiency of the electrolyzer is higher in the summer months.

M. Temiz and N. Javani (2018), floating photovoltaic systems with integrated hydrogen production units, as used in Turkey's Aegean Mumcular investigated with electricity demand data received from the Dam. They have used PvSyst and HOMER Pro software programs. The hydrogen produced was used to meet electricity needs when solar energy was not available in the fuel cell's generator, the land was saved, the damage to the environment was reduced. The system is commercially available. The fuel cell generator that produces and stores hydrogen has proven to be a good alternative and greatly reduces unmet electricity in the floating PV system.

The authors looked at hydrogen production in NaOH electrolyte of different concentration using zinc alloys. During hydrogen production, Zn90%Co10%, Zn95%Fe5%, Zn95%Cu5%, Zn90%Cr10% , Zn85%Cu15%, Zn95%Co5%, Zn85% Fe15%,Zn90%Cu10%, Zn95%Cr5%, Zn90%Fe10% was used as cathode at different mass alloy ratios. During the experiment, the effects of different current values, different voltage values and electrolyte concentration were observed. The highest efficiency reached 6mL hydrogen in 154 seconds at 5V, 0.45A with the Zn95%Cr5% electrode.

R. Solmaz (2004), bare and nickel-plated silver, brass and steel electrodes with different metal compositions, hydrogen gas evolution in acidic and basic environments was investigated. For this purpose, cathodic polarization curves and Nyquist curves at different potentials where hydrogen output occurs were obtained by using three electrode techniques. Electrolysis method was used to determine the hydrogen overvoltages of these electrodes. In addition, the volume of hydrogen gas released at the cathode was measured by applying a constant 5 V potential to the system. From the obtained results, it was determined that the hydrogen overvoltage decreased in nickel-coated electrodes.

M.E. Mert (2005), nickel-plated silver, copper and zinc electrodes in the basic environment hydrogen gas evolution was investigated. For this purpose, cathodic polarization curves and Nyquist curves at different potentials where hydrogen output occurs were obtained by using three electrode techniques. Electrolysis method was used to determine the hydrogen overvoltages of these electrodes. The volumes of hydrogen gas released at the cathode were measured by applying a constant 3 V potential to the system. From the obtained results, it was determined that the hydrogen overvoltage decreased in nickel-coated electrodes.

R. Solmaz and G. Kardaş (2007) investigated the catalytic effects of uncoated brass and Ni, NiZn, NiNiZn coated brass electrodes on hydrogen output by electrolysis in 1 M NaOH solution, current-potential curves and EIS measurements. The stability and corrosion resistance of the electrodes for 240 hours were determined. They determined that the zinc-removed NiZn coating was highly effective for HER. The catalytic effect of the electrode, its stability over time and corrosion resistance increased with the coating of a thin Ni film under the NiZn coating.

# 3. MATERIALS AND METHODS

## 3.1. Theoretical and simulation part

In the theoretical part, the experimental system parameters were simulated by MATLAB/Simulink. A module with experimentally used photovoltaic panel, DC-DC converter and electrolysis system features was created in a simulation environment. With this simulation, it is aimed to see the effect of different irradiations, temperatures and sizes of the electrodes used on hydrogen production. In addition, the basic relationship between current and cell voltage, reversible voltage, thermoneutral cell voltage, Faraday efficiency, energy efficiency and cell temperature can be calculated.

### 3.1.1. Photovoltaic panel and converter

#### 3.1.1.1. Photovoltaic panel

The solar cells inside are made up of semiconductors that convert the sunlight falling on them into electricity. Photovoltaic systems can convert sunlight directly into electrical energy. The working principle of the semiconductor material used is that light photons coming to the cell surface remove electrons and move these electron particles in the outer environment. Light enters a photovoltaic cell, revealing enough energy to activate electrons. This energy allows electrons to generate as much voltage as they can generate an electric current (Sick and Erge, 1996).

Solar panel cells are generally formed by combining N-type and P-type semiconductors. As seen in Figure 3.1, photons from the Sun hit the PV cell surface and set free electrons in motion. At this point, the system works and electricity is generated. Silicon, which is an important material in semiconductor production in electronics, is also one of the most common raw materials of solar cells. N-type and P-type semiconductors are formed by adding a very small amount of VA or IIIA group elements in the periodic table to the element silicon.

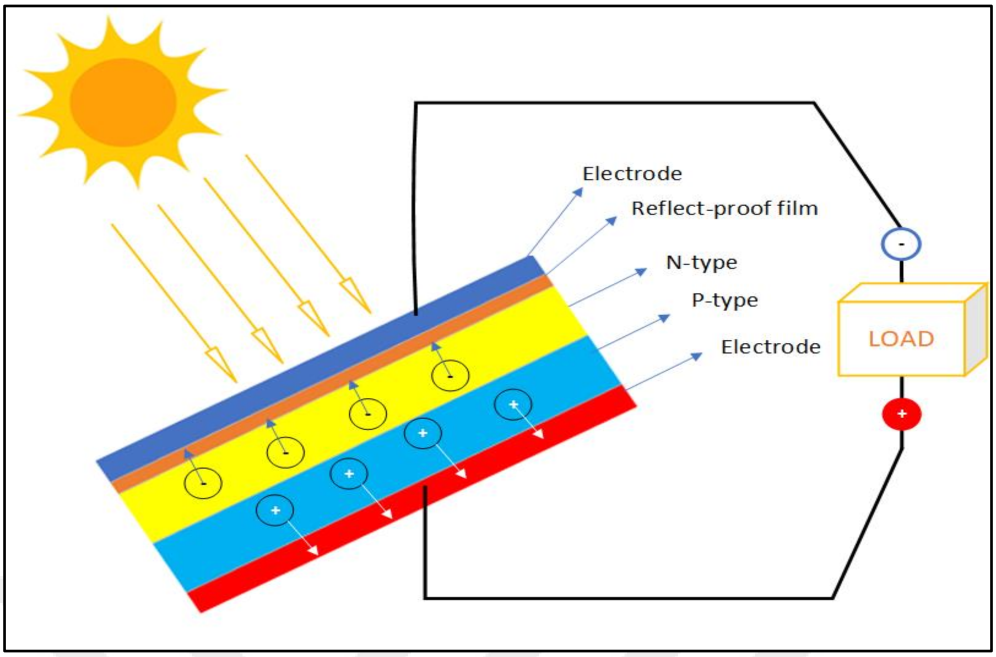


**Figure 3.1.** Solar cell structure.

N-type semiconductors; It is formed by adding the VA group elements to the IVA group semiconductors in a very small amount. Generally, silicon or germanium elements from the IVA group are used. However, silicon element is preferred most of the time. It is formed by adding the elements phosphorus, arsenic, bismuth and antimony from the VA group. Most of the time, the element phosphorus is used.

In P-type semiconductors, IIIA group elements are formed by adding very small amounts to IVA group elements. It is formed by adding elements such as boron, aluminum, gallium in IIIA group to silicon (Si) or germanium (Ge) in the IVA group. These semiconductors are brought together and the result is a solar cell.

Electricity generation from solar energy, like other renewable energy sources, was more expensive than electric energy produced from fossil sources. Due to high production costs, it has been used very little until recently. However, a decrease in costs is observed with the development of new production panels and storage systems with the developing technology. While the cost per watt of a solar cell panel was about 7.5 USD in 1990, this figure decreased to about 4 USD in 2005. By 2020, the cost of solar panels is 0.25 USD per watt.

The PV panel is one of the most crucial components of solar energy systems. It produces energy by absorbing sunlight with photovoltaic cells, generating direct current (DC) energy. Solar PV panels are constituted by an array of solar PV cells. The simplest one diode model of a PV cell equivalent circuit model is represented in Figure 3.2.

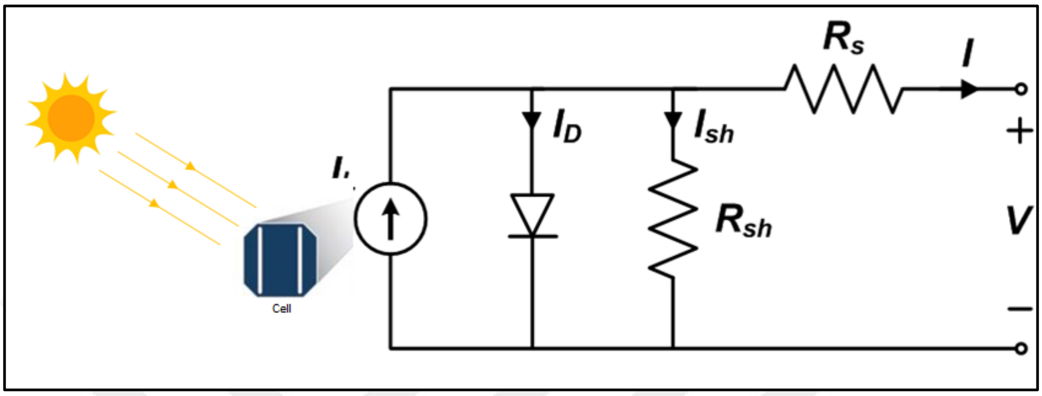


**Figure 3.2.** Equivalent circuit of solar PV cell.

In order to draw the I-V curve and P-V curve of a PV panel at any temperature and radiation, five basic parameters must be known. The parameters of an equivalent circuit of a PV are the open-circuit voltage ($V_{oc}$), the short-circuit current ($I_{sc}$), the maximum voltage ($V_{max}$), and the maximum power point (MPP). It is shown in Equation (1) that the current (I) is obtained by applying Kirchhoff's Current Law to the circuit.

$$I = I_L - I_D - I_{Sh} \qquad (1)$$

The $I_L$ current varies depending on the level of solar radiation to which the solar cell is exposed. The current passing through the diode ($I_D$) is the most important parameter in shaping the I-V characteristic of the PV cell. $I_{Sh}$ represents the shunt branch current. $I_{Sh}$ is obtained by applying Kirchhoff's Voltage Law to the circuit. The substitution of the related expressions for the shunt branch current $I_{Sh}$ and diode current $I_D$ in Equation (2) yields the following:

$$I_D = I_L - I_0\left[\exp\left(\frac{V+IR_S}{\frac{nkT_C}{q}}\right)-1\right] - \left(\frac{V+IR_S}{R_S}\right) \qquad (2)$$

$I_L$ represents the solar radiation current in Equation (3) and is a function of solar radiation at cell temperature.

$$I_L = I_{scR}\frac{G}{G_r}[1+\alpha_t(T_c - T_{cR})] \quad (3)$$

The current $I_0$ is the saturation current in Equation (4) and is called a function of the cell temperature.

$$I_0 = I_{0R}(\frac{T_c}{T_{cR}})\exp\left(\frac{1}{T_{cR}} - \frac{1}{T_c}\right)\frac{qe_g}{n_k} \quad (4)$$

where, $I_{0R}$ is the reverse saturation current of the cell at the reference temperature and solar irradiation. $e_g$ is the band gap energy of the semiconductor used in the cell ($e_g$ = 1.12 eV for the polycrystalline Si) at 25 C.

The output power of such PV systems can be calculated by Equation (5).

$$P_{PV(t)} = H_t(t) \times PVA \times \mu_c(t) \quad (5)$$

$H_t$ is the annual average solar radiation without shading. PV is the performance ratio and the loss coefficient varies between 0.5 and 0.9. The default value is 0.75.

#### 3.1.1.2. Types of solar panels

Solar panels, which are one of the most basic materials required to benefit from solar energy, are available in many different types. As shown in Figure 3.3, solar cells come together to form modules, and modules come together to form arrays.

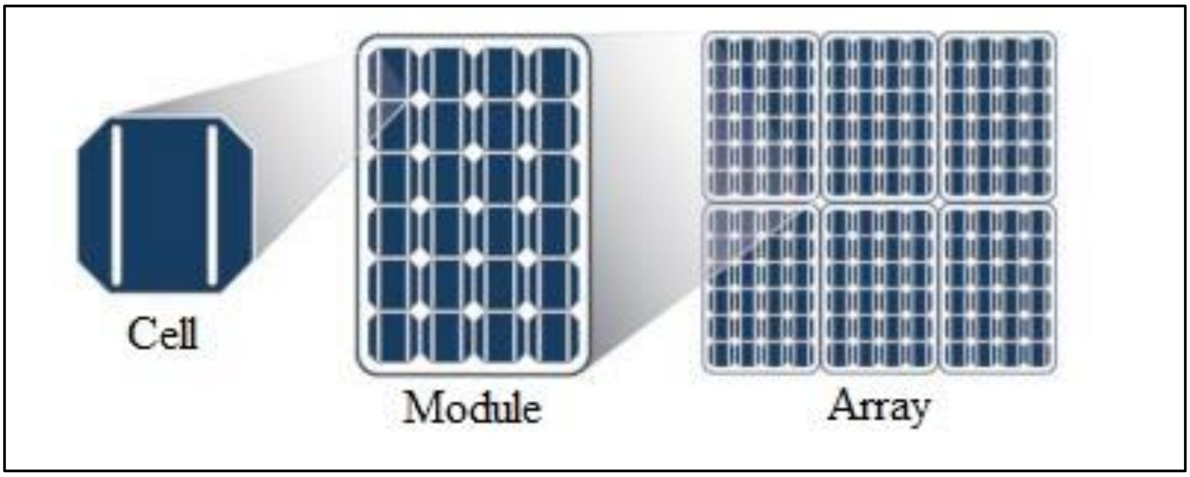


**Figure 3.3.** Solar cell, module and array structures.

Silicon is mostly used in the production of solar panels. There are many reasons why the element silicon is frequently used in solar cell production. These reasons; This is due to the fact that solar panels have a longer usage and electricity production life and that silicon can maintain its electrical, structural and optical properties for long periods of time. If we look at the types of solar panels, we first come across four types of panels. These are monocrystalline, polycrystalline, thin-film and flexible panels.

#### 3.1.1.2.1. Monocrystalline

The most efficient solar panel among solar panel types is monocrystalline. This type of solar panel generates great energy in a small space. Monocrystalline silicon based solar cells have excellent efficiency in converting light energy into electrical energy. The efficiency rate of monocrystalline solar cells is around 24%. This ratio is much higher than other solar energy panels available in the market. However, the price of monocrystalline energy panels is slightly more expensive than other solar panels. It is seen that monocrystalline silicon solar cells are frequently used in solar panel construction.

Monocrystalline solar panels can work more efficiently both in hot climates and in regions with less sunshine. In other words, the use of monocrystalline solar panels will be very beneficial in days or regions where the sunshine duration is short. Monocrystalline panels should be preferred so that you can always charge your batteries and use more solar energy. Monocrystalline solar panels are preferred in a country like Germany with a very short sunshine duration. In this way, energy is obtained from panels that have been used for more than 30 years.

Monocrystalline silicon technology is costly and difficult to manufacture. However, the unit price per watt can also be almost doubled compared to other energy panels. Quartz forms of the element silicon are widely used. Approximately 90% of quartz material consists of silicon. After the quartz is processed more than once, a 99% pure silica substance is obtained. Silicon element is obtained by going through the necessary processes of silica material. The silicon element is purified and the polycrystalline silicon element with semiconductor properties is obtained. The techniques used to obtain multicrystalline silicon are quite costly. A second disadvantage is the loss of material in the production stage of cells. While cutting processes are applied during production, approximately 40% of the raw material turns into dust or unused parts. For this reason, the cost per cell increases.

#### 3.1.1.2.2. Polycrystalline

It is the most preferred solar panel in the market. Its price is almost twice as cheap as monocrystals, but its service life and efficiency are low compared to monocrystals. Today, the efficiency of commercial polycrystalline solar cells is around 17%. Its electrical, optical and structural properties are the same as those of monocrystalline panels. In the production phase, the same processes are applied exactly as the single crystalline silicon is obtained in the first place. However, the pouring method is used in the production phase of Polycrystalline silicon material. The semiconductor silicon material in molten state is expected to cool by pouring it into molds. When the silicon is cooled slowly, it solidifies in the form of blocks. Blocks obtained from molds are cut in a square shape. Polycrystalline cells have a square shape, as if composed of amorphous small pieces, and a bluish appearance. The production of solar cells obtained from the materials produced using this method is relatively easier, the cost is low, and the efficiency is less. However, in the solidification process, the atoms are not aligned into a large single crystal as in the monocrystalline method. The size of the veins is directly proportional to the quality of the crystals. If there is discontinuity between the veins, there is some obstacle to the transfer of electrical charge carriers, especially.

#### 3.1.1.2.3. Thin-film

Thin-film solar panel has the smallest share in the solar power generation market. It has a usage rate that corresponds to only 7% of the market share. The main reason why thin-film solar cells are not preferred is their low efficiency. Although it absorbs the rays from the sun much, their efficiency is very low and very few people prefer these panels. The thin-film solar panel is designed on a flat surface that does not require connection with other cells, unlike conventional panels. Of course, the main purpose of the emergence of these products is to reduce the cost. As you know, when the cost is reduced, the quality also decreases, and this decrease is called the decrease in efficiency in solar energy systems. These thin-film solar cells take up a lot of space. But despite taking up so much space, it has a bad performance in terms of space-efficiency relationship. However, studies on increasing yields in the laboratory environment continue. Their efficiency is around 11% to 21% (Boz, 2011). This is really low efficiency. However, these solar panels have a very stylish appearance. It is preferred for more design. Today, thin-film solar energy panels are preferred for the operation of small devices and for the exterior of buildings. These modules are less affected by temperature than crystalline modules.

There are cell types that vary according to the elements used in their content, materials with high absorption of incoming rays are used during the construction of thin-film solar panels, and the amount of raw materials is low because they are generally produced in a thinner layer. For example, the absorption coefficient of solar panels using amorphous silicon is higher than solar panels using crystalline silicon. While solar radiation in a part with a wavelength coefficient of fewer than 0.7 microns can be absorbed by amorphous silicon with a thickness of 1 micron, a material with a thickness of 500 microns must be used in crystalline silicon to absorb the same radiation. Therefore, less material is used in amorphous solar cells and provides an advantage due to the ease of assembly (Erkul, 2010).

#### 3.1.1.2.4. Flexible

After the discovery and use of solar energy, the technological researches that started in this field have almost reached their peak as of today. The giant countries of technology have made a presentation to the users with excellent designs and low costs that go far beyond the classical forms of solar energy panels and continue to do so. One of the most striking panels of new and advanced technology is undoubtedly the flexible solar panel form. A flexible solar panel is a solar panel with so many uses. These solar panels are really very flexible and very light.

Because these panels do not have an aluminum frame and tempered glass. This makes them much lighter. Flexible solar panels are unbreakable and very durable. These panels, whose biggest feature is not to choose a flat floor, are easily portable and have taken their deserved place in the solar panel sector to a large extent.

The structure of this type of solar cell can be both monocrystalline and polycrystalline. In this case, it also diversifies the efficiencies of these energy panels. There are different types of such panels, which are essentially composed of crystal and thin-film cells. The most important feature of the panels consisting of thin-film cells is that they are flexible and in addition to that, they are easy to use with their laying feature. Flexible solar panels have a distinctive feature as they are easily portable. These panels, which can be rolled up when necessary, are preferred in military areas, especially in yachts. The usage areas are many. For example, rechargeable vehicles, rechargeable marine vehicles, bus stops, sloping factory roofs, sloping parking lots, etc. It is certain that flexible solar energy panels will make human life easier in the coming years. However, its weakness in productivity affects the continuation of productivity-enhancing efforts.

#### 3.1.1.3. Buck converter

Buck converters are converters whose voltage at the output part can be adjusted, reducing voltage from DC to a DC voltage. The important point is that the voltage you apply at the input must be higher than at the output. Thus, the open-circuit voltage obtained from the PV panel was reduced to the desired voltage levels required for the electrolysis system with the help of the converter. On-state is the state in which the switch is closed and the current flows. Off-state is the state in which the switch is open. The state that the switch is on or off is the MOSFET used in the key function.

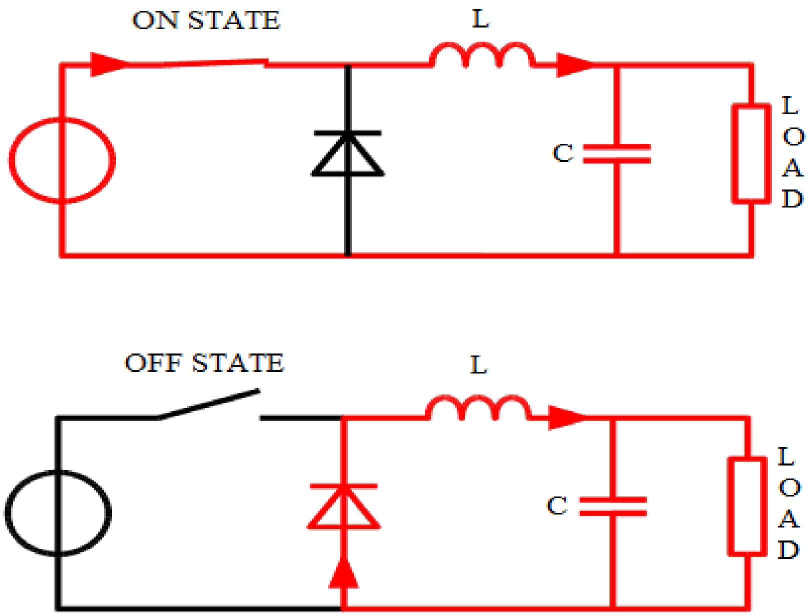


**Figure 3.4.** On-state and off-state buck converter circuit.

The first step to calculate the switch current is to determine the duty cycle (D) from Equation (6) for the maximum input voltage. The maximum input voltage ($V_i$) is used because this leads to the maximum switch current. We can find the duty cycle by proportioning the input voltage ($V_i$) to the output voltage ($V_o$) equation.

$$\text{Duty Cycle (D)}= \frac{V_i}{V_o} \tag{6}$$

The higher the inductor value (L), the higher is the maximum output current because of the reduced ripple current ($\Delta I_L$). In general, the lower the inductor value, the smaller is the solution size. Note that the inductor must always have a higher current rating than the maximum current; this is because the current increases with decreasing inductance. Using Equation (7), the inductor value was found to be 16.6 μH.

$$L = \frac{V_O.(1-D)}{f_S.\Delta I_L} \tag{7}$$

The best practice is to use capacitors to minimize the ripple on the output voltage. With external compensation, the following equations can be used to adjust the output capacitor values (C) for a desired output voltage ripple. Using Equation (8), the capacitor value was found to be 3.75 µF.

$$C = \frac{\Delta I_L}{8.f_S.\Delta V_O} \tag{8}$$

Calculated theoretical system parameters and PV panel values that we will use in the experiment were simulated in MATLAB/ Simulink. I created a module that has the characteristics of the PV panel and DC-DC buck converter. PV panel and converter design are given in Figure 3.5. I extracted the I-V curves and P-V curves of the PV panel to determine the maximum power point. In this way, I have provided energy with the highest efficiency from the PV panel.

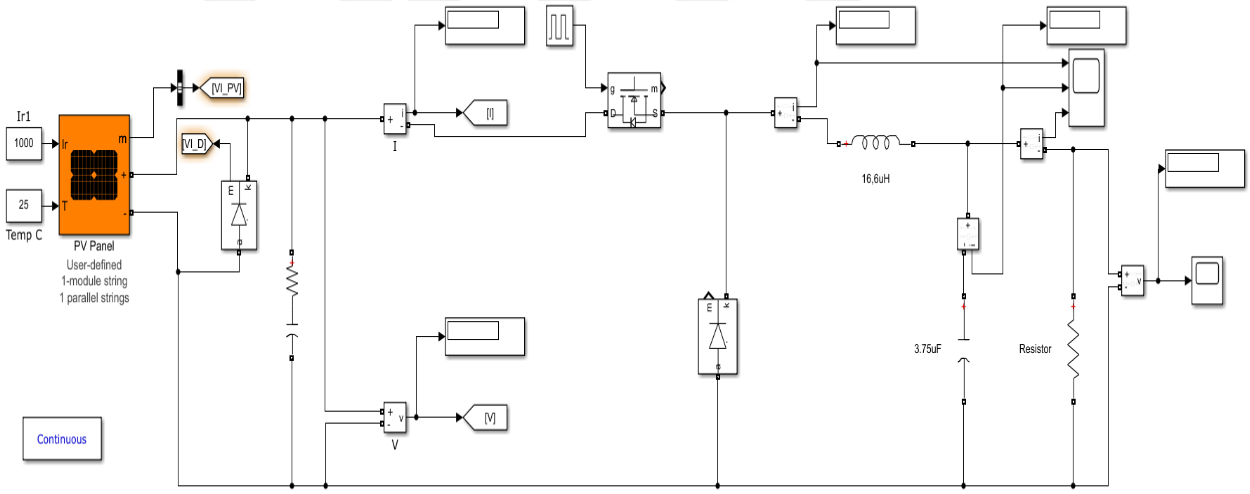


**Figure 3.5.** PV panel and converter design in MATLAB/Simulink.

### 3.1.2. Electrochemical model

The reversible cell voltage $V_{rev}$ is the lowest required voltage for the electrolysis to take place. In standard conditions (25º C and 1 bar), the change of Gibb's energy of water splitting is ΔGº = 237 kJ/mol. This voltage can be expressed as a function of ΔG by means of

$$V_{rev} = \frac{\Delta G}{z.F} \tag{9}$$

where z is the number of electron moles transferred per hydrogen mole (z = 2) and F is the Faraday constant, which represents the charge on one mole of electrons (96 485 C/mol). If the thermal energy T.ΔS is provided by means of electricity, as is the case in most commercial electrolysers, the minimum voltage for water electrolysis to occur is known as the thermo-neutral voltage $V_{tn}$. In addition to that, ΔH is the change of enthalpy between reactants and products in a reaction and is related to thermoneutral cell voltage as

$$V_{tn} = \frac{\Delta H}{z.F} \tag{10}$$

The energy required for water splitting in standard condition, $\Delta H^{o}$= 286 kJ/mol.
The kinetic properties around the electrodes in an electrolyser cell can be modelled based on empirical data of different proposed I-V curves. The basic relationship between current and cell voltage in a given temperature is

$$V = V_{rev} + \frac{I}{A}(r_1 + r_2 \mathrm{x} T) + s.\log\left[\frac{I}{A}\left(t_{1+}\frac{t_2}{T} + \frac{t_3}{T^2}\right) + 1\right] \tag{11}$$

where I is the current required for the electrolysis, A is the area of electrodes, r is the parameter related to ohmic overvoltage resistance of the electrolyte, s and t are the activation overvoltage coefficients on electrodes and $V_{rev}$ is the reversible voltage. The dynamic model describing cell voltage is shown in Figure 3.6.

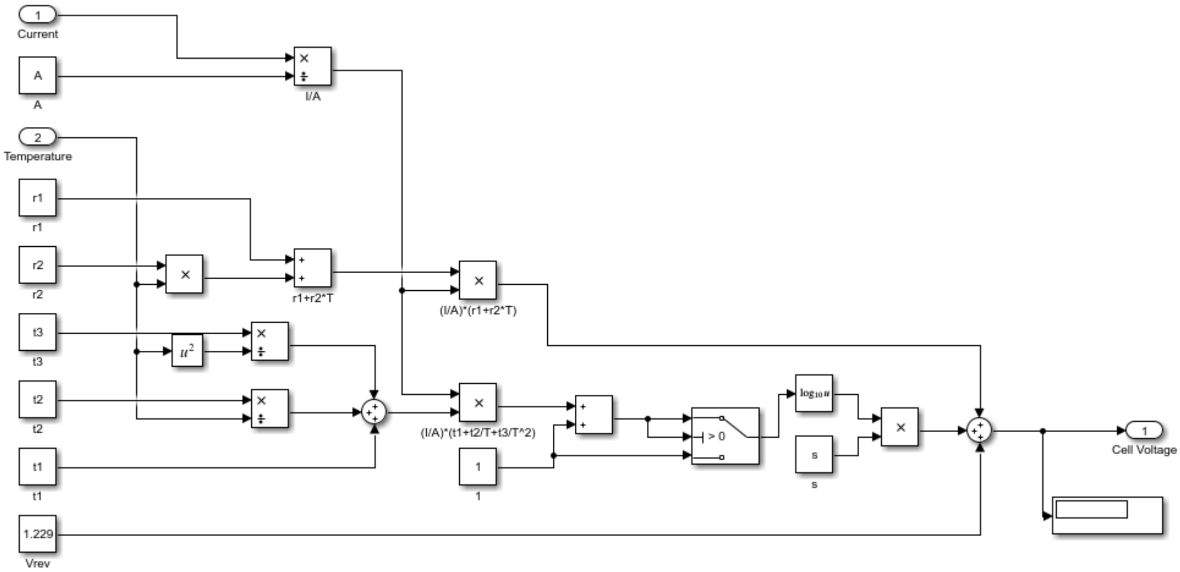


**Figure 3.6.** MATLAB/ Simulink block diagram of cell voltage.

Faraday efficiency is the proportion of the actual and theoretical hydrogen production in the electrolyzer. It will be shown later that one of the parameters that control the hydrogen production is current, so another name of Faraday efficiency is current efficiency. It can be noted that parasitic current increases with the decrement of current density and the increment of temperature resulting the reduction of Faraday efficiency. This phenomenon can be expressed as

$$n_F = \frac{\frac{I}{A}^2}{f_1 + \frac{I}{A}^2} \cdot f_2 \tag{12}$$

where f1 and f2 are the parameters related to Faraday efficiency. $f_1$ and $f_2$ are usually considered constant for the overall model. However, they vary with temperature. The assumption of linear relation with temperature depends on the temperature range of operation. In this research, a linear expression only applies for $f_1$ whereas for $f_2$ a limit value must be set to guarantee a range value between 0 and 1. Using the experimental data shown in Table 3.1, a linear empirical expression is obtained for $f_1$ as shown in Equation (13) and a quadratic for $f_2$ as shown in Equation (14). Note that an extra point was added to $f_2$ at 0°C to guarantee a limit value of 1.

$$f_1 = 2.5T + 50 \quad (13)$$

$$f_2 = 1 - 6.25x10^{-6}.T^2 \quad (14)$$

**Table 3.1.** The values of $f_1$ and $f_2$ parameters related to Faraday efficiency according to temperature.

| Temperature °C | $f_1$ | $f_2$ |
|---|---|---|
| 0 | | 1.00 |
| 40 | 150 | 0.99 |
| 80 | 250 | 0.96 |

Normally a number of electrolyser cells are connected in series in a stack and some stacks are connected in parallel. The number of such electrolyser cells has an impact on the total hydrogen production. The production rate is

$$\dot{n_{H2}} = n_F \frac{n_c I}{zF} \quad (15)$$

where $n_c$ is the number of electrolyser cells per stack.

A unit conversion is needed for the flow rate in Equation (15) to obtain a rate in kilograms rather than moles. This will facilitate comparisons in the result section. Using the volume of an ideal gas at standard conditions $V_{std}$ , the volumetric flow rate and the mass flow rate are given by Equation (16). The dynamic model describing mass flow rate is shown in Figure 3.7.

$$\dot{V} = \dot{n} V_{std} \rightarrow \dot{M} = \dot{V} c \quad (16)$$

where $\dot{V}$= 0.0224136 $m^3$/mol and c = 0.08988 kg/$m^3$.

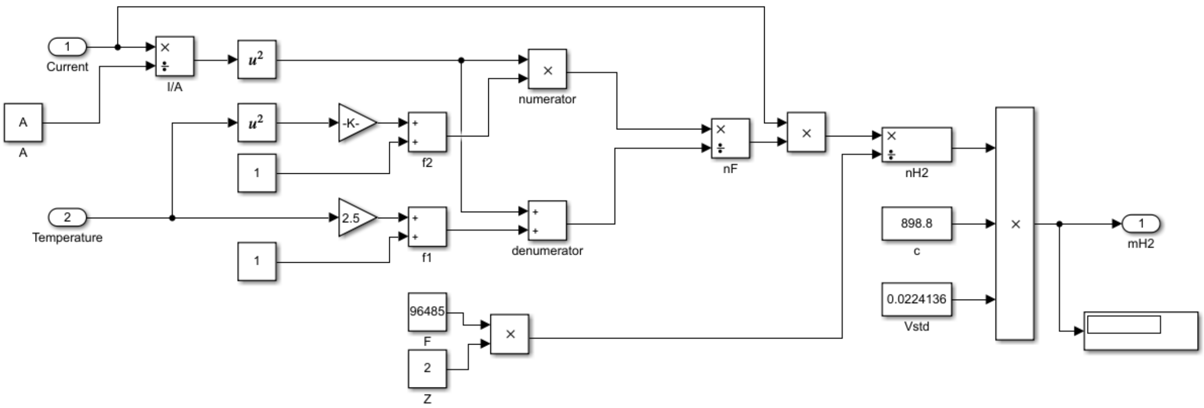


**Figure 3.7.** MATLAB/ Simulink block diagram of hydrogen mass flow rate.

Due to the presence of a logarithmic function in Equation (11), careful consideration is needed to avoid negative values that can produce unrealistic results. This is obvious at low levels of current where the model parameters cannot follow the electrolyser response properly.

Similarly, when the input current is zero, the electrolyser cell is equal to the reversible voltage and can potentially act as a voltage source feeding current to other elements of the electrical circuit. To avoid this situation, the mathematical element is disconnected from the circuit to block any current flow and to force the voltage to follow the external circuit.

Finally, production rate is given by Equation (17) only depends on the input current regardless of the voltage input. This is not accurate since water can only be divided into hydrogen and oxygen when the cell voltage is enough to provide the required activation energy. Special consideration is added to the model to produce hydrogen only if the cell voltage is greater than $V_{std}$. The final set of boundary conditions can be expressed in Equations (13) and (14). Using MATLAB/Simulink math blocks, Equations (9)–(19) are constructed for each input and output.

$$V = \begin{cases} V_{rev} + \frac{r_1+r_2T}{A} I + s\log\left(\left(t_1 + \frac{t_2}{T} + \frac{t_3}{T^2}\right)\frac{I}{A} + 1\right), & I > -A\left(t_1 + \frac{t_2}{T} + \frac{t_3}{T^2}\right)^{-1} \\ V_{rev} + \frac{r_1+r_2T}{A} I, & I \leq -A\left(t_1 + \frac{t_2}{T} + \frac{t_3}{T^2}\right)^{-1} \\ V_{outside}, & I = 0 \end{cases} \quad (17)$$

$$\dot{n}H_2 = \begin{cases} \left(\frac{(I/A)^2}{f_1+(I/A)^2} f_2\right)\frac{I}{zF}, & V > V_{rev} \\ 0, & V \leq V_{rev} \end{cases} \quad (18)$$

Energy efficiency is defined as the ratio of thermo neutral voltage and the cell voltage as follows

$$n_e = \frac{V_{tn}}{V} \quad (19)$$

Note that, the electrical inefficiencies result the unwanted heat generation in the electrolyser which has an indirect influence on Faraday efficiency. The dynamic model describing efficiency is shown in Figure 3.8.

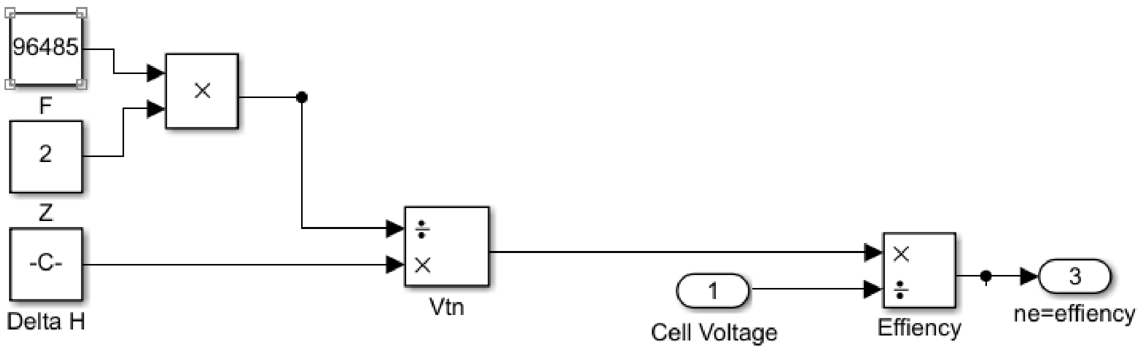


**Figure 3.8.** MATLAB/Simulink block diagram of efficiency.

## 3.2. Experimental part

In this section, the stages during the experimental setup of the proposed system that we simulated, the materials used and the working principle of the system are mentioned. The schematic structure of the PV assisted alkaline electrolysis system is shown in Figure 3.9.

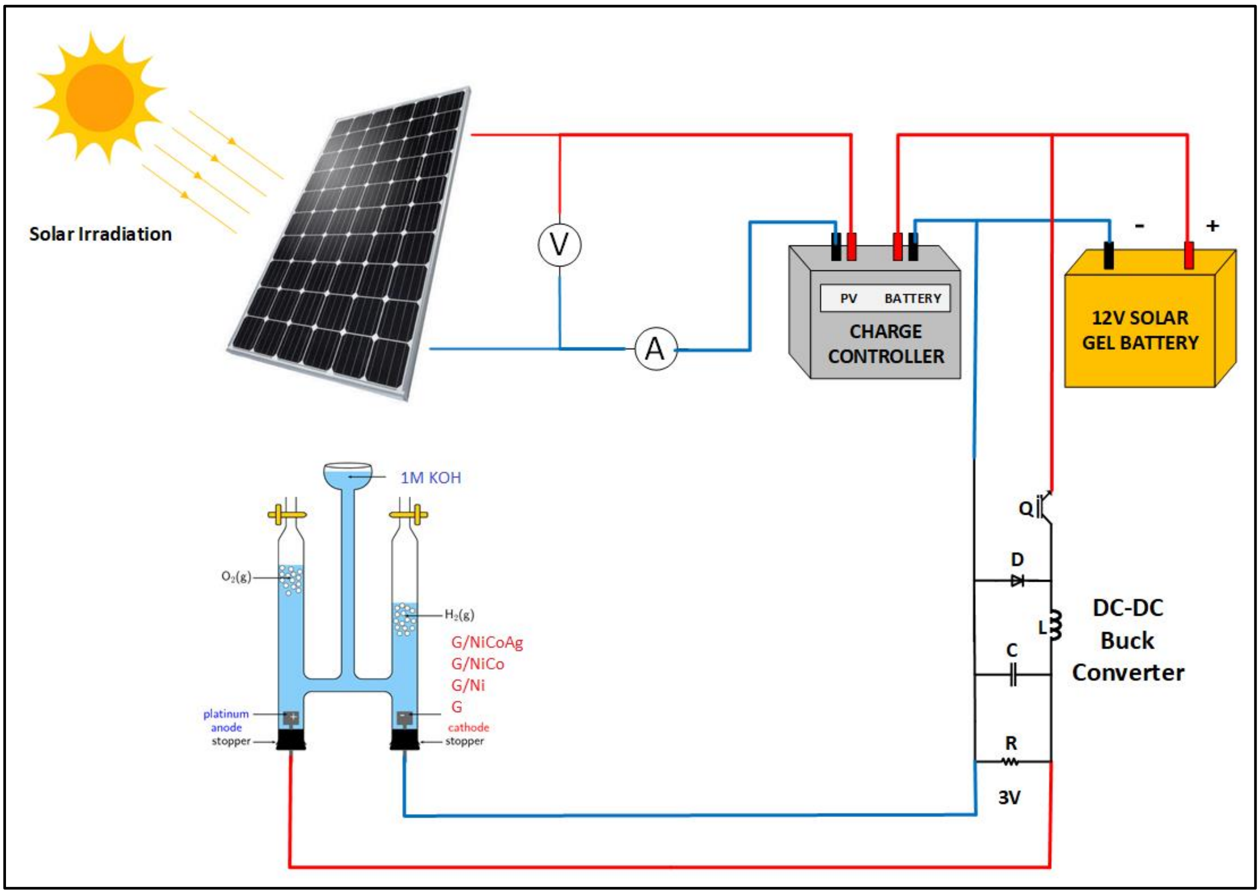


**Figure 3.9.** PV assisted alkaline electrolysis system.

### 3.2.1. Photovoltaic panel and converter

The PV panel is one of the most crucial components of solar energy systems. It produces energy by absorbing sunlight with photovoltaic cells, generating direct current (DC) energy. Solar PV panels are constituted by an array of solar PV cells. The 80-Watt solar PV panel was used for the electrolysis process. The characteristic features of the solar panel obtained by connecting 36 solar cells in series are given in Table 3.1.

**Table 3.2.** Characteristic features of the solar PV panel.

| Solar PV Panel | Parameter | Solar PV Panel | Parameter |
|---|---|---|---|
| Power rating | 80 Wp | Power tolerance | %±2.4 |
| Open circuit voltage ($V_{oc}$) | 22.68 V | MPPT range | 31.7 V |
| The voltage at the power point | 18.5 V | Protection class | IP65 |
| Short circuit current ($I_{sc}$) | 4.75 A | Dimensions | 800x670x30 mm |
| Current at the power point | 4.38 A | Series Fuse Rating | 15 A |
| Cell efficiency | %16.7 | Operating temperature | -40°C…+80°C |
| Module Efficiency | %13.6 | Weight | 8.5 kg |

It is also possible for a photovoltaic power plant to be independent or dependent on the grid. PV systems connected to the grid are called on grid systems, and PV systems not connected to the grid are called off grid systems. Off grid systems operate independently of the country's grid and the energy generated is consumed by itself. In this system, excess production energy is stored in batteries or converted to other alternative energy sources. On grid systems do not have a battery with a storage device. The generated energy is used in the system and the excess energy is converted into alternating current electrical energy and made available to the distribution network. At the same time, when the energy produced is insufficient, energy is purchased from the distribution network for cost.

In this study, off grid system was preferred. this system consists of a PV panel and DC-DC buck converter integrated into the electrolysis system. The 80 W solar PV panel is directly connected to the DC-DC step-down converter. Thus, the open-circuit voltage obtained from the PV panel is reduced to the desired voltage levels required for the electrolysis system with the help of the converter. Electrolysis was carried out with the energy from the solar panel and converter for hydrogen production. Excess energy is stored in batteries and used to ensure the continuity of the system at night or when the solar radiation is low.

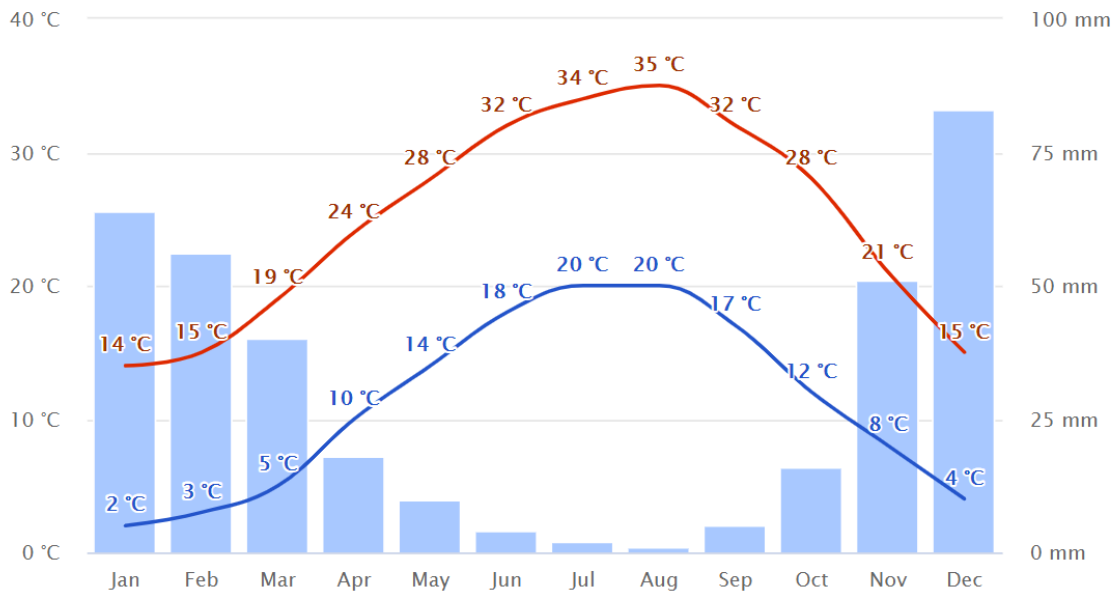


**Figure 3.10.** The highest and lowest temperature averages last 30 years in Adana.

I carried out my experiments in the city of Adana in the Mediterranean region. The sunshine duration and irradiation values of Adana city are 2,953 hours per year and 1564 $KWh/m^2$, respectively. These values are above Turkey's averages. As seen in Figure 3.10, Adana's monthly highest and lowest temperature averages and when we look at Figure 3.11, the average sunshine duration by months is given. The months with the highest temperatures and sunshine periods are June, July, August and September, above 30 °C.

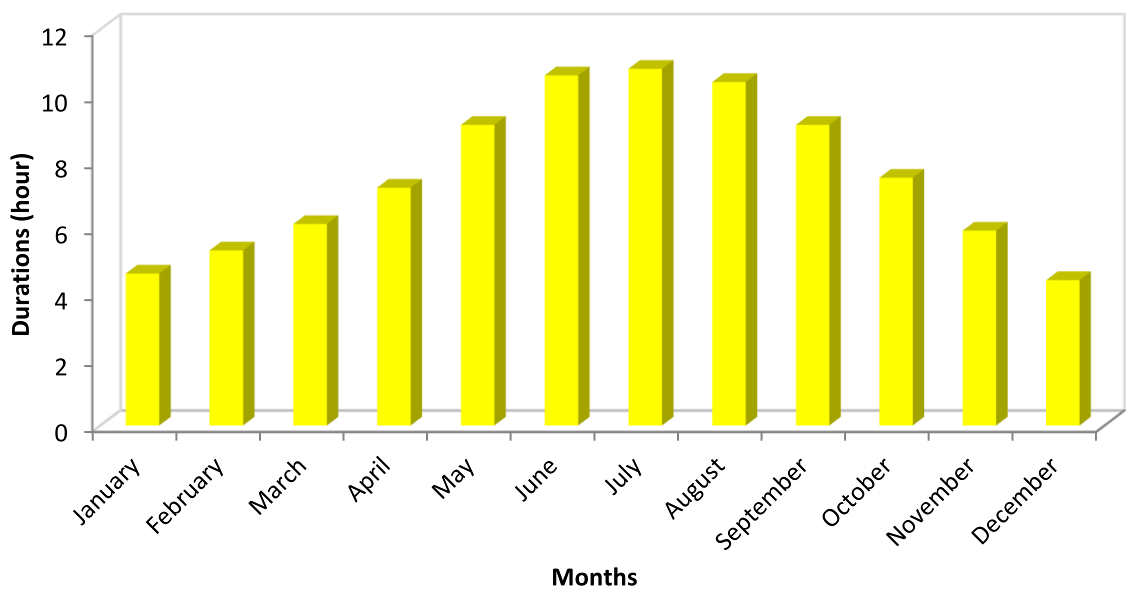


**Figure 3.11.** Average sunshine durations monthly last 30 years in Adana.

Solar PV panels formed by connecting a solar cell with serial or parallel connection of these cells are composed of a current source electrically, serial/parallel resistors, and parallel diodes. The relationship between the voltage of solar cell cells and the current it gives to the load gives the I-V and P-V characteristics of the cell. These two characteristics provide important clues about the conditions under which the power received from the panel should reach its highest value. Therefore, I-V curves and P-V curves of the PV panel were extracted to determine the maximum power point. In this way, energy was provided with the highest efficiency from the PV panel.

DC-DC step-down converters are systems that reduce the direct voltage at the converter input to a lower direct voltage level and transfer it to its output. DC-DC step down converters are used to the conversion process of solar PV panel generated voltage. These are monolithic integrated circuits ideally suited for easy and convenient design of a step-down switching regulator (buck converter). All circuits of this series are capable of driving a 3.0 A load with excellent line and load regulation. These devices are available in an adjustable output version. These regulators were designed to minimize the number of external components to simplify the power supply design. Since these types of converters are switch-mode power supply, its efficiency is significantly higher in comparison with popular three-terminal linear regulators, especially with higher input voltages. The proposed converter features are shown in Table 3.2.

**Table 3.3.** Characteristic features of the buck converter.

| **Description** | **Features** | **Description** | **Features** |
|---|---|---|---|
| Input voltage | 4-35V | Output voltage | 1.23V-30V |
| Rectifier | Non-Synchronous Rectification | Operating temperature | (-40°Cto +85°C ) |
| Module Properties | Non-isolated step-down module (buck) | Conversion efficiency | Up to 92% |
| Load regulation | ±0.5% | Switching Frequency | 150KHz |
| Voltage regulation | ±2.5% | Size | 48x23x14 mm |

### 3.2.2. Electrochemical part

In the production of hydrogen gas by electrolysis of water, aqueous solutions of KOH or NaOH are usually used due to the low electrical conductivity of pure water. At equilibrium concentrations, the conductivity of KOH solution is higher than that of NaOH solution. Also, some gases dissolved in the electrolyte solution (carbon dioxide, etc.), pollute the electrode and reduces its conductivity. For this reason, it is desirable that electrolyte solutions absorb these gases less. During the experiment, the 1 M KOH solution was preferred because the KOH solution absorbs less carbon dioxide than the NaOH solution and has better conductivity. The prepared electrolytes should be of high purity and especially not contain chloride. Because chloride has a corrosive effect on electrodes, especially on the anode. There should be no pollution in the water used in electrolysis, and high purity water should be used. When preparing the solution, distilled water from a high-quality water purifier was used. 56.11 grams of KOH was weighed on a precision scale and added to 1 liter of distilled water. The solution is mixed via magnetic stirrer.

Hydrogen production reactions consist of three stages in alkaline solution and these stages are the stages that affect the hydrogen production rate. The Volmer reaction, called the discharge reaction in the alkaline medium, is the first step in which the $H_2O$ molecule is separated into the absorbed hydrogen atom and the hydroxyl ion. For a hydrogen molecule to form, one of the usual two steps must occur. Tafel reaction, known as the combination step, selects the step in which two absorbed hydrogen atoms form a hydrogen molecule, or the hydrogen molecule is formed as a result of the interaction of the $H_2O$ molecule and the H atom, which is the Heyrovsky step.

$$\text{Volmer reaction: } H_2O + e^- \rightarrow H_{(ad)} + OH^- \tag{20}$$

$$\text{Tafel reaction: } H_{(ad)} + H_{(ad)} \rightarrow H_{2(ad)} \tag{21}$$

$$\text{Heyrovsky reaction: } H_2O + H_{(ad)} + e^- \rightarrow H_{2(ad)} + OH^- \tag{22}$$

Electrode selection has an important place in the electrochemical reaction. When selecting the electrodes, the cost and the potential for hydrogen production efficiency have been considered. To reduce the cost of the system, commercial electrodes were not used and prepared by ourselves in the laboratory. Graphite electrode is preferred as cathode in our system due to its low cost. Copper wire was passed to one end of a graphite rod to provide conductivity. The electrode is 5 cm in length and embedded in polyester. The surface area of the prepared graphite electrode, which is not covered with resin in contact with the solution, is 0.36 $cm^2$.

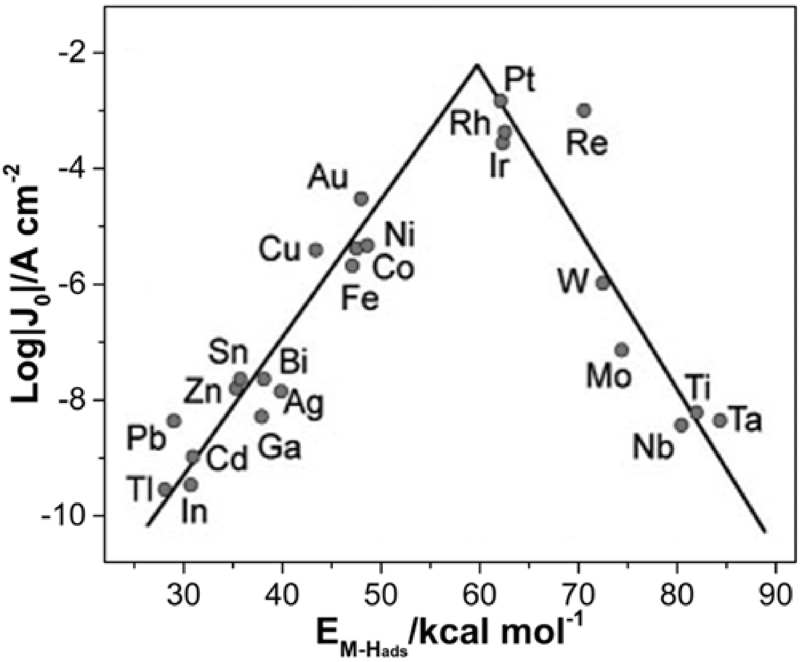


**Figure 3.12.** Volcano curve for hydrogen evolution reaction on metal electrodes.

Choosing metal with high electrocatalytic property as cathode will be good for hydrogen production reactions. According to the graph called the volcano curve in Figure 3.12, as the M-H bond energy increases, the charge changes current density first increases and then decreases. Accordingly, the metals with the highest charge change current density are metals such as Pt, Au, Ir, Rh. These metals are known to have high electrocatalytic properties. Another reason that increases the cost in hydrogen production is overvoltage. Since we want the overvoltage to below, Pt is chosen as the anode not only electrocatalytic activity but also higher corrosion resistance. Pt electrodes were prepared by attaching Pt wires to 1x1 cm Pt plates and then embedded in polyester so that only Pt plate remains outside. The surface area of the Pt electrode prepared in this way is 2 $cm^2$. In all the experiments, the Pt electrode was used.

The smallest potential difference that must be applied between the two electrodes in order to ensure a continuous separation in the electrolyte solution is called the decomposition voltage.

The theoretical decomposition voltage can be found by computing the electrode potentials corresponding to the equilibrium state of the anode and cathode by using Nernst equation;

$$E_d = E_{anode} - E_{cathode} \quad (23)$$

The $E_d$ obtained here is the theoretical decomposition voltage, based on the assumption that there is no overvoltage at the anode and cathode. Theoretically, the potential required for water decomposition at 25 ° C is 1.23 V. When $O_2$ overvoltage on Pt (0.47 V) is added to this value as the anode, a potential of at least 1.70 V must be applied to the system in order to start hydrogen gas output (Yazıcı,1995). However, a higher potential has to be applied due to the overvoltages caused by the solution and electrode metal and the internal resistance of the voltage source and the internal resistance of the cables used during the experiment. During electrolysis of alkaline water, oxygen is released at the anode and hydrogen gas is released at the cathode.

Anode : $4OH^- \rightarrow O_2 + 2H_2O + 4e^-$ $\quad E_A=0.401+0.0592pOH \quad (PO_2=1.0\ atm)$ (24)

Cathode: $4\ H_2O + 4e^- \rightarrow 4OH^- + 2H_2$ $\quad E_C=-0.828+0.0592pOH \quad (PH_2=1.0\ atm)$ (25)

$2H_2O \rightarrow O_2 + 2H_2$ $\quad E=E_A-E_C=1.229\ V$ (26)

A direct current source was used to perform electrolysis using two electrode techniques, obtain current-voltage curves, and determine hydrogen volumes with a certain constant potential. The current meter part of the multimeter was used to determine the current passing through the system. The decomposition voltages in 1 M KOH solution were determined using the two electrode technique of the system selected as platinum electrode anode and graphite electrode cathode. For this purpose, by applying potential from the direct current source from 1.3 V to 3 V at intervals of 0.1 V to the system, the current values passing through the system were determined and the current potential curves were extracted. The reason for not starting from 0 V is theoretically the decomposition voltage is approximately 1.3 V. The decomposition voltages of the electrolysis system were determined from the intersection points by extrapolating the linear parts. This experiment has been repeated 7 times and close results have been obtained.

After determining the decomposition voltage, the second part of our experiment, determining the hydrogen volumes, was started. In this part, hydrogen production volumes at different voltage values were observed. Graphite electrode and platinum electrode are immersed in 1 M KOH solution at a constant distance of 2 cm. The cathode, where there is an output of hydrogen gas, is placed on the electrode by reversing the cylinder. Thus, the volume of the amount of hydrogen produced was measured. Starting from 2.3 V, which is the decomposition voltage, to increase by 0.1 V, the volume of hydrogen produced at the entire voltage value of up to 3 V and the current values passing through the system at each volt value were measured. The volume amounts displayed in the cylinder with an interval of 5 minutes at each volt are noted. Each voltage value was applied to the system for 30 minutes. Considering that in the same environment, water vapor will also collect in the cylinder, volume correction was made as given below.

$$P_{H_2} = P_T - P_{H_2O} \tag{27}$$

When the vapor pressure of water ($P_{H_2O}$) under these conditions is 23.756 mmHg and the total atmospheric pressure ($P_T$) is 756 mmHg, the pressure of hydrogen ($P_{H_2}$) gas under these conditions is determined as 732.244 mmHg. Hydrogen volume ($V_{H_2}$) is;

$$V_{H_2} = \frac{732.244}{756} \text{ x } V_{measuring} \tag{28}$$

determined by the relation. The $V_{measuring}$ here is the total volume of gas collected experimentally in the cylinder.

In order to see the effect of nickel plating on hydrogen production, 0.36$cm^2$ graphite electrode was coated with nickel. 30 grams $NiSO_4.7H_2O$, 1 gram $NiCl_2.6H_2O$, and 1.25 grams $H_3BO_3$ were weighed and put in the volumetric flask to prepare the Ni bath. The solution had a volume of 100 mL. The galvanostatic method was used to achieve the 10 µm thick Ni coating by the Ivium stat electrochemical analyzer. The current density was 50 $mA/cm^2$. A three-electrode system was used Ni electrode was used as counter electrode, Ag / AgCl (3M KCl) as reference electrode, and graphite as working electrode.

$$Ni^{+2} + 2e^{-} \longrightarrow Ni_{(s)} \quad (29)$$

The decomposition voltages in 1 M KOH solution were determined using the two electrode technique of the system selected as platinum electrode anode and G/Ni electrode cathode. For this purpose, by applying potential from the direct current source from 1.3 V to 3 V at intervals of 0.1 V to the system, the current values passing through the system were determined and the current potential curves were extracted. The decomposition voltages of the electrolysis system were determined from the intersection points by extrapolating the linear parts. This experiment has been repeated 7 times and close results have been obtained.

After determining the decomposition voltage of the G/Ni electrode, the second part of our experiment was to determine the hydrogen volumes. In this part, hydrogen production volumes at different voltage values were observed. G/Ni electrode and platinum electrode are immersed in 1 M KOH solution at a constant distance of 2 cm. The cathode, where there is an output of hydrogen gas, is placed on the electrode by reversing the cylinder. Thus, the volume of the amount of hydrogen produced was measured. The volume of hydrogen produced at all voltage values starting from 2.3 V, increasing by 0.1 V up to 3 V and the current values passing through the system at each volt value were measured.

Cobalt was decorated on the G/Ni electrode to see its contribution to hydrogen production. Cobalt bath was prepared for the preparation of the new G/NiCo electrode. In order to prepare Co bath, 30 grams $CoSO_4.7H_2O$, 1 gram $CoCl_2.6H_2O$, 1.25 grams $H_3BO_3$ were weighed and put into the volumetric flask. The volume of solution was 100 mL. The 10 µg Co decorated per 1 $cm^2$ of electrode surface with the help of galvanostatic method by Ivium stat electrochemcial analyzer. The current density was 50 $mA/cm^2$. A three-electrode system was used Pt electrode was used as counter electrode, Ag / AgCl (3M KCl) as reference electrode.

$$Co^{+2}_{(aq)} + 2e^{-} \longrightarrow Co_{(s)} \quad (30)$$

The decomposition voltages in 1 M KOH solution were determined using the two electrode technique of the system selected as platinum electrode anode and G/NiCo electrode cathode. For this purpose, by applying potential from the direct current source from 1.3 V to 3 V at intervals of 0.1 V to the system, the current values passing through the system were determined and the current potential curves were extracted. The decomposition voltages of the electrolysis system were determined from the intersection points by extrapolating the linear parts. This experiment has been repeated 7 times and close results have been obtained.

After determining the decomposition voltage of the G/NiCo electrode, the second part of our experiment was to determine the hydrogen volumes. In this part, hydrogen production volumes at different voltage values were observed. G/NiCo electrode and platinum electrode are immersed in 1 M KOH solution at a constant distance of 2 cm. The cathode, where there is an output of hydrogen gas, is placed on the electrode by reversing the cylinder. Thus, the volume of the amount of hydrogen produced was measured. The volume of hydrogen produced at all voltage values starting from 2.3 V, increasing by 0.1 V up to 3 V and the current values passing through the system at each volt value were measured.

Silver was decorated on the G/NiCo electrode to see its contribution to hydrogen production. Silver bath was prepared for the preparation of the new G/NiCoAg electrode. In order to prepare Ag bath, 12.75 miligrams $AgNO_3$ was weighed and put into the volumetric flask. The volume of solution was 100 mL. The 10 μg Ag decorated per 1 $cm^2$ of electrode surface with the help of galvanostatic method by Ivium stat electrochemcial analyzer. The current density was 50 $mA/cm^2$. A three-electrode system was used Pt electrode was used as counter electrode, Ag / AgCl (3M KCl) as reference electrode.

$$Ag^{+1} + 1e^- \longrightarrow Ag_{(s)} \quad (31)$$

The decomposition voltages in 1 M KOH solution were determined using the two electrode technique of the system selected as platinum electrode anode and G/NiCoAg electrode cathode. For this purpose, by applying potential from the direct current source from 1.3 V to 3 V at intervals of 0.1 V to the system, the current values passing through the system were determined and the current potential curves were extracted. The decomposition voltages of the electrolysis system were determined from the intersection points by extrapolating the linear parts. This experiment has been repeated 7 times and close results have been obtained.

After determining the decomposition voltage of the G/NiCoAg electrode, the second part of our experiment was to determine the hydrogen volumes. In this part, hydrogen production volumes at different voltage values were observed. G/NiCoAg electrode and platinum electrode are immersed in 1 M KOH solution at a constant distance of 2 cm. The cathode, where there is an output of hydrogen gas, is placed on the electrode by reversing the cylinder. Thus, the volume of the amount of hydrogen produced was measured. The volume of hydrogen produced at all voltage values starting from 2.3 V, increasing by 0.1 V up to 3 V and the current values passing through the system at each volt value were measured.

# 4. RESULTS AND DISCUSSIONS

## 4.1. Photovoltaic panel

Extracted the I-V curves and P-V curves of the PV panel to determine the maximum power point. In this way, energy was provided with the highest efficiency from the PV panel. This application was implemented both in MATLAB/Simulink and experimentally. During the simulation and experiment, the air temperature was 25 °C and the irradiation was 1000 W/m$^2$. As a result of the simulation, the MPP point was obtained as 81 W at 18.5 V and 4.38 A current. The resulting I-V curve is shown in Figure 4.1.

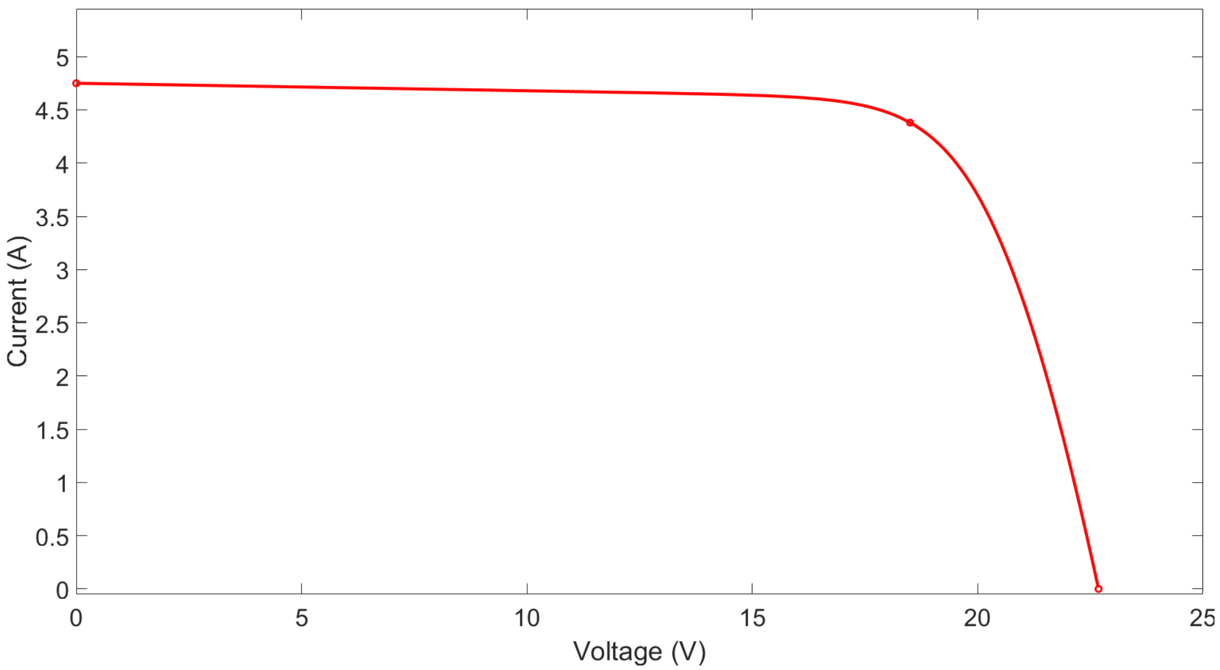


**Figure 4.1.** I-V curve of 80W PV panel at 25°C and 1000 W/m$^2$ irradiance in MATLAB/Simulink.

As a result of the experiment, the MPP point was obtained as 77.15 W at 16.7 V and 4.62 A. The resulting I-V curve is shown in Figure 4.2.

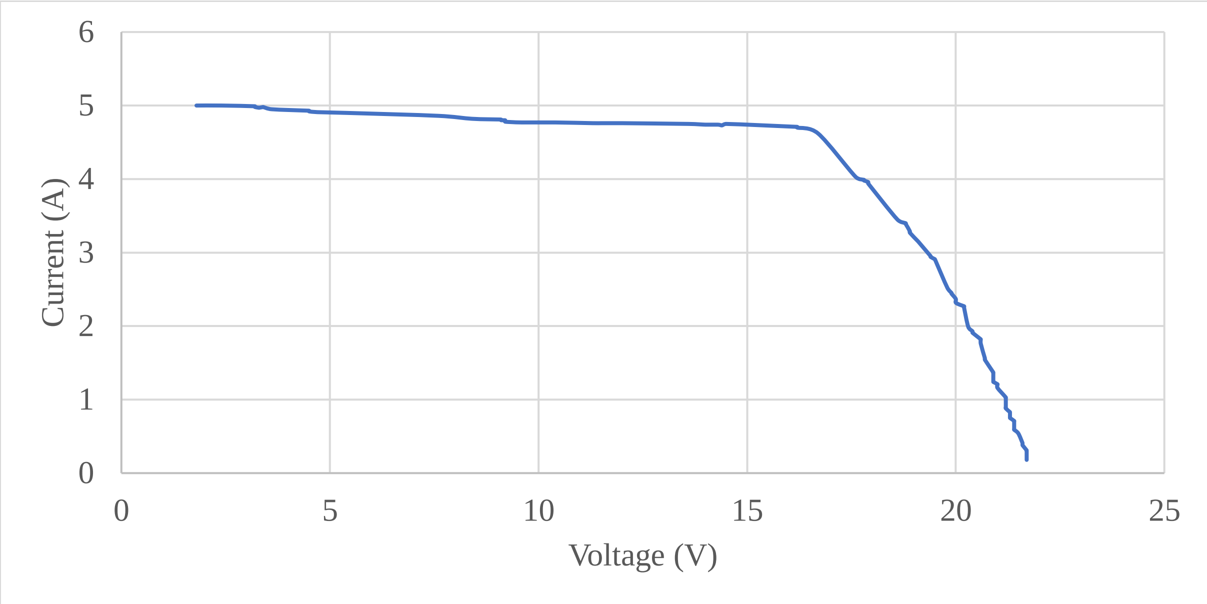


**Figure 4.2.** I-V curve of 80W PV panel at 25℃ and 1000 W/m$^2$ irradiance experimentally.

As a result of the simulation, the MPP point was obtained as 81 W at 18.5 V The resulting P-V curve is shown in Figure 4.3.

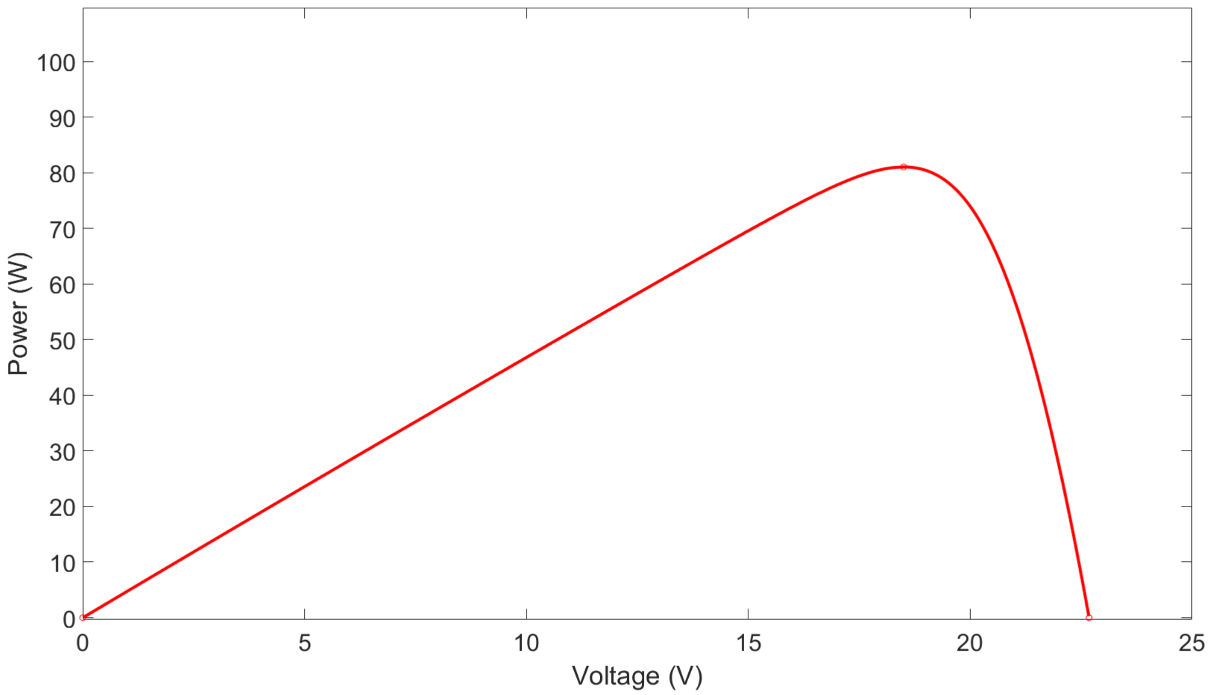


**Figure 4.3.** P-V curve of 80W PV panel at 25℃ and 1000 W/m$^2$ irradiance in MATLAB/Simulink.

As a result of the experiment, the MPP point was obtained as 77.15 W at 16.7 V The resulting P-V curve is shown in Figure 4.4.

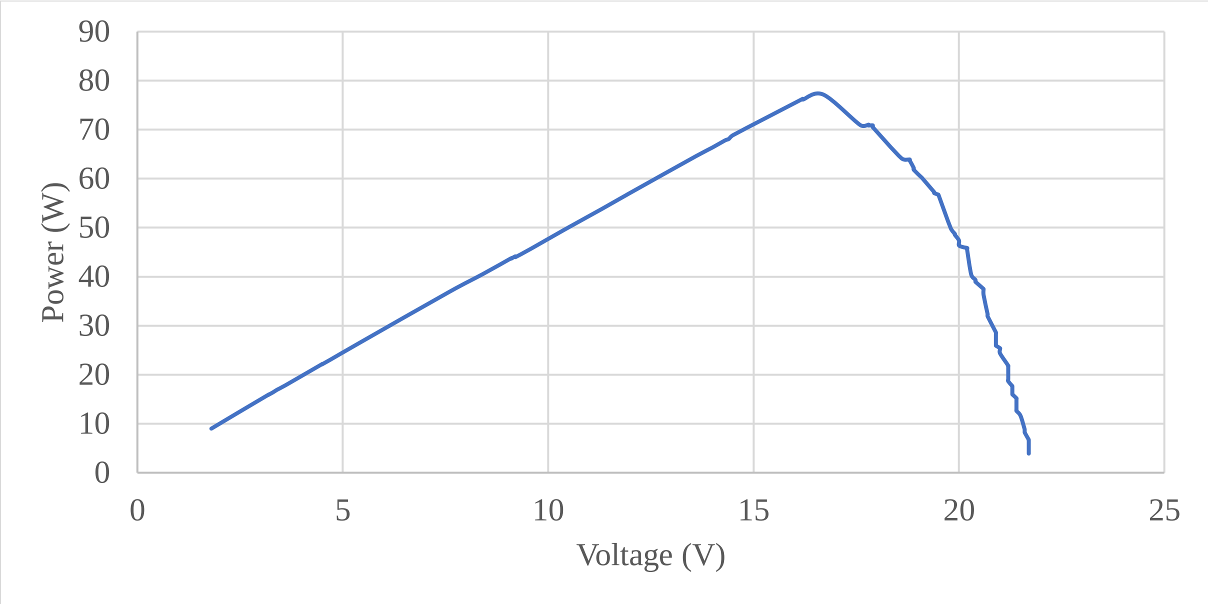


**Figure 4.4.** P-V curve of 80W PV panel at 25°C and 1000 W/m$^2$ irradiance experimentally.

As a result of the simulation, the power of our panel was calculated as 81 W, and as a result of the experiment, it was found as 77.15 W. This difference is tolerable. There are definitely differences between ideal conditions and real life conditions. In addition, looking at the datasheet of our panel, it is seen that it has a power tolerance of 2.5 percent. As can be seen, these values are close to each other.

## 4.2. Hydrogen production

Theoretically, the potential required for water dissociation at 25°C is 1.229 V. When the $O_2$ overvoltage (0.47 V) on Pt as the anode is added to this value, a potential of at least 1.70 V must be applied to the system to initiate the hydrogen gas output (Yazıcı,1995). The hydrogen gas was measured on the working electrodes used as the cathode in 1 M KOH. Experimental dissociation voltage was calculated for each electrode in order to compare the volumes and the effectiveness of the coatings with each other. The decomposition voltage ($E_d$) for the graphite electrode was 2.1 V and the overvoltage $E_{over}$ was 0.8V in Equation (32).

$$E_{over} = E_d - 1.3 = 2.1 - 1.3 \quad (32)$$

$$E_{over} = 0.8 \text{ V}$$

The decomposition voltages in 1 M KOH solution were determined using the two electrode technique of the system selected as platinum electrode anode and graphite electrode cathode. For this purpose, by applying potential from the direct current source from 1.3 V to 3 V at intervals of 0.1 V to the system, the current values passing through the system were determined and current density ($mA/cm^2$)- potential (V) curves were extracted in Figure 4.5.

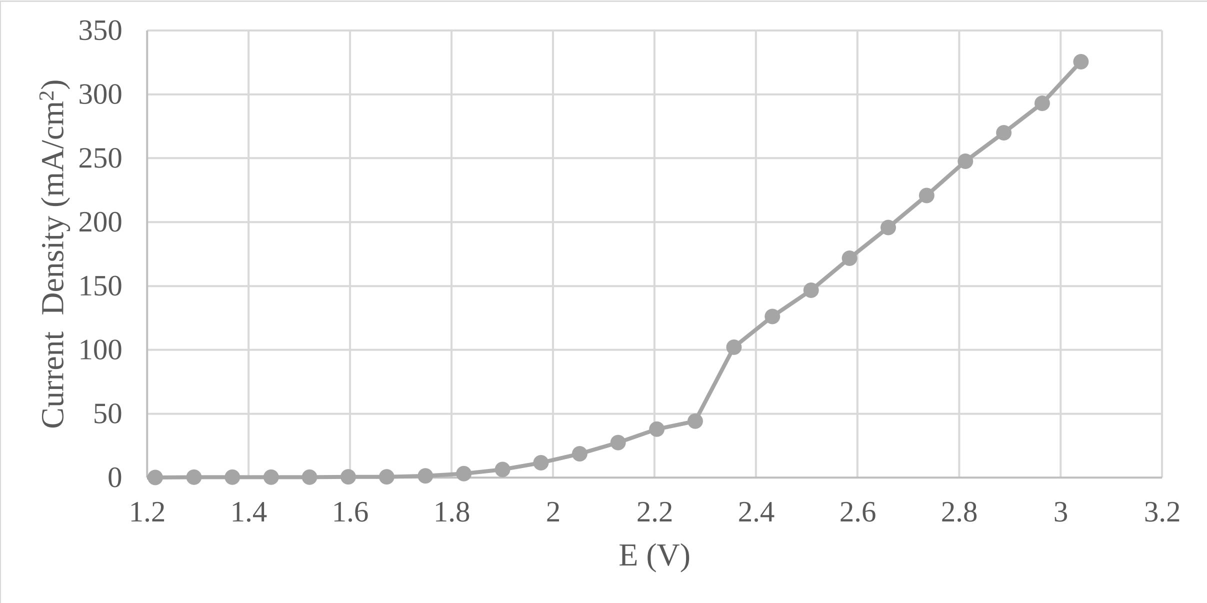


**Figure 4.5.** The voltage-current density curve of G in 1 M KOH at 298 K.

Hydrogen production volumes at different voltage values were observed. Graphite electrode and platinum electrode are immersed in 1 M KOH solution at a constant distance of 2 cm. The cathode, where there is an output of hydrogen gas, is placed on the electrode by reversing the cylinder. Thus, the volume of the amount of hydrogen produced was measured. The volume of hydrogen produced at all voltage values starting from 2.3 V, increasing by 0.1 V up to 3 V and the current values passing through the system at each volt value were measured.

**Table 4.1.** Total charge (Q) during 30 minutes electrolysis, theoretical ($V_t$) and experimental ($V_e$) hydrogen volumes at the end of 30 minutes for various voltages (E) for G electrode.

| E (V) | Q (Coulomb) | $V_t$ (mL) | $V_e$(mL) |
|---|---|---|---|
| 2.3 | 78 | 9.09 | 7.0 |
| 2.4 | 100 | 11.59 | 9.5 |
| 2.5 | 126 | 14.59 | 12.5 |
| 2.6 | 147 | 17.09 | 15.0 |
| 2.7 | 173 | 20.09 | 18.0 |
| 2.8 | 199 | 23.09 | 21.0 |
| 2.9 | 259 | 30.09 | 28.0 |
| 3 | 276 | 32.09 | 30.0 |

At the end of 30 minutes, 30 mL of hydrogen was obtained with a graphite electrode. Current values at different voltages and hydrogen production amounts are given in Table 4.5. Different voltages and hydrogen production volumes every 5 minutes are given in Figure 4.6.

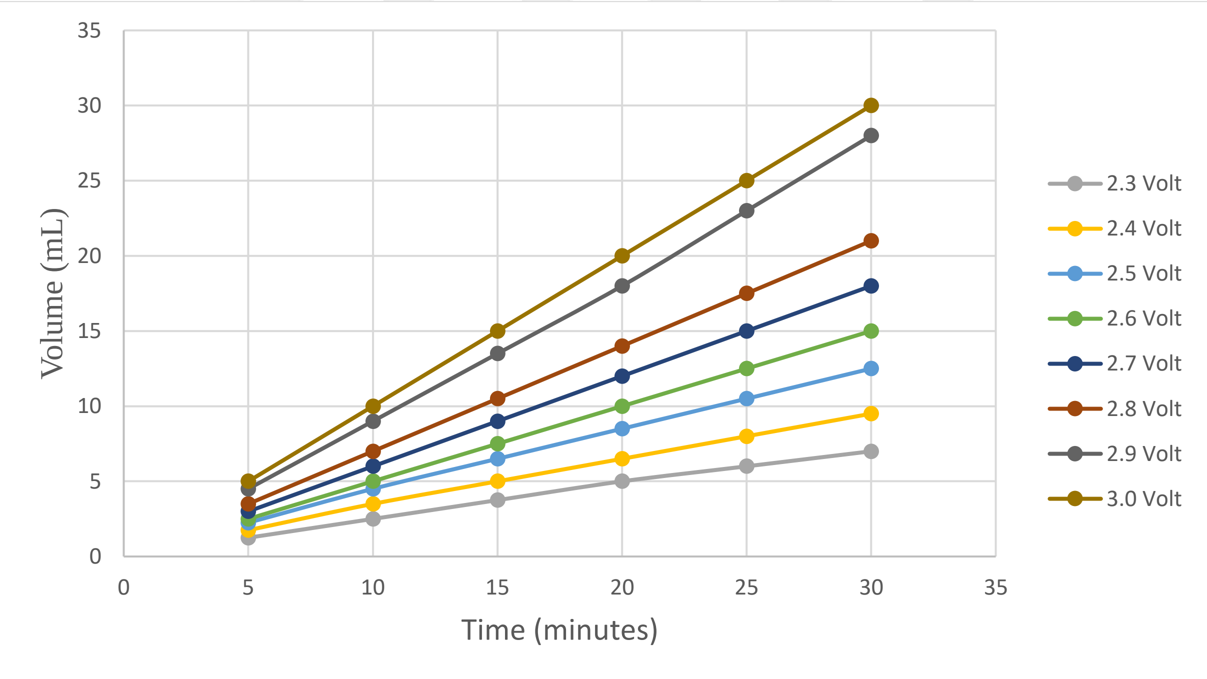


**Figure 4.6.** Amount of hydrogen volume value with Graphite from 2.3 V up to 3 V at each volt during the 30 minutes.

The hydrogen gas measured on the working electrodes used as the cathode in 1 M KOH. Experimental dissociation voltage was calculated for each electrode in order to compare the volumes and the effectiveness of the coatings with each other. The decomposition voltage ($E_d$) for the G/Ni electrode was 1.9 V and the overvoltage $E_{over}$ was 0.6 V in Equation (33).

$$E_{over} = E_d - 1.3 = 1.9 - 1.3 \tag{33}$$

$$E_{over} = 0.6 \text{ V}$$

The decomposition voltages in 1 M KOH solution were determined using the two electrode technique of the system selected as platinum electrode anode and G/Ni electrode cathode. For this purpose, by applying potential from the direct current source from 1.3 V to 3 V at intervals of 0.1 V to the system, the current values passing through the system were determined and current density (mA/cm$^2$)- potential (V) curves were extracted in Figure 4.7.

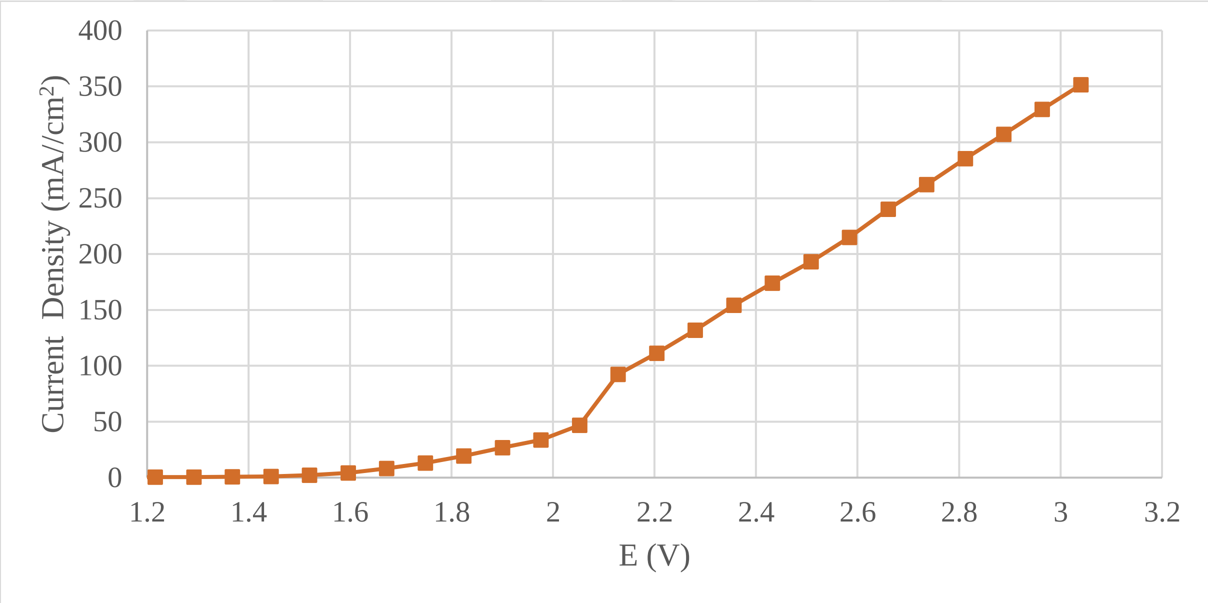


**Figure 4.7.** The voltage-current density curve of G/Ni in 1 M KOH at 298 K.

Hydrogen production volumes at different voltage values were observed. G/Ni electrode and platinum electrode are immersed in 1 M KOH solution at a constant distance of 2 cm. The cathode, where there is an output of hydrogen gas, is placed on the electrode by reversing the cylinder. Thus, the volume of the amount of hydrogen produced was measured. The volume of hydrogen produced at all voltage values starting from 2.3 V, increasing by 0.1 V up to 3 V and the current values passing through the system at each volt value were measured.

**Table 4.2.** Total charge (Q) during 30 minutes electrolysis, theoretical ($V_t$) and experimental ($V_e$) hydrogen volumes at the end of 30 minutes for various voltages (E) for G/Ni electrode.

| E (V) | Q (Coulomb) | $V_t$ (mL) | $V_e$(mL) |
|---|---|---|---|
| 2.3 | 94 | 10.92 | 9.25 |
| 2.4 | 137 | 15.92 | 14.25 |
| 2.5 | 144 | 16.67 | 15.00 |
| 2.6 | 174 | 20.17 | 18.50 |
| 2.7 | 200 | 23.17 | 21.50 |
| 2.8 | 243 | 28.17 | 26.50 |
| 2.9 | 256 | 29.67 | 28.00 |
| 3 | 281 | 32.67 | 31.00 |

At the end of 30 minutes, 31 mL of hydrogen was obtained with a G/Ni electrode. Current values at different voltages and hydrogen production amounts are given in the Table 4.2. Different voltages and hydrogen production volumes in every 5 minutes are given in the Figure 4.8.

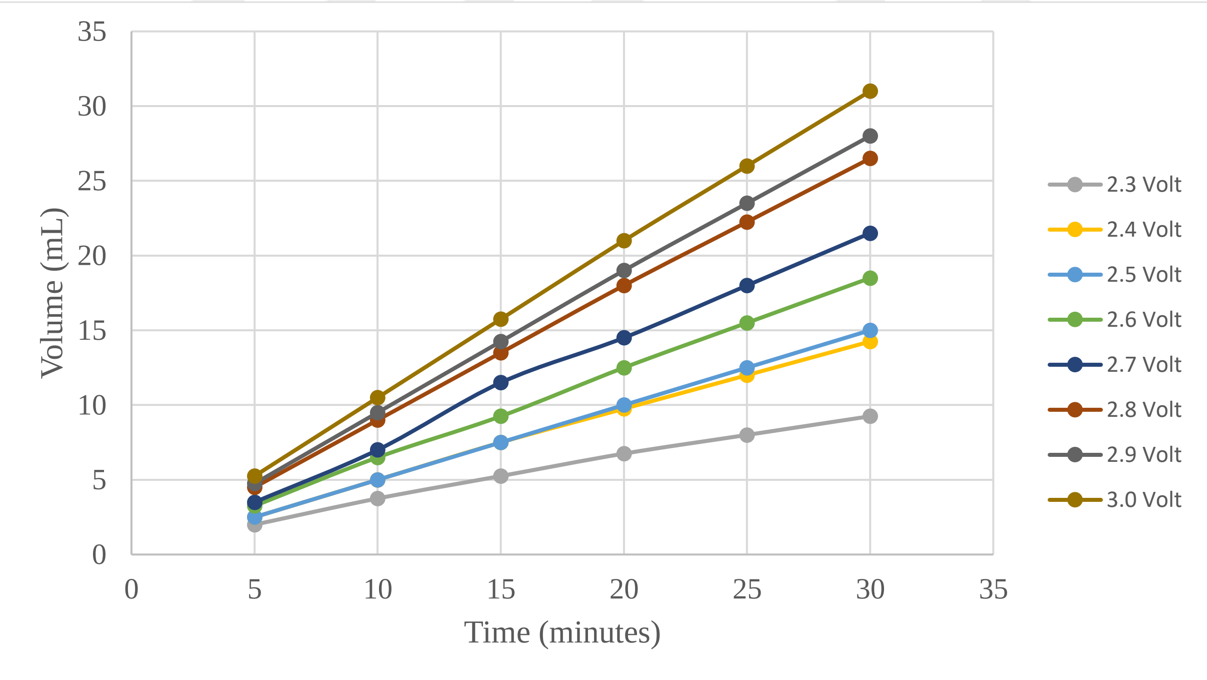


**Figure 4.8.** Amount of hydrogen volume value with G/Ni from 2.3 V up to 3 V at each volt during the 30 minutes.

The hydrogen gas measured on the working electrodes used as the cathode in 1 M KOH. Experimental dissociation voltage was calculated for each electrode in order to compare the volumes and the effectiveness of the coatings with each other. The decomposition voltage ($E_d$) for the G/NiCo electrode was 1.7 V and the overvoltage $E_{over}$ was 0.4V in Equation (34).

$$E_{over} = E_d - 1.3 = 1.7 - 1.3 \quad (34)$$

$$E_{over} = 0.4 \text{ V}$$

The decomposition voltages in 1 M KOH solution were determined using the two electrode technique of the system selected as platinum electrode anode and G/NiCo electrode cathode. For this purpose, by applying potential from the direct current source from 1.3 V to 3 V at intervals of 0.1 V to the system, the current values passing through the system were determined and current density (mA/cm$^2$)- potential (V) curves were extracted in Figure 4.9.

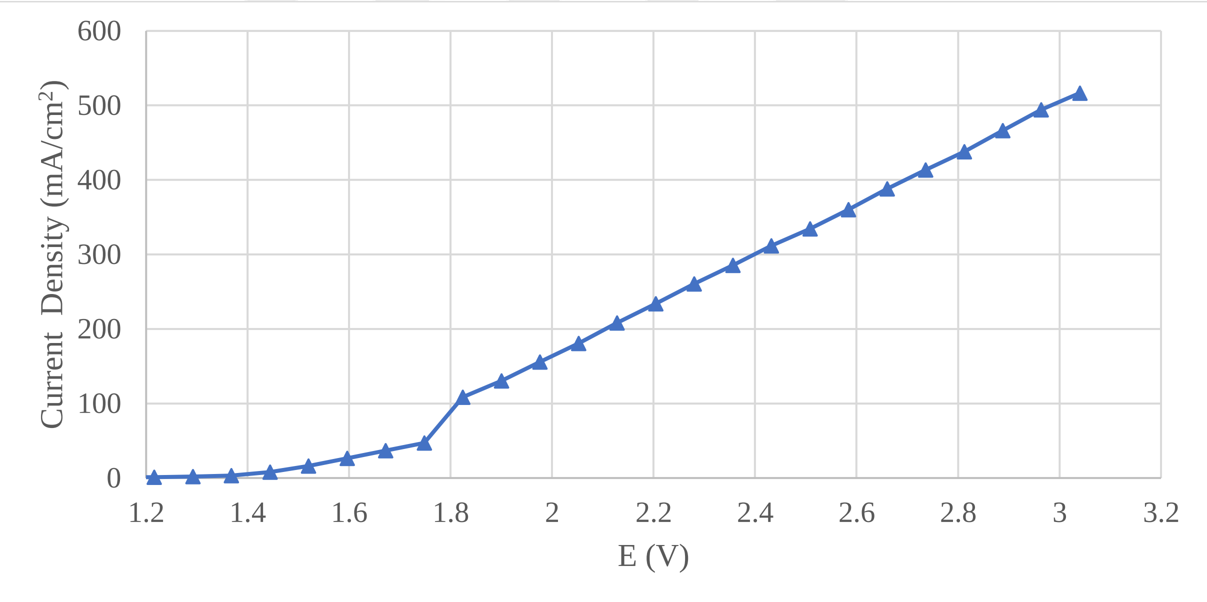


**Figure 4.9.** The voltage-current density curve of G/NiCo in 1 M KOH at 298 K.

Hydrogen production volumes at different voltage values were observed. G/NiCo electrode and platinum electrode are immersed in 1 M KOH solution at a constant distance of 2 cm. The cathode, where there is an output of hydrogen gas, is placed on the electrode by reversing the cylinder. Thus, the volume of the amount of hydrogen produced was measured. The volume of hydrogen produced at all voltage values starting from 2.3 V, increasing by 0.1 V up to 3 V and the current values passing through the system at each volt value were measured.

**Table 4.3.** Total charge (Q) during 30 minutes electrolysis, theoretical ($V_t$) and experimental ($V_e$) hydrogen volumes at the end of 30 minutes for various voltages (E) for G/NiCo electrode.

| E (V) | Q (Coulomb) | $V_t$ (mL) | $V_e$(mL) |
|---|---|---|---|
| 2.3 | 200 | 23.25 | 22.00 |
| 2.4 | 218 | 25.25 | 24.00 |
| 2.5 | 243 | 28.25 | 27.00 |
| 2.6 | 261 | 30.25 | 29.00 |
| 2.7 | 295 | 34.25 | 33.00 |
| 2.8 | 312 | 36.25 | 35.00 |
| 2.9 | 334 | 38.75 | 37.50 |
| 3 | 373 | 43.25 | 42.00 |

At the end of 30 minutes, 42 mL of hydrogen was obtained with a G/NiCo electrode. Current values at different voltages and hydrogen production amounts are given in Table 4.3. Different voltages and hydrogen production volumes in every 5 minutes are given in Figure 4.10.

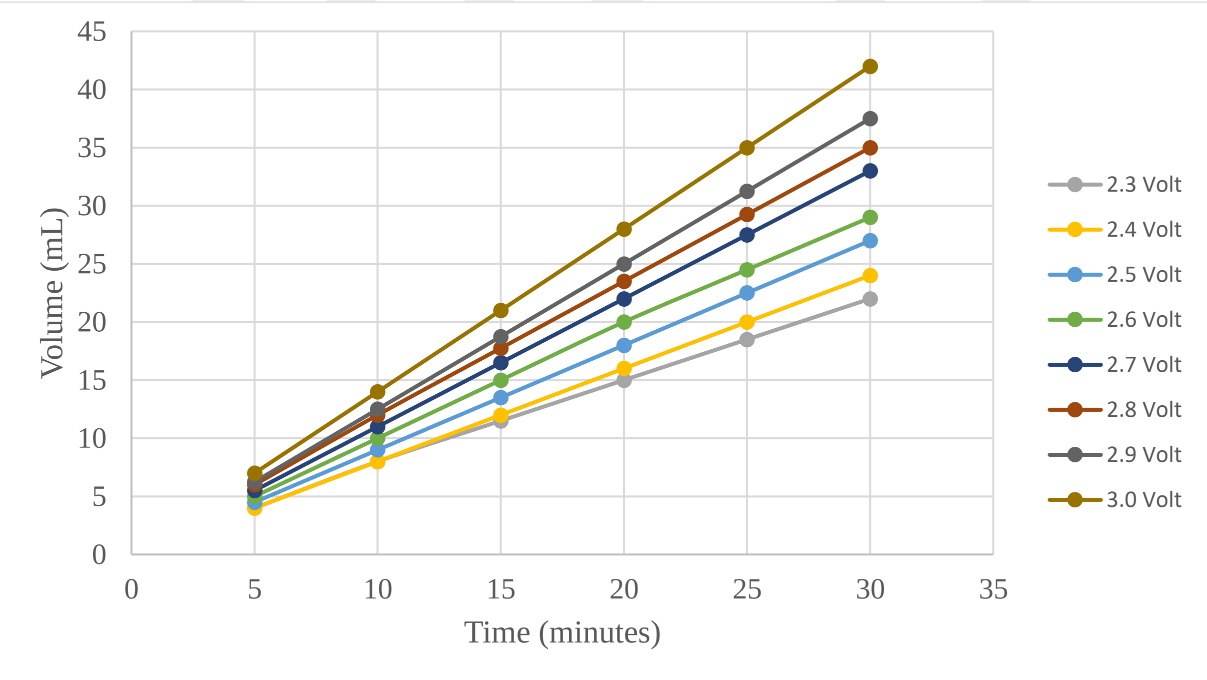


**Figure 4.10.** Amount of hydrogen volume value with G/NiCo from 2.3 V up to 3 V at each volt during the 30 minutes.

The hydrogen gas measured on the working electrodes used as the cathode in 1 M KOH. Experimental dissociation voltage was calculated for each electrode in order to compare the volumes and the effectiveness of the coatings with each other. The decomposition voltage ($E_d$) for the G/NiCoAg electrode was 1.55 V and the overvoltage $E_{over}$ was 0.25 V in Equation (35).

$$E_{over} = E_d - 1.3 = 1.55 - 1.3 \quad (35)$$

$$E_{over} = 0.25 \text{ V}$$

The decomposition voltages in 1 M KOH solution were determined using the two electrode technique of the system selected as platinum electrode anode and G/NiCoAg electrode cathode. For this purpose, by applying potential from the direct current source from 1.3 V to 3 V at intervals of 0.1 V to the system, the current values passing through the system were determined and the current density (mA/cm$^2$)- potential (V) curves were extracted.

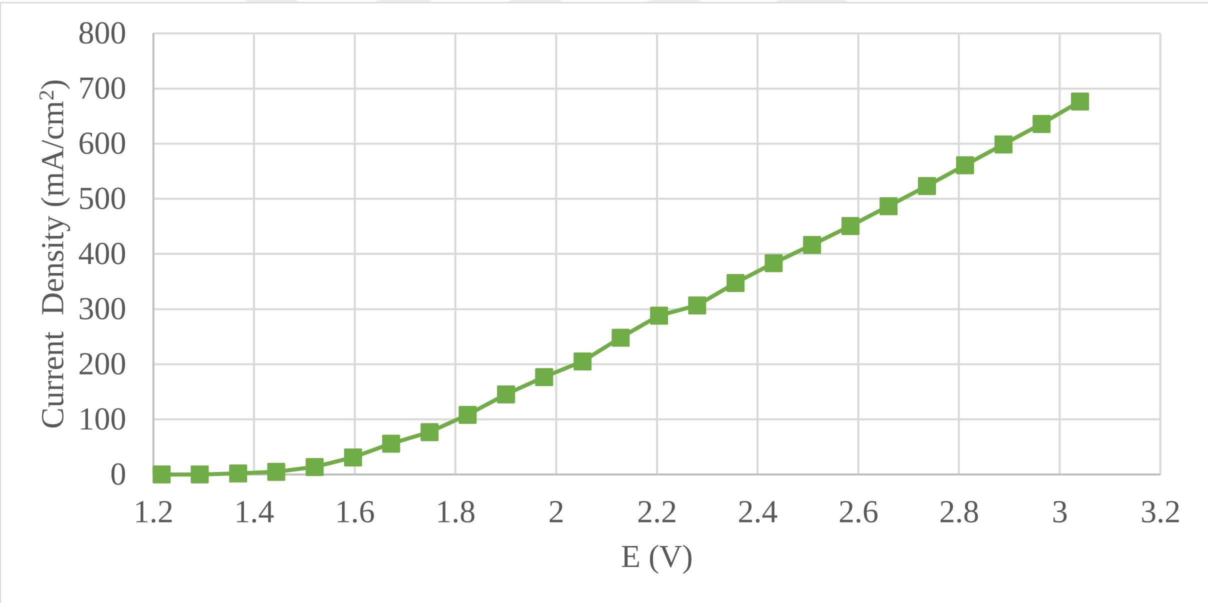


**Figure 4.11.** The voltage-current density curve of G/NiCoAg in 1 M KOH at 298 K.

Hydrogen production volumes at different voltage values were observed. G/NiCoAg electrode and platinum electrode are immersed in 1 M KOH solution at a constant distance of 2 cm. The cathode, where there is an output of hydrogen gas, is placed on the electrode by reversing the cylinder. Thus, the volume of the amount of hydrogen produced was measured. The volume of hydrogen produced at all voltage values starting from 2.3 V, increasing by 0.1 V up to 3 V and the current values passing through the system at each volt value were measured.

**Table 4.4.** Total charge (Q) during 30 minutes electrolysis, theoretical ($V_t$) and experimental ($V_e$) hydrogen volumes at the end of 30 minutes for various voltages (E) for G/NiCoAg electrode.

| E (V) | Q (Coulomb) | $V_t$ (mL) | $V_e$(mL) |
|---|---|---|---|
| 2.3 | 266 | 30.84 | 30.00 |
| 2.4 | 317 | 36.84 | 36.00 |
| 2.5 | 472 | 54.84 | 54.00 |
| 2.6 | 498 | 57.84 | 57.00 |
| 2.7 | 550 | 63.84 | 63.00 |
| 2.8 | 576 | 66.84 | 66.00 |
| 2.9 | 628 | 72.84 | 72.00 |
| 3 | 679 | 78.84 | 78.00 |

At the end of 30 minutes, 78 mL of hydrogen was obtained with a G/NiCoAg electrode. Current values at different voltages and hydrogen production amounts are given in Table 4.4. Different voltages and hydrogen production volumes in every 5 minutes are given in Figure 4.12.

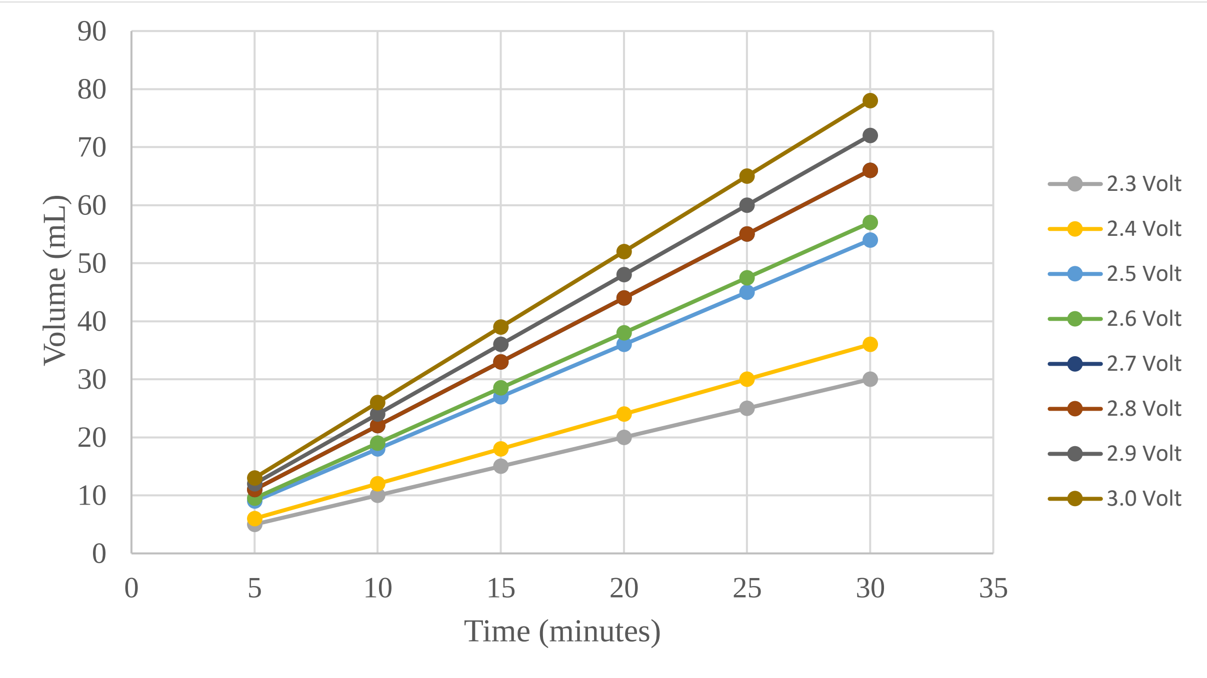


**Figure 4.12.** Amount of hydrogen volume value with G/NiCoAg from 2.3 V up to 3 V at each volt during the 30 minutes.

The scanning electron microscope is used to illuminate the surface structures of materials. The electrons detached from the electron source are dropped on the sample with the help of collector lenses in a column under vacuum, the particles and x-rays that come out as a result of the interaction of the electron beam with the atoms on the sample surface are detected, passed through signal amplifiers and sent to the screen of the cathode ray tube. Information about the topography and chemical composition of the sample under investigation is obtained. Secondary electrons scattered from the surface atoms provide information about the sample surface, while backscattered electrons are used to detect elemental differences on the sample surface through the contrast difference between regions with different chemical compositions.

In this study, The FESEM device used in this study is the Quanta 650 model of the FEI brand. After the surface of the graphite electrode was coated with G/NiCoAg, the structure of the coatings formed on the surface was examined by taking Field Emission Scanning Electron Microscopy (FESEM) images. The surface image of the uncoated graphite electrode was also taken for comparison. SEM image of the graphite electrode is given in Figure 4.13. SEM images of typical morphological features of graphite. Graphite is characterized by a surface consisting of irregularly shaped graphite flakes.

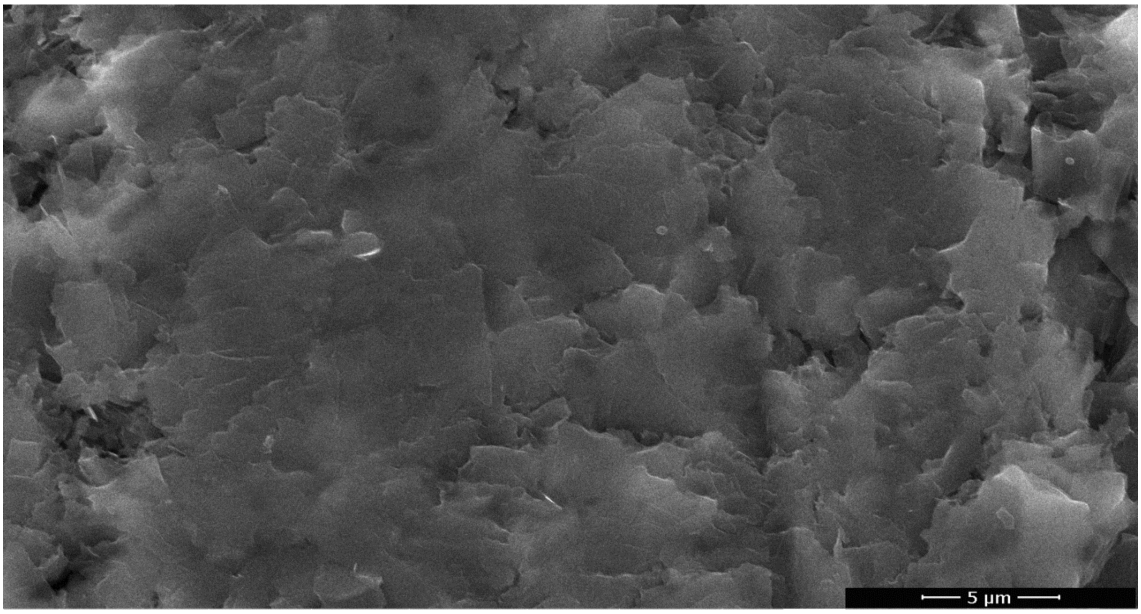


**Figure 4.13.** FESEM images of G, scale bar is 5 μm.

Figure 4.14 shows the SEM image of the G/NiCoAg electrode. On the surface of the graphite, it is seen that there are rough structures in the form of islands in the image of a clustered cauliflower.

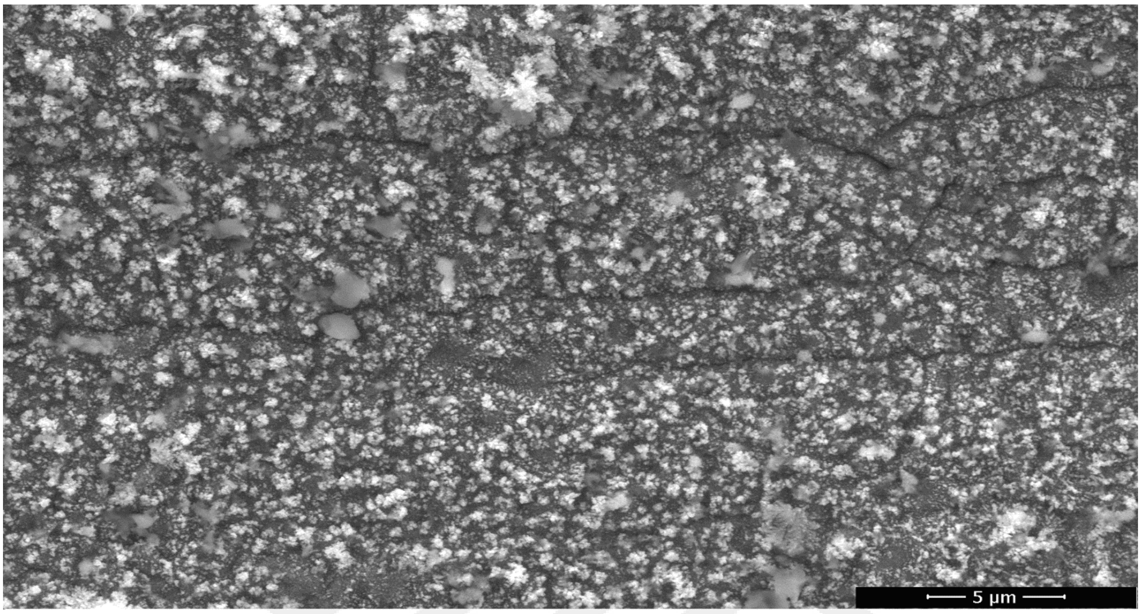


**Figure 4.14.** FESEM images of G/NiCoAg, scale bar is 5 µm.

In the study of Chakik et al. (2017), 20g / L NaOH solution was used as the electrolyte, and zinc (Zn) alloys in various proportions were used as cathodes. As a result of the experiment, the highest hydrogen production was obtained when Zn90% Cr10% alloy was used as cathode. When 3 V constant DC voltage was applied, 1 mL hydrogen production was achieved in 246 seconds, 2 mL hydrogen production in 382 seconds, 3 mL hydrogen production in 536 seconds. In the study of Koca et al. (2019), 1 M KOH solution was used as the electrolyte, Platinum (Pt) was used as the reference electrode, CF, CF / Ni, CF / NiGa were used as the cathode electrodes and 3V DC voltage was used in the electrolysis circuit for 30 minutes. has been applied. At the end of the experiment, the highest hydrogen production occurred when CF / NiGa electrode was used with 27.5 mL. In the study of Döner (2008), platinum was used as anode in 1 M KOH solution, and Cu, Cu / Cu, Cu / Ni, Cu / Co, Cu / NiCo electrodes were used as cathodes. In the experiments, the maximum amount of hydrogen was obtained in 141 mL with Cu / NiCu electrode in 60 minutes. Considering the production amount in 30 minutes, which is the current test period, assuming that 70.5 mL of hydrogen will be produced. In this study, Dayana ve ark designed a cylindrical electrolytic cell made of acrylic and 304 stainless steel electrodes to produce hydrogen. The electrolyte used was sodium hydroxide (NaOH 2-5 mol $L^{-1}$), and the direct current voltages applied were 2.0, 2.7, and 3.4 V. The maximum hydrogen production was achieved with 5.0 mol $L^{-1}$ NaOH and 3.4 V electric voltage. The system was connected to a photovoltaic panel of 20 W and exposed to solar radiation from 10 a.m. to 2 p.m. Approximately 2 L of hydrogen was produced within a period, and an average irradiance of 800.0 W $m^{-2}$ ± 60 W $m^{-2}$ was achieved. Kaya et al. looked at the power consumption of 4 different low-cost electrodes and selected the 2 electrodes with the lowest power consumption, graphite and high carbon steel. They investigated their production in KOH solution by alkaline electrolysis method with different concentrations. After 2 hours at 4V at room temperature, 141.1 mL of hydrogen was obtained in KOH solution with 15% concentration. Graphite was used as the anode and HCS was used as the working electrode. The authors looked at hydrogen production in NaOH electrolyte of different concentration using zinc alloys. During hydrogen production, Zn90%Co10%, Zn95%Fe5%, Zn95%Cu5%, Zn90%Cr10% , Zn85%Cu15%, Zn95%Co5%, Zn85% Fe15%,Zn90%Cu10%, Zn95%Cr5%, Zn90%Fe10% was used as cathode at different mass alloy ratios. During the experiment, the effects of different current values, different voltage values and electrolyte concentration were observed. The highest efficiency reached 6mL hydrogen in 154 seconds at 5V, 0.45A with the Zn95%Cr5% electrode. Döner et al. compared the hydrogen production values of 4 different electrodes. In this study, Pt as anode, bare graphite, Co, CoZn and CoZn-Pt electrodes as cathode were used. 1 hour measurements were made in 1M KOH solution by applying a constant voltage of 3V. Hydrogen production of 73 mL/$cm^2$ in bare graphite, 294 mL/$cm^2$ in Co, 428 mL/$cm^2$ in CoZn and 520 mL/$cm^2$ in CoZn-Pt was achieved.

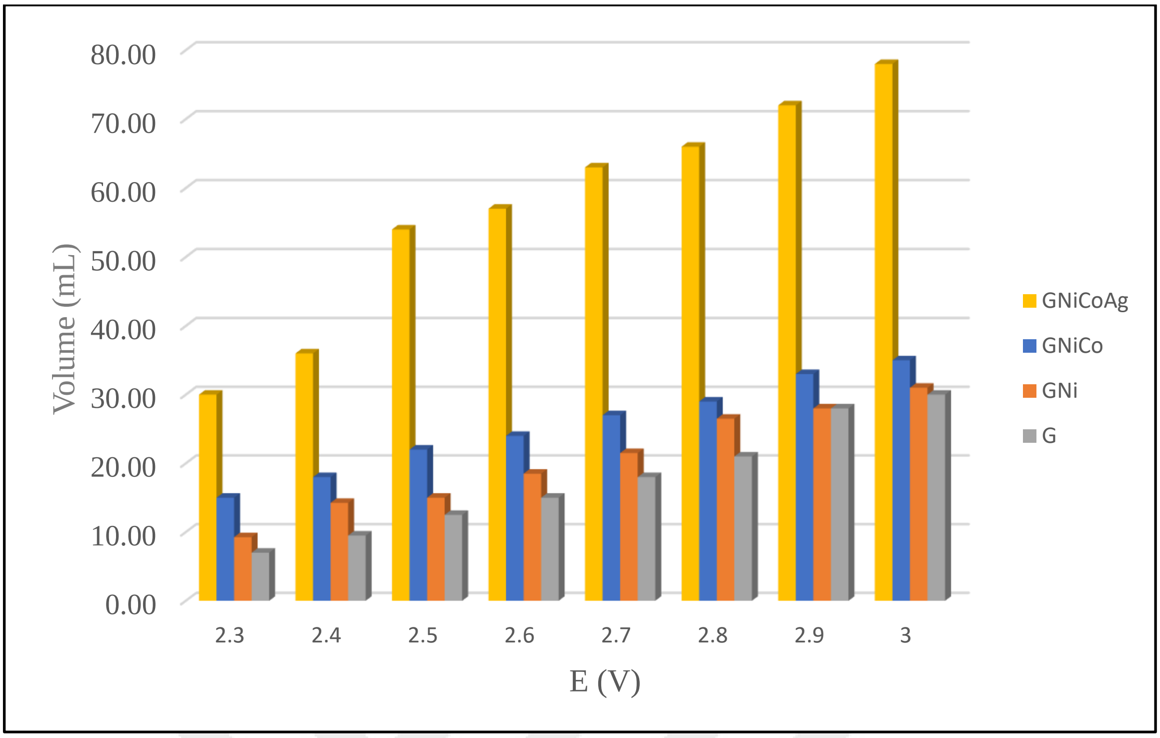


**Figure 4.15.** Comparison of hydrogen production amounts of G, G/Ni, G/NiCo, and G/NiCoAg electrodes after 30 minutes at 3V.

The hydrogen gas volume was determined with a graduated cylinder filled with 1 M KOH electrolyte. The hydrogen performance of G, G/Ni, G/NiCo and G/NiCoAg was compared in Figure 4.15. G, G/Ni, G/NiCo, and G/NiCoAg produced 30 mL, 31 mL, 42 mL and 78 mL of hydrogen gas, respectively, end of 30 minutes of electrolysis time by applying a voltage of 3V. Thanks to these thin coatings and decorations, the electrocatalytic properties of the electrodes were increased and it was proved that there was a serious increase in hydrogen production.

As a result, the performance of the produced G/NiCoAg electrode is comparable to the literature and has good results at low cost as a cathode in an alkaline electrolysis cell provided by a PV system.

# 5. CONCLUSIONS

In this study, we aimed to create alternative energy applications based on solar and hydrogen-based systems in order to reduce the global warming problem that threatens the world. Off-grid system parameters are given in this study, but we believe that on-grid system applications will be suitable for hydrogen production.

Calculated theoretical system parameters and PV panel values that we will use in the experiment were simulated in MATLAB/ Simulink. The module was created according to the characteristics of the PV panel and DC-DC buck converter. I-V and P-V curves of the PV panel were extracted to determine the maximum power point (MPP). In this way, the highest efficiency from the PV panel was provided. By comparing the results obtained by the simulation with the experimental results, compatible results were obtained. During the simulation and experiment, the ambient temperature was 25 ℃ and the irradiation was 1000 W/m2. As a result of the simulation, the MPP point was obtained as 81 W at 18.5 V and 4.38 A. As a result of the experiment, the MPP point was obtained as 77.15 W at 16.7 V and 4.62 A.

The graphite electrode was preferred as the cathode (working) electrode because of its low cost. Initially, the hydrogen production and current values of graphite at different potentials were observed. After 30 minutes at 3V, 30 mL of hydrogen gas was obtained. The results are remarkable when compared with similar studies in the literature. Then the graphite surface was coated with 10 μm Ni and the same experiments were repeated for the G/Ni electrode, with the highest volume of 31 mL. The G/Ni electrode was decorated with cobalt and the same experiments were repeated in the G/NiCo electrode. A significant increase was seen compared to G/Ni and 43mL of hydrogen gas was obtained. The G/NiCo electrode was also decorated with silver and its performance was examined. After 30 minutes, 78 mL of hydrogen gas was produced. Thus, high amount of hydrogen production was realized at low cost. Compared to bare electrode, G, more than 2.5 times increase was achieved with the G/NiCoAg electrode.

# 6. RECOMMENDATIONS

Due to the increasing human population and industrialization, it is seen that pollution has increased, global warming has accelerated and fossil fuel reserves have decreased. In order to leave a livable green world for the future and not to interfere with their right to live in a good world, countries should invest in renewable energy sources as soon as possible. On the other hand, it has been seen that economic prosperity and freedom from foreign dependency on energy side can only be achieved with renewable energy in Turkey. Our country has potential especially in solar energy, wind energy, hydroelectric energy. This potential should be supported and evaluated with government incentives.

Looking at the literature, it is seen that the energy carrier hydrogen will reach an important point in the near future. Studies in this area should be increased and new cathode materials should be produced. Thus, the cost will be reduced and it will reach the position it deserves. For the development of the solar assisted alkaline electrolysis system, a fuel cell may be added to this system in the future. In addition, MATLAB/Simulink simulation can also be developed and added to the thermal analysis and fuel cell parts of the system.

# REFERENCES

Akyuz, E., Coskun, C., Oktay, Z., & Dincer, I. (2011). Hydrogen production probability distributions for a PV-electrolyser system. *International Journal of Hydrogen Energy, 36*(17), 11292-11299. doi: 10.1016/j.ijhydene.2010.11.125

Albarghot, M., & Rolland, L. (2016). MATLAB/Simulink modelling and experimental results of a PEM electrolyzer powered by a solar panel. *2016 IEEE Electrical Power and Energy Conference (EPEC),* 1-6. Ottawa, ON, Canada: IEEE. doi: 10.1109/EPEC.2016.7771691

Aldaoudeyeh, A. I. (2016). Photovoltaic-battery scheme to enhance PV array characteristics in partial shading conditions. *IET Renewable Power Generation*, *10*(1), 108-115. doi: 10.1049/iet-rpg.2015.0177

Alemdaroğlu, Nusret, (2007). Enerji Sektörünün Geleceği Alternatif Enerji Kaynakları ve Türkiye'nin Önündeki Fırsatlar, İstanbul: İstanbul Ticaret Odası Yayınları.

Al-Refai, M. A. (2014). MATLAB/Simulink Simulation of Solar Energy Storage System. *International Journal of Electrical and Computer Engineering*, *8*(2), 6.

Amores, E., Rodríguez, J., & Carreras, C. (2014). Influence of operation parameters in the modeling of alkaline water electrolyzers for hydrogen production. *International Journal of Hydrogen Energy*, *39*(25), 13063-13078. doi: 10.1016/j.ijhydene.2014.07.001

Awasthi, A., Scott, K., & Basu, S. (2011). Dynamic modeling and simulation of a proton exchange membrane electrolyzer for hydrogen production. *International Journal of Hydrogen Energy*, *36*(22), 14779-14786. doi: 10.1016/j.ijhydene.2011.03.045

Aydoğan, H. (2019). KÖMÜR (LİNYİT) SEKTÖR RAPORU. 115.

Bartık, A. (2018). Türkiye'nin enerji ihtiyacını ve bu ihtiyacın giderilmesinde yenilenebilir enerji kaynaklarının önemi. (Yayımlanmamış Yüksek Lisans Tezi). Kafkas

Üniversitesi/Sosyal Bilimler Enstitüsü, Kars.

Bilim, N. (2016). TÜRKİYE NİN ELEKTRİK ENERJİSİ ÜRETİMİNDEKİ DIŞA BAĞIMLILIĞIN AZALTILMASI İÇİN UYGULANMASI GEREKEN POLİTİKALAR. *Selcuk University Journal of Engineering ,Science and Technology*, *4*(2), 145-145. doi: 10.15317/Scitech.2016218526

Boudries, R., Khellaf, A., Aliane, A., Ihaddaden, L., & Khida, F. (2014). PV system design for powering an industrial unit for hydrogen production. *International Journal of Hydrogen Energy*, *39*(27), 15188-15195. doi: 10.1016/j.ijhydene.2014.04.166

https://www.bp.com/en/global/corporate/energy-economics/energy-charting-tool-desktop.html

Chaudhary, A., & Ozansoy, C. R. (t.y.). *Microbial electrolysis cell modelling and simulation using MATLAB*. 6.

Coro G, Trumpy E, Predicting geographical suitability of geothermal power plants, Journal of Cleaner Production (2020), doi: https://doi.org/10.1016/j.jclepro.2020.121874.

de Fátima Palhares, D. D., Vieira, L. G. M., & Damasceno, J. J. R. (2018). Hydrogen production by a low-cost electrolyzer developed through the combination of alkaline water electrolysis and solar energy use. *International Journal of Hydrogen Energy*, *43*(9), 4265-4275. doi: 10.1016/j.ijhydene.2018.01.051

Demir, M. (2013). Enerji ithalatı cari açık ilişkisi, var analizi ile Türkiye üzerine bir inceleme. Akademik Araştırmalar ve Çalışmalar Dergisi, 5(9), 2-26.

Demirdelen, T., Ekinci, F., Mert, B. D., Karasu, İ., & Tümay, M. (2020). Green touch for hydrogen production via alkaline electrolysis: The semi-flexible PV panels mounted wind turbine design, production and performance analysis. *International Journal of Hydrogen Energy*, *45*(18), 10680-10695. doi: 10.1016/j.ijhydene.2020.02.007

Department of Electronic Telecommunication, Mechanical & Automotive Engineering and High Safety Vehicle Core Technology Research Center, INJE University, 197 Inje-ro, Gimhae-si, Gyeongsangnam-do 50834, Republic of Korea, & Je, C.-H. (2019). A Study on the Water Splitting using Polymer Electrolyte Membrane for producing Hydrogen and Oxygen. *International Journal of Electrochemical Science*, 6948-6975. doi: 10.20964/2019.07.64

Dieguez, P., Ursua, A., Sanchis, P., Sopena, C., Guelbenzu, E., & Gandia, L. (2008). Thermal performance of a commercial alkaline water electrolyzer: Experimental study and mathematical modeling. *International Journal of Hydrogen Energy*, *33*(24), 7338-7354. doi: 10.1016/j.ijhydene.2008.09.051

Döner, A., Solmaz, R., & Kardaş, G. (2011). Enhancement of hydrogen evolution at cobalt–zinc deposited graphite electrode in alkaline solution. *International Journal of Hydrogen Energy*, *36*(13), 7391-7397. doi: 10.1016/j.ijhydene.2011.03.083

Đukić, A., & Firak, M. (2011). Hydrogen production using alkaline electrolyzer and photovoltaic (PV) module. *International Journal of Hydrogen Energy*, *36*(13), 7799-7806. doi: 10.1016/j.ijhydene.2011.01.180

Ghribi, D., Khelifa, A., Diaf, S., & Belhamel, M. (2013). Study of hydrogen production system by using PV solar energy and PEM electrolyser in Algeria. *International Journal of Hydrogen Energy*, *38*(20), 8480-8490. doi: 10.1016/j.ijhydene.2012.09.175

Gibson, T., & Kelly, N. (2008). Optimization of solar powered hydrogen production using photovoltaic electrolysis devices. *International Journal of Hydrogen Energy*, *33*(21), 5931-5940. doi: 10.1016/j.ijhydene.2008.05.106

Hammoudi, M., Henao, C., Agbossou, K., Dubé, Y., & Doumbia, M. L. (2012). New multi-physics approach for modelling and design of alkaline electrolyzers. *International Journal of Hydrogen Energy*, *37*(19), 13895-13913. doi: 10.1016/j.ijhydene.2012.07.015

Haussener, S., Xiang, C., Spurgeon, J. M., Ardo, S., Lewis, N. S., & Weber, A. Z. (2012).

Modeling, simulation, and design criteria for photoelectrochemical water-splitting systems. *Energy & Environmental Science*, *5*(12), 9922. doi: 10.1039/c2ee23187e

Henao, C., Agbossou, K., Hammoudi, M., Dubé, Y., & Cardenas, A. (2014). Simulation tool based on a physics model and an electrical analogy for an alkaline electrolyser. *Journal of Power Sources*, *250*, 58-67. doi: 10.1016/j.jpowsour.2013.10.086

Holladay, J. D., Hu, J., King, D. L., & Wang, Y. (2009). An overview of hydrogen production technologies. *Catalysis Today*, *139*(4), 244-260. doi: 10.1016/j.cattod.2008.08.039

Huang, P.-H., Kuo, J.-K., & Wu, Z.-D. (2016). Applying small wind turbines and a photovoltaic system to facilitate electrolysis hydrogen production. *International Journal of Hydrogen Energy*, *41*(20), 8514-8524. doi: 10.1016/j.ijhydene.2016.02.051

Hug, W., Divisek, J., Mergel, J., Seeger, W., & Steeb, H. (1992). Highly efficient advanced alkaline electrolyzer for solar operation. *International Journal of Hydrogen Energy*, *17*(9), 699-705. doi: 10.1016/0360-3199(92)90090-J

Ismail, T. M., Ramzy, K., Elnaghi, B. E., Abelwhab, M. N., & El-Salam, M. A. (2019). Using MATLAB to model and simulate a photovoltaic system to produce hydrogen. *Energy Conversion and Management*, *185*, 101-129. doi: 10.1016/j.enconman.2019.01.108

Joshi, A. S., Dincer, I., & Reddy, B. V. (2011). Solar hydrogen production: A comparative performance assessment. *International Journal of Hydrogen Energy*, *36*(17), 11246-11257. doi: 10.1016/j.ijhydene.2010.11.122

Kabadayı, Ş. (t.y.). *GÜNEŞ PANELLERİNDE GÜNEŞ İLE GÖLGE ARASINDAKİ ORANLARIN VERİMLİLİK ÜZERİNE ETKİLERİ VE ANALİZİ*. 85.

Karagöl, E. T., & Kavaz, İs. (t.y.). *DÜNYADA VE TÜRKİYE'DE YENİLENEBİLİR ENERJİ*. 32.

Kardaş, G., Solmaz, R., Yazıcı, B., & Erbil, M. (t.y.). *ELEKTROLİZ YÖNTEMİYLE HİDROJEN GAZI ELDESİ*. 5.

Kaya, M. F., Demir, N., Albawabiji, M. S., & Taş, M. (2017). Investigation of alkaline water electrolysis performance for different cost effective electrodes under magnetic field. *International Journal of Hydrogen Energy, 42*(28), 17583-17592. doi: 10.1016/j.ijhydene.2017.02.039

Kermadi, M., & Berkouk, E. M. (2015). A maximum power point tracker based on particle swarm optimization for PV-battery energy system under partial shading conditions. *2015 3rd International Conference on Control, Engineering & Information Technology (CEIT)*, 1-6. Tlemcen, Algeria: IEEE. doi: 10.1109/CEIT.2015.7233061

Khalilnejad, A., & Riahy, G. H. (2014). A hybrid wind-PV system performance investigation for the purpose of maximum hydrogen production and storage using advanced alkaline electrolyzer. *Energy Conversion and Management, 80*, 398-406. doi: 10.1016/j.enconman.2014.01.040

Khaselev, O. (1998). A Monolithic Photovoltaic-Photoelectrochemical Device for Hydrogen Production via Water Splitting. *Science, 280*(5362), 425-427. doi: 10.1126/science.280.5362.425

Kuzoluk, Elif,(2014), Farklı Miktar Ve Özellikteki Kömür Yığınlarının Kendiliğinden Yanma Davranışları, Önlenmesi Ve Önceden Tespit Edilmesine Bir Örnek; Çayırhan Kömür Stokları T.C. Selçuk Üniversitesi Fen Bilimleri Enstitüsü

Manabe, A., Kashiwase, M., Hashimoto, T., Hayashida, T., Kato, A., Hirao, K., … Nagashima, I. (2013). Basic study of alkaline water electrolysis. *Electrochimica Acta, 100*, 249-256. doi: 10.1016/j.electacta.2012.12.105

Martinez, D., & Zamora, R. (2018). *MATLAB Simscape Model of An Alkaline Electrolyser and Its Simulation with A Directly Coupled PV Module*. *8*(1), 9.

Martinez, D., & Zamora, R. (2019). *Electrical Implementations of an Empirical Electrolyser Model for Improved Matlab/Simulink Simulations*. 11.

Maruf-ul-Karim, Md., & Iqbal, M. T. (2009). Dynamic modeling and simulation of alkaline type electrolyzers. *2009 Canadian Conference on Electrical and Computer Engineering*, 711-715. St. John’s, NL, Canada: IEEE. doi: 10.1109/CCECE.2009.5090222

Mert, B. D., Ekinci, F., & Demirdelen, T. (2019). Effect of partial shading conditions on off-grid solar PV/Hydrogen production in high solar energy index regions. *International Journal of Hydrogen Energy*, *44*(51), 27713-27725. doi: 10.1016/j.ijhydene.2019.09.011

Mert, M. E. (t.y.). *ÇUKUROVA ÜNİVERSİTESİ FEN BİLİMLERİ ENSTİTÜSÜ*. 120.

Morales Pedraza, J. (2015). *Electrical Energy Generation in Europe*. Cham: Springer International Publishing. doi: 10.1007/978-3-319-08401-5

Olivier, P., Bourasseau, C., & Bouamama, Pr. B. (2017). Low-temperature electrolysis system modelling: A review. *Renewable and Sustainable Energy Reviews*, *78*, 280-300. doi: 10.1016/j.rser.2017.03.099

Özgener, Ö., & Özgener, L. (2020). *Türkiye’de Yenilenebilir Enerji Uygulamaları, Mevcut Durum ve Gelecek Öngörüleri Renewable Energy Applications in Turkey, Current Status and Future Forecasts*. 13.

Paola, A., Fabrizio, Z., & Fabio, O. (2011). Techno-economic optimisation of hydrogen production by PV – electrolysis: “RenHydrogen” simulation program. *International Journal of Hydrogen Energy*, *36*(2), 1371-1381. doi: 10.1016/j.ijhydene.2010.10.068

Peharz, G., Dimroth, F., & Wittstadt, U. (2007). Solar hydrogen production by water splitting with a conversion efficiency of 18%. *International Journal of Hydrogen Energy*, *32*(15), 3248-3252. doi: 10.1016/j.ijhydene.2007.04.036

Pregger, T., Graf, D., Krewitt, W., Sattler, C., Roeb, M., & Möller, S. (2009). Prospects of solar thermal hydrogen production processes. *International Journal of Hydrogen Energy*, *34*(10), 4256-4267. doi: 10.1016/j.ijhydene.2009.03.025

Qiu, Z. (t.y.). *Transition Metal-Based Electrocatalysts for Alkaline Water Splitting and CO2 Reduction*. 89.

Rashid, M., Mesfer, M. K. A., Naseem, H., & Danish, M. (t.y.). *Hydrogen Production by Water Electrolysis: A Review of Alkaline Water Electrolysis, PEM Water Electrolysis and High Temperature Water Electrolysis*. *4*(3), 14.

Ratlamwala, T. A. H., Gadalla, M. A., & Dincer, I. (2011). Performance assessment of an integrated PV/T and triple effect cooling system for hydrogen and cooling production. *International Journal of Hydrogen Energy*, *36*(17), 11282-11291. doi: 10.1016/j.ijhydene.2010.11.121

Sharifian, S., Asasian Kolur, N., & Harasek, M. (2020). Transient simulation and modeling of photovoltaic-PEM water electrolysis. *Energy Sources, Part A: Recovery, Utilization, and Environmental Effects*, *42*(9), 1097-1107. doi: 10.1080/15567036.2019.1602220

Shukla, P. K., Karn, R. K., Singh, A. K., & Srivastava, O. N. (2002). Studies on PV assisted PEC solar cells for hydrogen production through photoelectrolysis of water. *International Journal of Hydrogen Energy*, *27*(2), 135-141. doi: 10.1016/S0360-3199(01)00095-7

Slama, R. B. (2013). Hydrogen Production by Water Electrolysis Effects of the Electrodes Materials Nature on the Solar Water Electrolysis Performances. *Natural Resources*, *04*(01), 1-7. doi: 10.4236/nr.2013.41001

Solmaz, R. (t.y.). *ÇUKUROVA ÜNİVERSİTESİ FEN BİLİMLERİ ENSTİTÜSÜ*. 181.

Soylu, B. N. (t.y.). *SELÇUK ÜNİVERSİTESİ SOSYAL BİLİMLER ENSTİTÜSÜ İKTİSAT ANABİLİM DALI İKTİSAT BİLİM DALI*. 109.

Tebibel, H., Khellaf, A., Menia, S., & Nouicer, I. (2017). Design, modelling and optimal power and hydrogen management strategy of an off grid PV system for hydrogen production using methanol electrolysis. *International Journal of Hydrogen Energy*, *42*(22), 14950-14967. doi: 10.1016/j.ijhydene.2017.05.010

Thesis, M., & Vural, M. (t.y.). *ANKARA YILDIRIM BEYAZIT UNIVERSITY GRADUATE SCHOOL OF NATURAL AND APPLIED SCIENCES*. 128.

Tijani, A. S., Yusup, N. A. B., & Rahim, A. H. A. (2014a). Mathematical Modelling and Simulation Analysis of Advanced Alkaline Electrolyzer System for Hydrogen Production. *Procedia Technology*, *15*, 798-806. doi: 10.1016/j.protcy.2014.09.053

Tijani, A. S., Yusup, N. A. B., & Rahim, A. H. A. (2014b). Mathematical Modelling and Simulation Analysis of Advanced Alkaline Electrolyzer System for Hydrogen Production. *Procedia Technology*, *15*, 798-806. doi: 10.1016/j.protcy.2014.09.053

Turner, J. A. (2004). Sustainable Hydrogen Production. *Science*, *305*(5686), 972-974. doi: 10.1126/science.1103197

Turner, J., Sverdrup, G., Mann, M. K., Maness, P.-C., Kroposki, B., Ghirardi, M., … Blake, D. (2008). Renewable hydrogen production. *International Journal of Energy Research*, *32*(5), 379-407. doi: 10.1002/er.1372

Türkmen, Ü. (t.y.). *ÇUKUROVA ÜNİVERSİTESİ FEN BİLİMLERİ ENSTİTÜSÜ*. 104.

Ulleberg, O. (2003). Modeling of advanced alkaline electrolyzers: A system simulation approach. *International Journal of Hydrogen Energy*, *28*(1), 21-33. doi: 10.1016/S0360-3199(02)00033-2

Ursua, A., Gandia, L. M., & Sanchis, P. (2012). Hydrogen Production From Water Electrolysis: Current Status and Future Trends. *Proceedings of the IEEE*, *100*(2), 410-426. doi: 10.1109/JPROC.2011.2156750

Yazıcı , B., Tatlı, G., Galip, H., Erbil, M. (1995). Investigation of suitable cathodes for the production of hydrogen gas by electrolysis. *Int. J. Hydrogen Energy*, 20 (12):957–965.

Yuvaraj, A. L., & Santhanaraj, D. (2013). A systematic study on electrolytic production of hydrogen gas by using graphite as electrode. *Materials Research*, *17*(1), 83-87. doi: 10.1590/S1516-14392013005000153

Zhang, H. L., Van Gerven, T., Baeyens, J., & Degrève, J. (2014). Photovoltaics: Reviewing the European Feed-in-Tariffs and Changing PV Efficiencies and Costs. *The Scientific World Journal*, *2014*, 1-10. doi: 10.1155/2014/4049